

พฤติกรรมการอัดตัวคายนํ้าด้วยวิธีสุญญากาศสำหรับการปรับปรุงคุณภาพดินอ่อน

นาย เดชา ตรุง ใจ

วิทยานิพนธ์นี้เป็นส่วนหนึ่งของการศึกษาตามหลักสูตรปริญญาวิศวกรรมศาสตรดุษฎีบัณฑิต

สาขาวิชาวิศวกรรมโยธา ภาควิชาวิศวกรรมโยธา

คณะวิศวกรรมศาสตร์ จุฬาลงกรณ์มหาวิทยาลัย

ปีการศึกษา **2555**

ลิขสิทธิ์ของจุฬาลงกรณ์มหาวิทยาลัย

บทคัดย่อและแฟ้มข้อมูลฉบับเต็มของวิทยานิพนธ์ตั้งแต่ปีการศึกษา 2554 ที่ให้บริการในคลังปัญญาจุฬาฯ (CUIR)
เป็นแฟ้มข้อมูลของนิสิตเจ้าของวิทยานิพนธ์ที่ส่งผ่านทางบัณฑิตวิทยาลัย

The abstract and full text of theses from the academic year 2011 in Chulalongkorn University Intellectual Repository(CUIR)
are the thesis authors' files submitted through the Graduate School.

**PERFORMANCE OF VACUUM CONSOLIDATION
METHOD FOR SOFT GROUND IMPROVEMENT**

Mr. Duong Trung Ngo

A Dissertation Submitted in Partial Fulfillment of the Requirements
for the Degree of Doctor of Philosophy Program in Civil Engineering
Department of Civil Engineering
Faculty of Engineering Chulalongkorn University
Academic Year **2012**
Copyright of Chulalongkorn University

Thesis Title	PERFORMANCE OF VACUUM CONSOLIDATION METHOD FOR SOFT GROUND IMPROVEMENT
By	Mr. Duong Trung Ngo
Field of Study	Geotechnical Engineering
Thesis Advisor	Associate Professor Wanchai Teparaksa, Ph.D.
Thesis Co-Advisor	Professor Hiroyuki Tanaka, Ph.D.

Accepted by the Faculty of Engineering, Chulalongkorn University in
Partial Fulfillment of the Requirements for the Doctoral Degree

.....Dean of the Faculty of Engineering
(Associate Professor Boonsom Lerthirunwong, Ph.D.)

THESIS COMMITTEE

..... Chairman
(Associate Professor Boonsom Lerthirunwong, Ph.D.)

..... Thesis Advisor
(Associate Professor Wanchai Teparaksa, Ph.D.)

..... Thesis Co-advisor
(Professor Hiroyuki Tanaka, Ph.D.)

..... Examiner
(Associate Professor Tirawat Boonyatee, Ph.D.)

..... Examiner
(Assistant Professor Tanate Srisirojanakorn, Ph.D.)

..... External Examiner
(Associate Professor Korchoke Chantawarangkul, Ph.D.)

เดา ตรง โง: พฤติกรรมการอัดตัวคายน้ำด้วยวิธีสุญญากาศสำหรับการปรับปรุงคุณภาพดินอ่อน. (PERFORMANCE OF VACUUM CONSOLIDATION METHOD FOR SOFT GROUND IMPROVEMENT) อ.ที่ปรึกษาวิทยานิพนธ์หลัก :รศ.ดร.วันชัย เทพรักษ์,ศ.ดร.อิโรยูกิ ทานากะ, 110 หน้า.

งานวิจัยนี้ดำเนินการโดยการวิเคราะห์ไฟไนต์เอลิเมนต์และผลการทดลองในห้องปฏิบัติการเพื่อนำเสนอวิธีการที่เหมาะสมและสามารถนำไปประยุกต์ใช้กันอย่างแพร่หลายในการปรับปรุงคุณภาพดินอ่อนโดยการใช้วิธีการเพิ่มน้ำหนักแบบสุญญากาศ

การทำนายพฤติกรรมของการปรับปรุงดินโดยใช้วิธีการเพิ่มน้ำหนักแบบสุญญากาศควรจะคำนึงอย่างมีนัยสำคัญทั้งในห้องปฏิบัติการและในสนามโดยมีวัตถุประสงค์เพื่อหลีกเลี่ยงความเสี่ยงจากความไม่เสถียรภาพและการพังทลายของคันดินในระหว่างการก่อสร้างในส่วนวิธีการจำลองการเพิ่มน้ำหนักแบบสุญญากาศโดยใช้เครื่องทดสอบสามแกนถูกนำเสนอในการคาดการณ์ล่วงหน้าไม่เพียงแต่พฤติกรรมของการปรับปรุงดินอ่อนแต่รวมไปถึงพฤติกรรมของแรงเฉือนแบบไม่ระบายน้ำที่เพิ่มขึ้นของตัวอย่างดินที่ระดับการยุบตัวของ การอัดตัวคายน้ำในห้องปฏิบัติการแบบจำลองนี้มีแนวโน้มว่าเป็นวิธีที่มีประสิทธิภาพในการกำหนดอัตราการเพิ่มความแข็งแรงของดินที่สอดคล้องกับอัตราการเพิ่มขึ้นของแรงในระหว่างกระบวนการอัดตัวคายน้ำและเป็นการจำกัดการใช้สนามทดสอบในระหว่างการก่อสร้างที่จะทำให้เกิดความเสียหายของเยื่อหุ้มสุญญากาศและการสูญเสียความดันสุญญากาศ.

กรณีศึกษาได้ทำการศึกษาที่สนามบินจังหวัดนครศรีธรรมราชในช่วงการปรับปรุงดินเครื่องมือวัดในสนามถูกใช้ในการประเมินการปรับปรุงพฤติกรรมของดินอ่อนและลดปัญหาความไม่เสถียรภาพของถนนเพื่อเพิ่มประสิทธิภาพของวิธีนี้ในงานวิจัยนี้มีวัตถุประสงค์เพื่อสนับสนุนการทำงานวิศวกรรมอย่างมีประสิทธิภาพนอกจากนี้ยังคาดว่าจะทำให้วิธีที่มีอยู่กลายเป็นวิธีที่สามารถนำไปใช้ในทางจริงได้อย่างแพร่หลายในอนาคต.

ภาควิชา : วิศวกรรมโยธา ลายมือชื่อนิสิต

สาขาวิชา : วิศวกรรมธรณีเทคนิค ลายมือชื่อ อ.ที่ปรึกษาวิทยานิพนธ์หลัก

ปีการศึกษา 2555 ลายมือชื่อ อ.ที่ปรึกษาวิทยานิพนธ์ร่วม

ACKNOWLEDGEMENTS

I would like to express my grateful admiration to the hearted supports of JICA – Japan, represented by AUN-Seed/Net scholarship program in training for Asian countries' human resources. The program sponsors not only for scientific development but also for deep humanity. Experiences in the international environment have helped us understand the culture of the different ethnic groups in the world, especially in the Asian countries and Japan. With all the knowledge gained in the past years, I believe that I am able to promote the program's noble in my future work.

Ho Chi Minh University of Technology (HCMUT), Chulalongkorn University, Hokkaido University, and the Lectures have provided the most favourable conditions and equipments to help me complete the PhD research. I greatly appreciate all their kind supports. Furthermore, I would like to thank Assoc. Prof. Phan Dinh Tuan and Assoc. Prof. Le Van Nam, Vice Rectors of HCMUT, Assoc. Prof. Nguyen Thanh Nghi, Deputy Minister of Construction Viet Nam, who have supported and encouraged me to pursue my PhD study. I also would like to express my gratitude to Mr. Nakakuma, Dr. Nipon, Mr. Wanna and Dr. Yamazoe, N who have given me suggestions and data to complete my research.

My profound thanks go to The Thesis Committee for their important comments that have been helping me improve my thesis with a good progress as well as figure out the future research directions. I am sincerely grateful to **Professor Hiroyuki Tanaka**, my co-advisor, for his enthusiasm, but strict attitude in working which helped me experience the professional research environment that I have ever been. In addition, several trips together with him give me good impressions of Japanese cuisine and people here as well as strong spirit to conduct my research in Hokkaido University. I am deeply indebted to my advisor, Associate Professor **Wanchai Teparaksa** from Chulalongkorn University, whose helps, stimulating suggestions and encouragement have instructed me in doing PhD research. I have learned a lot from him, an exemplary teacher in class with numerous experiences in the industry, which has motivated me to overcome some difficult periods in research.

Additionally, I would specially like to send my acknowledgement to my family, my friends, and my co-workers, who always have been supported, taken care and given me the possibility to perform my thesis. Especially, I give my honest thanks to my wife and my little daughter Uyen Nhi whose patient love enabled me to complete the doctoral study.

CONTENTS

	Page
Abstract in Thai.....	iv
Abstract in English.....	v
Acknowledgments.....	vi
Contents.....	vii
List of Tables.....	x
List of Figures.....	xi
CHAPTER 1 INTRODUCTION.....	1
1.1 Introduction.....	1
1.2 Statement of Research.....	3
1.3 Purpose of Research Works.....	3
1.4 The Scope of Research Works.....	4
CHAPTER 2 LITERATURE REVIEW.....	5
2.1 Soil Improvement.....	5
2.1.1 Soft Clay.....	5
2.1.2 The Basic Compression Theory to Improve Soft Soil.....	6
2.1.3 The Fundamentals of Consolidation.....	7
2.1.4 The Primary Consolidation (Terzaghi theory).....	9
2.2 Compact Vacuum Consolidation Method.....	10
2.2.1 Introduction on Vacuum Method.....	10
2.2.2 Mechanisms of Vacuum Preloading Method.....	13
2.3 Recent Studies on Vacuum Consolidation Method (CVM).....	16
2.4 The Techniques of Vacuum Preloading Method.....	17
2.5 Degree of Consolidation (DOC).....	18
2.5.1 Calculation of Degree of Consolidation by The Settlement (Terzaghi).....	18
2.5.2 Yoshikuni 's Method (1979).....	21
2.5.3 Hansbo's Method (1981).....	22

2.5.4	Car-rillo Theory to Calculate DOC.....	22
2.5.5	Asaoka (Empirical Method).....	23
2.5.6	Degree of Consolidation Based on Pore Water Pressure.....	24
2.6	Laboratory Test.....	25
2.7	Field Test Results.....	26
2.8	Numerical Method	26
2.8.1	Three-Dimensional Finite-Element Analysis	28
2.8.2	Two-Dimensional Plane Strain Finite-Element Analysis.....	28
2.8.3	One - D Finite-Element Analysis.....	30
CHAPTER 3 RESEARCH METHODOLOGY.....		32
3.1	Introduction.....	32
3.2	Simulation Vacuum Preloading Method by Tri-Axial Apparatus	32
3.3	Tri-axial Apparatus	33
3.4	Prediction of DOC of Vacuum Preloading Method.....	35
3.4.1	Field Monitoring and Instrumentation.....	35
3.4.2	Asaoka Method	37
CHAPTER 4 RESEARCH AND ANALYSIS.....		39
4.1	Finite Element Method of Analysis for Drainage Boundary Condition Analysis.....	39
4.1.1	The Theory of Axisymmetric Consolidation	39
4.1.2	Solution for Axisymmetric Unit Cell under Vacuum Pressure	41
4.2	Solution for Axisymmetric Unit Cell under Vacuum Combine Surcharge Loading.....	46
4.3	Simulation in Laboratory Test	52
4.3.1	Soil Specimen	52
4.3.2	Test Procedure to control the instability of soil specimen under vacuum preloading.....	53
4.3.3	Test Results and Analysis	57
4.4	Summary Conclusions	61

4.5 Case study of Vacuum Consolidation at Nakhorn Sri Thammarat Air port.....	63
4.5.1 Site Description.....	63
4.5.2 Soil Conditions.....	64
4.5.3 Construction and Field Monitoring Work of Vacuum Preloading Method.....	67
4.5.4 Behavior and Performance of Vacuum Consolidation Method.....	70
4.5.5 Summary Conclusions	77
CHAPTER 5 CONCLUSIONS AND DISCUSSIONS	79
5.1 Research Conclusions	79
5.1.1 The Gain of the Research.....	79
5.1.2 The Advantages of Using the Vacuum Preloading Method	80
5.1.3 The Factors Effect on Effectiveness of This Method	81
5.2 Limitations of the Study:	81
REFERENCES	83
BIBLIOGRAPHY	86
APPENDIX	87

LIST OF TABLES

	Page
Table 2.1. Mechanism of consolidation of soil.....	8
Table 2.2: The effective of vacuum-preloading method.....	11
Table 2.3. Equivalent diameter (d_w) of PVD.....	20
Table 2.4. The period method to define the DOC.....	23
Table 3.1. List of functions and frequency of field instrumentation.	36
Table 4.1. The case studies for axisymmetric unit cell.....	43
Table 4.2. The ratio of Time factor.....	46
Table 4.3. The ratio of time factor for $n=20$, Vacuum combine surcharge.....	50
Table 4.4. Kasaoka clay's properties	52
Table 4.5. Parameter in vacuum proceed by tri-axial apparatus ($U=10\%$).....	56
Table 4.6. Parameter analysis in vacuum proceed.....	57
Table 4.7. The data of vacuum procedure simulation to control instability of soil	58
Table 4.8. Summary of field investigations in soft soil.....	64
Table 4.9. Summary Index and Engineering Properties of soil at depth 0.00-4.00m..	65
Table 4.10. The lists and nos of field instrumentation works.....	69
Table 4.11. The stage of embankment filling period and vacuum operation	76
Table 4.12. Degree of consolidation and rate of settlement	76

LIST OF FIGURES

	Page
Figure 1.1. Layout of the Chevron Air Terminal.....	1
Figure 1.2. Layout of the project	2
Figure 2.1. The Sharp of settlement of soil clay	6
Figure 2.2. Principal of consolidation.....	7
Figure 2.3. One-dimensional settlement calculation (a) is for Eq. 2.5);.....	10
Figure 2.4. Air water separation vacuum pump system (et al. 2004)	12
Figure 2.5. The lateral movement of soil due to by vacuum preloading	13
Figure 2.6. The mechanisms vacuum preloading method	14
Figure 2.7. The consolidation process	15
Figure 2.8. The stress path ($p' \sim q$).....	15
Figure 2.9. Vacuum system (after Masse et al., 2001)	17
Figure 2.10. Arrangement method of drain board	19
Figure 2.11. Pore water pressure distributions under vacuum preloading.....	25
Figure 2.12. PVDs configuration	27
Figure 3.1. Scheme Tri-axial apparatus	34
Figure 3.2. The modeling of axisymmetric cell in FEM.....	35
Figure 3.3. Arrangement of instrumentations	36
Figure 3.4. Schematic illustration of Asaoka's method.....	37
Figure 4.1. The boundary condition of axisymmetric cell.....	42
Figure 4.2. Case n=10, vacuum only; $V_a=50$ kPa	44
Figure 4.3. Case n=20, Vacuum only; $V_a=50$ kPa	44
Figure 4.4. Case n=10, Vacuum only; $V_a=100$ kPa	45
Figure 4.5. Case n=20, Vacuum only; $V_a=100$ kPa	45
Figure 4.6. Ratio of Time factor $\sim U(\%)$ for Vacuum stage only.....	46
Figure 4.7. Vacuum combine surcharge preloading	47
Figure 4.8. Case n=20, Vacuum - Surcharge;.....	48
Figure 4.9. Case n=20, Vacuum - Surcharge;.....	48

Figure 4.10. Case n=20, Vacuum - Surcharge; $V_a=50\text{kPa}$, $U=100\%$	49
Figure 4.11. Ratio of Time factor $\sim U(\%)$ for Vacuum - Surcharge preloading	49
Figure 4.12. Case n=20, Vacuum - Surcharge;	50
Figure 4.13. Case n=20, Vacuum - Surcharge;	51
Figure 4.14. Case n=20, Vacuum - Surcharge;	51
Figure 4.15. Void ratio $\sim \log(p')$ graph	53
Figure 4.16. Predict shear strength by effective stress and earth ratio	53
Figure 4.17. Behavior of soil mass under vacuum and surcharge preloading	54
Figure 4.18. Excess pore water pressure in vacuum condition	55
Figure 4.19. Soil specimen under Vacuum condition	56
Figure 4.20. Case n=20, Vacuum only; $V_a=50\text{ kPa}$, $U=100\%$	58
Figure 4.21. Case n=20, Vacuum - Surcharge; $V_a=50\text{kPa}$, $U=100\%$	59
Figure 4.22. Case n=20, Vacuum - Surcharge; $V_a=50\text{kPa}$, $U=100\%$	59
Figure 4.23. Increasing un-drain shear strength	60
Figure 4.24. Stress path	60
Figure 4.25. Increasing undrained shear strength	61
Figure 4.26. The CVM is applied	63
Figure 4.27. The cross section of the Taxiway	63
Figure 4.28. Soil profile of the project	64
Figure 4.29. Log of boring	66
Figure 4.30. Arrangement of instrumentations	68
Figure 4.31. The schematic of CVM	69
Figure 4.32. The vacuum preloading stages	70
Figure 4.33. The final settlement-Zone GI-1 by Asaoka's method	71
Figure 4.34. The settlement at zone GI-1	72
Figure 4.35. Field monitoring Zone 1&2	72
Figure 4.36. Pore water pressure from piezometer data	73
Figure 4.37. Problem during surcharge applying in Zone 3,4	73

Figure 4.38. Dissipation of excess pore water pressure.....	74
Figure 4.39. Predict DOC by dissipation of the excess pore water pressure (EPWP).75	
Figure 4.40. The discharge of zone GI-1 & GI-2	75
Figure 4.41. The real excess pore water pressure	77

CHAPTER I

INTRODUCTION

1.1 Introduction

The vacuum preloading consolidation method furthermore has become the popular effective method to improve soft soil introduced by Kjellman in early 1952 and enhanced in recent years with the merging of new materials and technologies. The prediction behavior of improved soft soil should be concerned significantly not only in the laboratory but also at the field to predict and avoid the instability of embankment during performance of vacuum consolidation.

The new method is proposed using tri-axial apparatus to simulate the comprehensive behavior of soft soil improved by vacuum preloading method in the laboratory, to support the engineering task quickly, and to make this method become familiar in the future. Stability of embankment during vacuum preloading consolidation should be concerned to ensure that the project can be performed well and safety. A case study of vacuum consolidation at Nakhorn Sri Thammarat Airport is proposed.

The project is at serving airport in Nakhorn Sri Thammarat, a town in the south of Thailand. It is located in Muang District, about 14 km from city. Capacity of passenger building arrival is 300 people and departure 300 people per hour. The Chevron Co,Ltd planned to settle their hub. The transportation to the oil platform from the sea is required and should be located together with the airport. The separated airport terminal is fixed about 0.5 km away from the existing way. The taxiway links from the new terminal to the existing runway as shown in Figure 1.1.

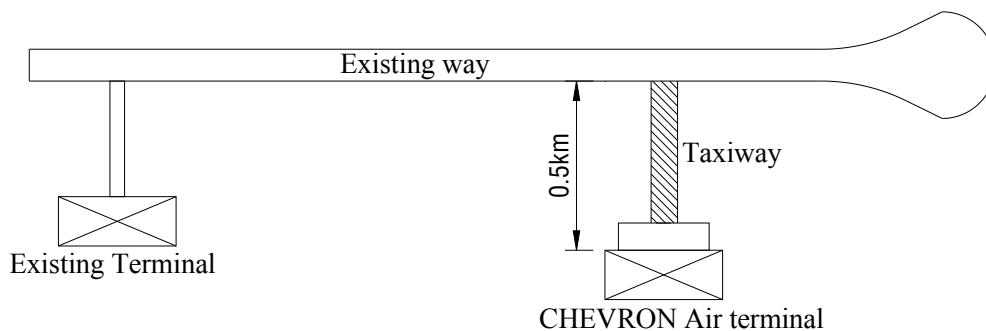


Figure 1.1. Layout of the Chevron Air Terminal

The construction area is located on the low land and marshy area. The high embankment from 4.00m to 4.50 m is designed for Apron and Taxiway construction area approximately 30,000 m².

The layout of the project is shown as the **Figure 1.2**.

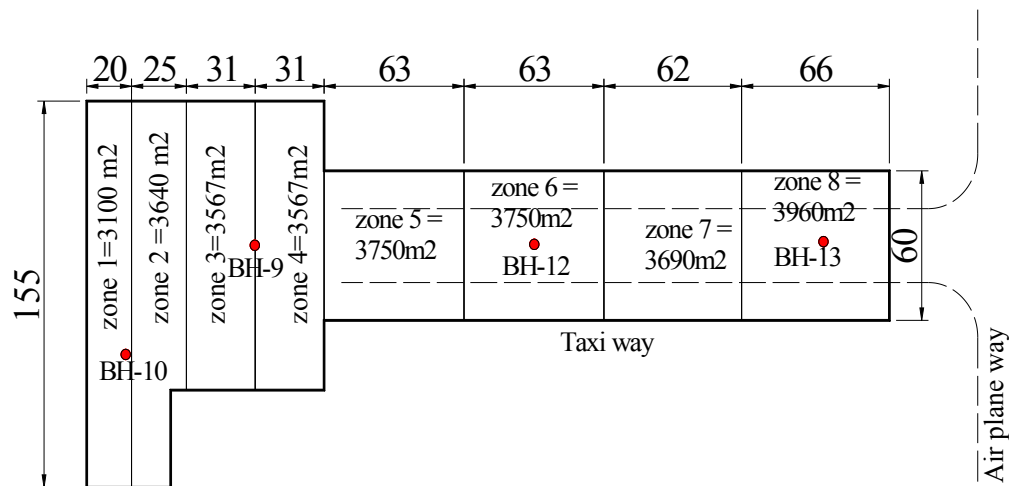


Figure 1.2. Layout of the project

The soil condition consists of 6.0 m thick of very soft dark gray clay in the swamp area, having water content over 100%, with low shear strength from 15.6 to 23kPa with depth. Due to very poor engineering properties of soft to very soft clay, low shear strength and high compressibility, the soil improvement techniques would be become major consideration for this project. In point of views of construction management, geotechnical engineering, and economic issues, vacuum method has been applied to be a method of soft ground treatment works to fulfill the construction's requirements.

The soil improvement by vacuum consolidation method (CVM), which has so many advantages; is selected to improve the very soft clay with required shorten time construction.

The most advantage of CVM is the time of construction of embankment shorter than that of conventional method. The surcharge can be applied immediately without any stability issues; therefore, it can save time and money. However, the technique should be performed gradually and has to research more to make it more perfectly and effectively in soft clay improvement.

1.2 Statement of Research

Vacuum preloading method was used in Survanabhumi Airport by cap drain technique method. The first time; the Vacuum Consolidation technique from Maruyama Co,Ltd has been used in Thailand. Research behaviors of soft clay before and after improvement by vacuum preloading method have to conduct to estimate the effectiveness of this method, applying in the future in Thailand and the lowland areas.

The modeling vacuum method to improve soft soil in the laboratory has been performed by Indaratna 2008 by the large-scale apparatus and follows one-dimensional consolidation theory (Terzaghi). The results obtained from this modeling get somewhat evaluated the behavior of soft soil reinforced by vacuum preloading method in the laboratory. However using the large specimen 45cm x 90cm in diameter and height respectively in the large-scale apparatus, the testing time was more than one month. In addition, the horizontal deformation (ϵ_r) during test time, which is the typical deformation of soft soil improvement by vacuum, and the increasing of undrained shear strength of soil specimen, could not be measured; so far, the controlling surcharge processing during vacuum construction has not been discussed sufficiently.

1.3 Purpose of Research Works

By using Vacuum Consolidation Method (CVM) to improve the soft clay at the taxiway of the Nakhorn Sri Thammarat Airport, the time of construction will be reduced remarkable by increasing of the rate of consolidation. The specific objectives of this research are follows:

- (1) Assessment the behaviors and performance of soil ground during improvement by CVM;
- (2) Assessment the effectiveness of the CVM ;
- (3) Assessment the behavior of ground after completion of CVM and embankment loading;
- (4) Performance the laboratory test to simulate the soil improvement behavior under vacuum preloading;

- (5) Back analysis the performance of CVM with embankment loading compare with field measurement.

1.4 The Scope of Research Works

- (1) Measure the data during soil improvement to control the step of construction of embankment by CVM. To estimate the behavior of this method by analysis the data measured at the site.
- (2) Carry out the test in the laboratory to simulate the behavior of soft clay improvement by Tri-axial apparatus.
- (3) Numerical and back analysis by finite element method (FEM).

CHAPTER II

LITERATURE REVIEW

2.1 Soil Improvement

2.1.1 *Soft Clay*

The design and construction of infrastructure facilities in the soft soil of coastal regions is necessary due to extensive urbanization and industrialization and quite often in many lowland areas.

It is necessary to determine the compressibility, shear strength and permeability characteristics of clays to find practical solutions to the geotechnical problems encountered in soft clay.

Clay is regarded as very soft stage if the unconfined compressive strength ($s_u = q_u/2$) is less than 25kPa and as soft stage with strength is presented in the range of 25 to 50kPa (Terzaghi & Peck 1967). The natural soft clay's permeability is increasingly realized in solving many geotechnical problems.

All soft soil improvement techniques seek to improve the soft soil characteristics that match the desired results of a project, such as an increase in density and shear strength to prevent problems of stability, the reduction on soil compressibility, influencing permeability to reduce and control ground water flow or to increase the rate of consolidation, or to improve soil homogeneity.

It is very important to improve unfavorable ground for the particular requirements that poses a challenge to geotechnical engineers. So many researchers focus on soft soil improvement. At various stages, different methods have been published Kjellman (1952), (Mitchell 1970, 1981, Hansbo (1987), Broms 1979, 1987, Kamon 1991, Kamon & Bergado 1991, Bell 1993, and others). The recent book by Bergado et al. (1996) provides extensive details of the application of many soft soil improvement techniques.

The various techniques are to:

- Reduce the settlement of embankment or structure;
- Improve the shear strength of soil and hence increase the bearing capacity of foundations;

- Increase the safety factor against possible slope failure of embankments and earth dams;
- Reduce the shrinkage and swelling of soil during operation stage.

2.1.2 The Basic Compression Theory to Improve Soft Soil

The stress increase of soil caused by the construction of foundations or other loads compresses the soil layers for improvement. The general shape of the deformation of the specimen against time for a give load increment is shown in **Figure 2.1**.

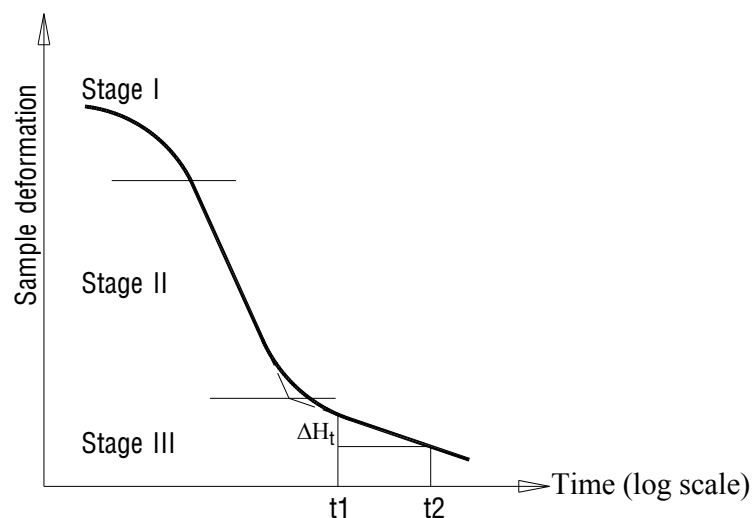


Figure 2.1. The Sharp of settlement of soil clay

From the plot, it can be observed that there are three distinct stages, which may be described as follows:

- **Stage I:** Initial compression (S_i), which is mostly caused by preloading, by the elastic deformation of dry soil and of moist and saturated soils, without any change in the moisture content. Initial compression calculations are generally based on equations derived from the elasticity theory.
- **Stage II:** Primary consolidation (S_c) occurs during the excess pore water pressure, is gradually transferred into effective stress because of the pore water dissipation.
- **Stage III:** Secondary consolidation (S_s) appears after the excess pore water pressure dissipates completely, deformation of the specimen takes

place because of the plastic readjustment of soil fabric. It follows the primary consolidation settlement under a constant effective stress.

The total settlement of ground $S(t)$ at time t can be represented as follow:

$$S_t = S_i + S_c + S_s \quad (2.1)$$

2.1.3 The Fundamentals of Consolidation

When a saturated soil layer is subjected to a stress increase (under loading), the pore water pressure (PWP) immediately increases to gain the loading with soil skeleton. In sand that has high permeability; the drainage caused by the increasing in the pore water pressure is completed immediately. Pore water drainage is accompanied by a reduction in the volume of soil mass, resulting in settlement. Because of rapid drainage of the pore water in sand, elastic settlement and consolidation take place simultaneously. For cohesive soil (clay), which has low hydraulic conductivity, the consolidation settlement is time dependent.

Consider a clay layer of thickness H_c located below the groundwater level and between two highly permeable sand layers as shown in **Figure 2.2**.

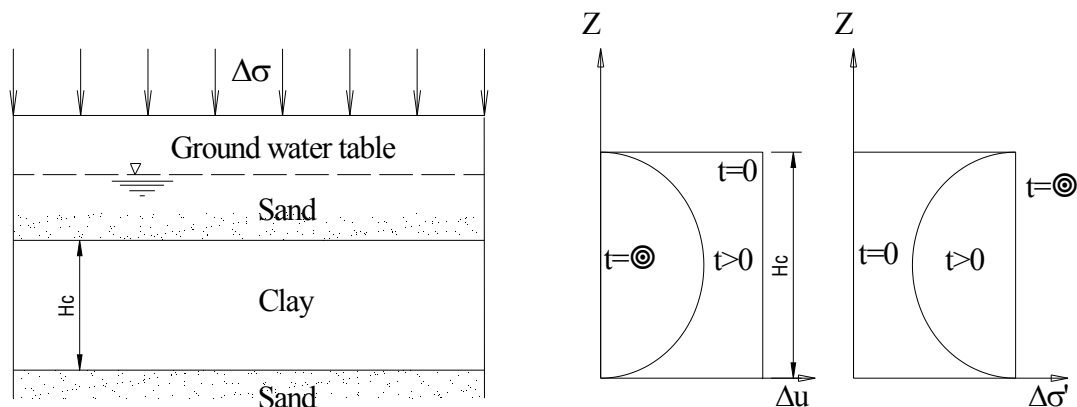


Figure 2.2. Principal of consolidation

If an increasing surcharge of $\Delta\sigma$ is applied at the ground surface over a giant area, the pore water pressure in the clay layer will increase. For a surcharge of *infinite extent*, the immediate increase of the pore water pressure Δu , at all depths of the clay layer will be equal to the increase of the total stress $\Delta\sigma$.

Thus, immediately after the application of the surcharge

$$\Delta u = \Delta \sigma$$

Since the total stress is equal to the sum of the effective stress ($\Delta\sigma'$) and the pore water pressure (Δu), at all depths of the clay layer the increase of effective stress due to the surcharge (immediately after application) will be equal to zero (i.e., $\Delta\sigma' = 0$, where $\Delta\sigma'$ is the increase of effective stress).

In other words, at time $t = 0$, the entire stress increase at all depths of the clay is taken by the pore water pressure and none by the soil skeleton. It must be pointed out that, for loads applied over a limited area, it may not be true that the increase of the pore water pressure is equal to the increase of vertical stress at any depth at time $t = 0$.

After application of the surcharge (i.e., at time $t > 0$), the water in the void spaces of the clay layer will be squeezed out and will flow toward both the highly permeable sand layers, thereby reducing the excess pore water pressure. This, in turn, will increase the effective stress by an equal amount, since $\Delta\sigma' + \Delta u = \Delta\sigma$.

Thus at time $t > 0$,

$$\Delta\sigma' > 0 \quad \text{and} \quad \Delta u < \Delta\sigma$$

Following is a summary of the variation of $\Delta\sigma$, Δu , and $\Delta\sigma'$ at various times. **Figure 2.2** shown the general nature of the distribution of Δu and $\Delta\sigma'$ with depth.

This gradual process of increase in effective stress in the clay layer due to the surcharge will result in a settlement that is time-dependent, and is referred to as the process of consolidation.

Table 2.1. Mechanism of consolidation of soil

Time, t	Total stress increase, $\Delta\sigma$	Excess pore water pressure, Δu	Effective stress increase, $\Delta\sigma'$
0	$\Delta\sigma$	$\Delta\sigma$	0
>0	$\Delta\sigma$	$<\Delta\sigma$	>0
∞	$\Delta\sigma$	0	$\Delta\sigma$

2.1.4 The Primary Consolidation (Terzaghi theory)

The one-dimensional primary consolidation settlement (caused by an additional load) of the clay layer, having a thickness H_c calculates as:

$$S_c = \frac{\Delta e}{1 + e_o} H_c ; \quad (2.2)$$

$$\frac{\Delta e}{1 + e_o} = \varepsilon_v \quad (2.3)$$

Where:

S_c : primary consolidation settlement

Δe : total change of void ratio caused by additional load applied

e_o : initial void ratio of the clay layer before application of the load

ε_v : vertical strain.

For normally consolidated clay, the field e - $\log \sigma'$ curve is be as shown in Figure 2.3a (Das, 2004). If σ'_o is the initial average effective overburden stress on the clay layer and $\Delta \sigma'$ is the average effective increase in pressure on the clay layer caused by the added load, the change in void ratio caused by the load is

$$\Delta e = C_c \log \frac{\sigma'_o + \Delta \sigma'}{\sigma'_o} \quad (2.4)$$

Where:

C_c : the compression index, or can be defined as the slope of the e - $\log \sigma'$ graph as shown in **Figure 2.3a**, combining Eq. (2.2) and Eq. (2.4) yields.

$$S_c = \frac{C_c H_c}{1 + e_o} \log \frac{\sigma'_o + \Delta \sigma'}{\sigma'_o} \quad (2.5)$$

For over-consolidated clay, the field e - $\log \sigma'$ curve is as shown in **Figure 2.3b**. In this case, depending on the value of $\Delta \sigma'$, two condition may arise.

First, if $\sigma'_o + \Delta \sigma' < \sigma'_c$ then

$$\Delta e = C_s \log \frac{\sigma'_o + \Delta \sigma'}{\sigma'_o} \quad (2.6)$$

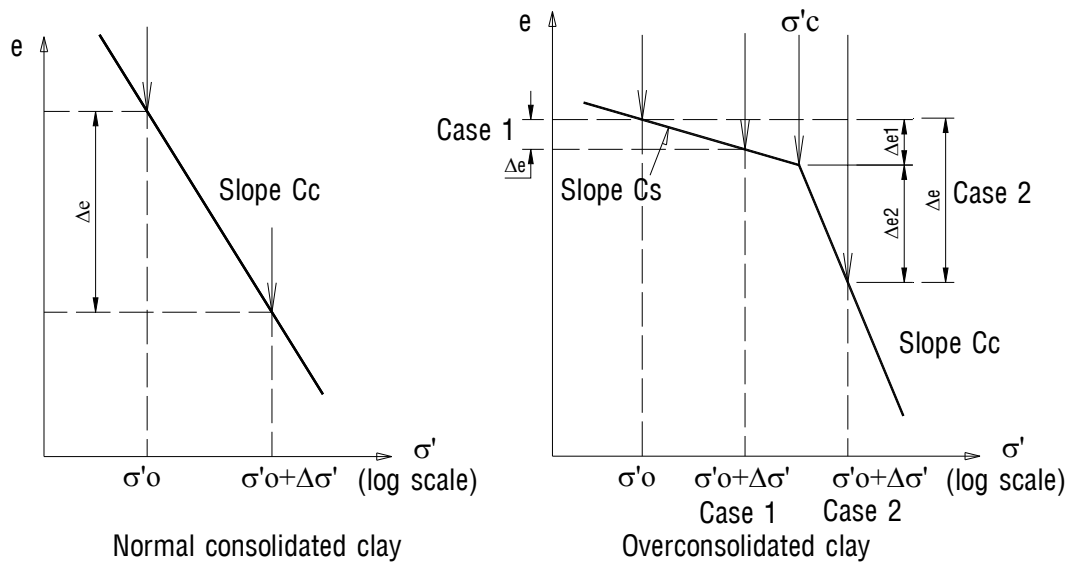


Figure 2.3. One-dimensional settlement calculation (a) is for Eq. 2.5);
(b) is for Eq. (2.7) and (2.9) (after Das, 2004)

Where:

C_s is the swelling index. In most case, the value of the swelling index is 0.20 to 0.25 of the compression index (Das, 2004). Combining Eq. (2.2) and Eq.(2.6) gives

$$S_c = \frac{C_s H_c}{1 + e_0} \log \frac{\sigma'_o + \Delta\sigma'}{\sigma'_o} \quad (2.7)$$

Second, if $\sigma'_c < \sigma'_o + \Delta\sigma'$ then

$$\Delta e = \Delta e_1 + \Delta e_2 = C_s \log \frac{\sigma'_c}{\sigma'_o} + C_c \log \frac{\sigma'_o + \Delta\sigma'}{\sigma'_c} \quad (2.8)$$

Now combine Eq.2.2 and Eq. 2.8 gives

$$S_c = \frac{C_s H_c}{1 + e_0} \log \frac{\sigma'_c}{\sigma'_o} + \frac{C_c H_c}{1 + e_0} \log \frac{\sigma'_o + \Delta\sigma'}{\sigma'_c} \quad (2.9)$$

2.2 Compact Vacuum Consolidation Method

2.2.1 Introduction on Vacuum Method

There are so many methods to treat soft soil; they can be classified in several ways such as mechanical stabilization, hydraulic modification, chemical stabilization and inclusion of confinement materials such as geosynthetics into the soil. Nowadays the vacuum preloading method becomes the most popular method to improve soft soil. A technique using atmospheric pressure as a

temporary loading is principally the compact vacuum consolidation method. It is concerned as an effective method of improving soft soil conditions, which was introduced by Kjellman (1952); this method has been successfully used for soil improvement in a number of countries (Holtz (1975); Chen and Bao (1983); Bergado et al. (1998); Chu et al. (2000); Indraratna et al. (2005)). With the merging of new material and new technologies, this method has been further improved in recent years and was applied several projects in Asian countries, which is shown in the *Table 2.2*

Table 2.2: The effective of vacuum-preloading method

Project	Tanjin New Harbour, China	Northeast New Railway, Japan	Factory in Lianyungang City, China
Soil type	Silty clay	Peat and silt	Marine clay
Water content (%)	55	580-860	69-85
Void ratio	1.4	-	1.62 – 2.36
Natural bulk density (g/cc)	1.73	1.05	1.54-1.61
Initial shear strength (kPa)	16.7-20.6	3.4-5.9	5.7-19.6
Area of involvement (m ²)	1250	1950	4000
Thickness (m)	16	13	10
Degree of vacuum (mm Hg)	600	700	650
Increase in shear strength (kPa)	131-190	186-190	170-440
Increase in bearing capacity (%)	300	200-300	250
Estimated settlement (mm)	811	2040	1000
Measure settlement (mm)	565	1490	700
Reduction in settlement (%)	69.5	73	70

To achieve best results, this method should combine with prefabricated vertical drains (PVDs), which are installed before vacuum pressure applying. The airtight plastic sheet is buried in the surrounding separation walls. Water and air in soft soil can be drawn out from the vertical drains through the system of perforated pipes by a pump (see **Figure 2.4**). With new technique from Maruyama Ltd,Co, the water and air are pumped out by two separately trends, hence the vacuum pressure can be maintained during construction procedure at high pressure and the surcharge can be applied above the airtight sheet immediately. When pore water and air are pumped out of the ground, a

difference in pressure is formed at the separation surface, which induces compression of the clay.

A common vacuum pressure from 60 to 80kPa is usually used in design; however, a higher vacuum pressure of up to 90kPa may be achieved sometimes at the field. When the surcharge loading more than 80kPa is required, a combined vacuum and fill surcharge should be applied for a good result.

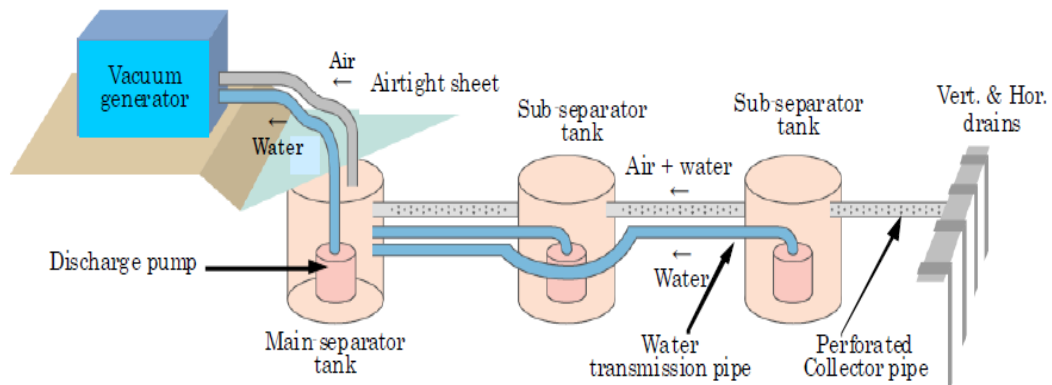


Figure 2.4. Air water separation vacuum pump system (et al. 2004)

For treatment of very soft ground, the time of vacuum preloading method is faster than that of surcharge preloading method, because the 80kPa vacuum pressure can be applied instantly, without causing instability problem. The vacuum preloading method is also cheaper than the surcharge preloading method for an equivalent load (Chu et al. 2000).

Yan and Chu (2003) showed that the cost of soil improvement by vacuum preloading reduces over one-third that by conventional surcharge alone. The effectiveness of this system relies on: (a) reliability (airtight) of membrane, (b) effectiveness of the seal between the ground surface and the membrane edges, and (c) soil conditions and the location of ground water level (Cognon et al., 1994).

The mechanisms of vacuum preloading and conventional and innovative techniques relate to equipment, materials, monitoring, analysis and numerical simulation that are discussed in the followings.

The increase the effective stress tends towards isotropic with the compressive lateral deformations (**Figure 2.5**). Since there no shear failure, preloading can be applied at rapid rate. The method is based on the idea of applying vacuum suction to an isolated soil mass to reduce the atmospheric pressure in it, thus by

the way of reducing the pore water pressure in the soil the effective stress is increased without changing the total stress.

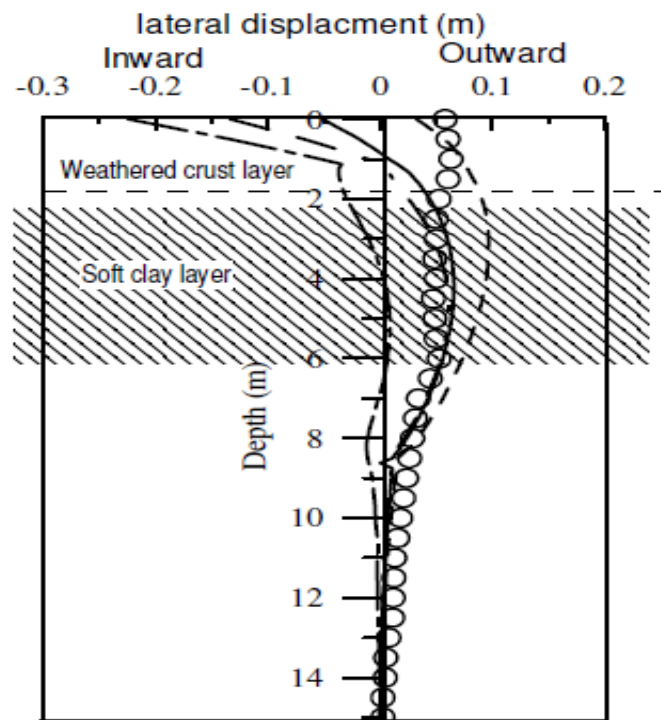


Figure 2.5. The lateral movement of soil due to by vacuum preloading

2.2.2 Mechanisms of Vacuum Preloading Method

The mechanisms vacuum preloading method is shown as the **Figure 2.6** and **Figure 2.7**. In saturated soils, the total stress (σ) at any point within the soil mass is the combination of the effective stress (σ') and the pore water pressure (u) (Terzaghi, 1943).

Thus, the total stress at any point within the soil mass can be written as Eq(2.10):

$$\sigma' = \sigma - (+u_{\Delta p}) \quad (2.10)$$

Under the surcharge loading only, the effective stress is gained by the dissipation of positive excess pore water pressure after the load application. In contrast, the effective stress is increased by the applied negative pore pressure ($-u_{vac}$) under the vacuum condition. Equation (1) can be rewritten based on the vacuum and fill preloading as Eq.(2.11):

$$\sigma' = \sigma - (+u_{\Delta p}) - (-u_{vac}) \quad (2.11)$$

It can be seen that the effective stress increases by negative suction, thereby, reducing the risk of shear failure. The performance of this system depends on the vacuum condition under the airtight membrane (Indraratna et al. 2004). The intensive pore pressure measurement under membrane and inside the PVD with depth should be performed to verify the reliability of the vacuum system.

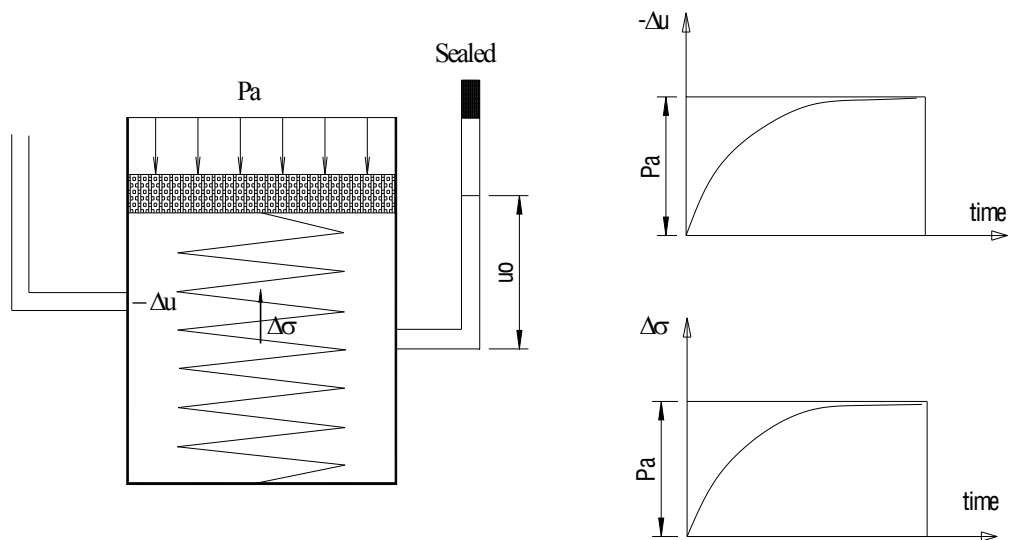


Figure 2.6. The mechanisms vacuum preloading method

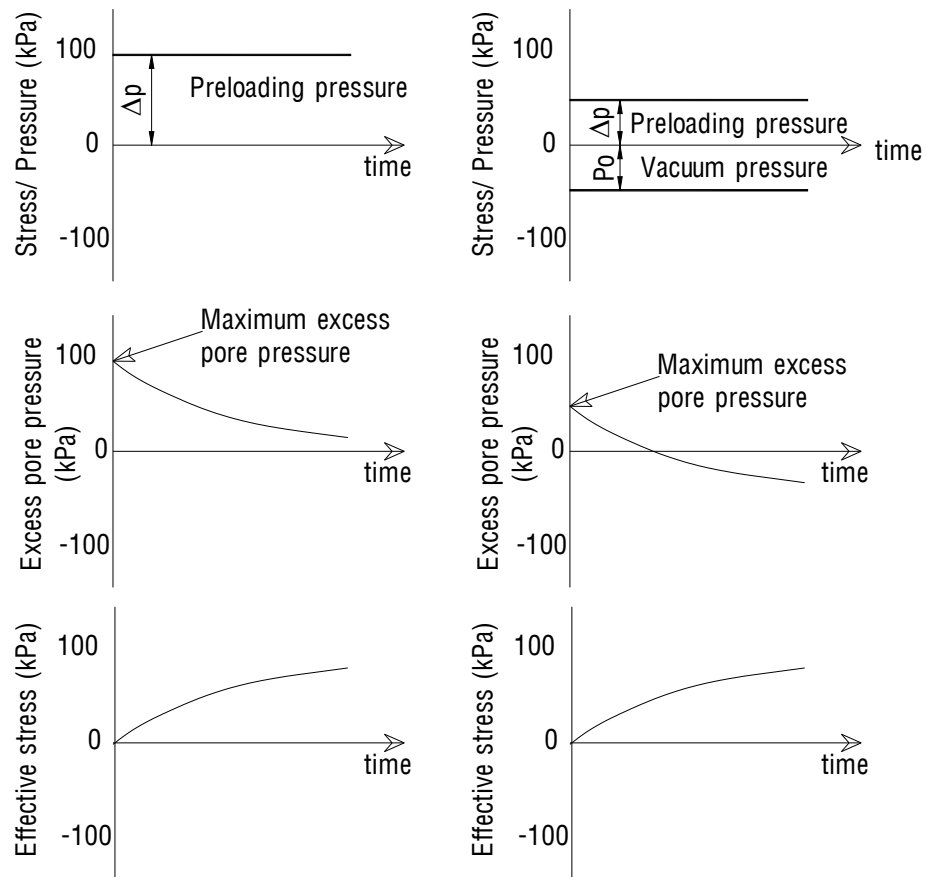
In terms of stress path distributions, the stress state can be described in tri-axial space with mean effective stress p' and the deviator stress q , defined as Eq.(2.12) and Eq.(2.13) respectively:

$$q = \frac{(\sigma'_1 - \sigma'_3)}{2}; \quad (2.12)$$

$$p' = \frac{(\sigma'_1 + \sigma'_3)}{2} \quad (2.13)$$

Where:

σ'_1, σ'_3 : are the principal normal stresses.



(a) Preloading; (b) Combine preloading and vacuum (Indraratna et al. 2004)

Figure 2.7. The consolidation process

In **Figure 2.8** different stress paths are described. Starting from an in situ stress state at point A, the curve ABC describes the case of conventional preloading.

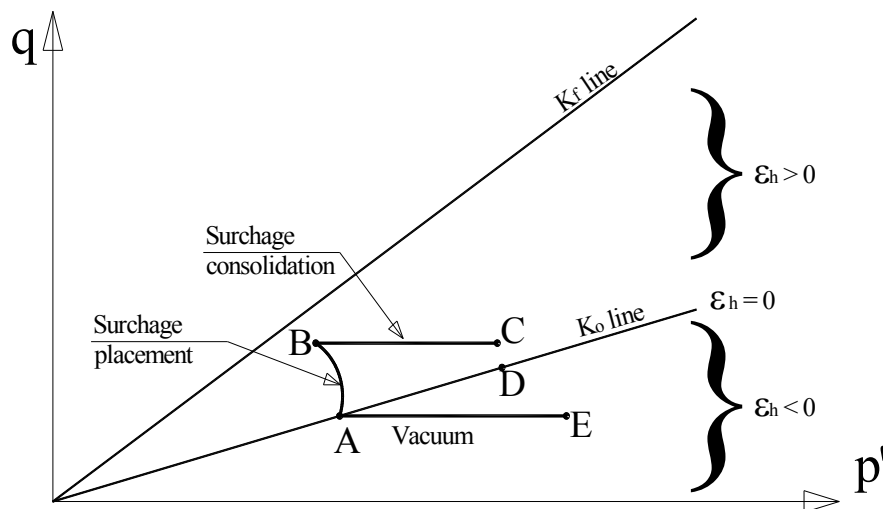


Figure 2.8. The stress path ($p' \sim q$)

When the surcharge is applied, it follows curve AB with a possible failure if point B would cross the failure K_f line. Consolidation will take place from B to C in the area of $\varepsilon_h > 0$ above the K_o -line and hence, outward lateral deformation will occur.

Line AD corresponds to oedometric consolidation. As for vacuum induced preloading, the stress path follows the line AE. This is because during vacuum consolidation, the soil is under isotropic conditions and thus the principal normal stresses are equal. It can be seen that the entire stress path is under the K_o -line with the field of $\varepsilon_h < 0$, and hence, under horizontal compression or inward lateral displacement respectively.

2.3 Recent Studies on Vacuum Consolidation Method (CVM)

Wangthong (2008) studied the ground improvement of soft clay using PVDs with and without vacuum in field and in the laboratory by large scale consolidometer. The specimens were reconstituted with the surcharge of 50kPa until 90% degree of consolidation as predicted by Asaoka (1978) method. The rate of settlement of soil improvement with vacuum pressure is higher than PVD only due to the higher flow rate of water to the PVD channel with vacuum pressure. However, the final settlement of both two methods is the same value. After consolidation, the variation of shear strength in the consolidometer is higher than the shear strength for PVD with vacuum. Water content was measured shown higher percent decrease of water content for PVD with vacuum. However, the settlement rate increased with corresponding increased in the coefficient of horizontal consolidation C_h .

Indraratna (2008) carried out a system of PVDs with surcharge load to accelerate consolidation by shortening the drainage path. The study is proposed based on radial soil permeability and changing of vacuum pressure. The prediction of smear zone and effects of drain unsaturated compared with laboratory data from large-scale radial consolidation tests. In this method, the vacuum creates a suction head that increases the effective stress. The effectiveness of vertical drains on cyclic loading was also performed in laboratory. The research show that vertical drains can dissipate the built up excess pore pressure under repeated loading, and that short drains can be sufficient in certain cases better than driving the drains to install the entire

depth of soft clay deposits. The effects of soil disturbance and vacuum pressure can affect soil consolidation considerably, which means that these aspects need to be modeled correctly in any numerical approaches.

For estimating of the behavior of soil clay improved by vacuum preloading the laboratory test on the large – scale radial drainage consolidometer has been carried out by Indraratna (2008). However, the specimen with the size 45 cm in diameter and 90 cm high could not be feasible to obtain undisturbed sample of this size, and the clay mixed with water for several days to be ensure saturation before making the samples.

2.4 The Techniques of Vacuum Preloading Method

The common vacuum system is shown as **Figure 2.9**. For the vacuum preloading technique, the PVDs and the horizontal pipes are used for the distribution of vacuum pressure and dissipation of pore water.

The horizontal pipes and the top ends of PVDs are buried in a sand blanket made of coarse sand, which transmits the vacuum to PVDs. Corrugated flexible pipes (50 to 100 mm in diameter) are normally used as horizontal pipes. These pipes are perforated and wrapped with a permeable fabric textile to act as a filter to prevent sand get in to the pipes. The horizontal pipes are connected to the main vacuum distribution pipes.

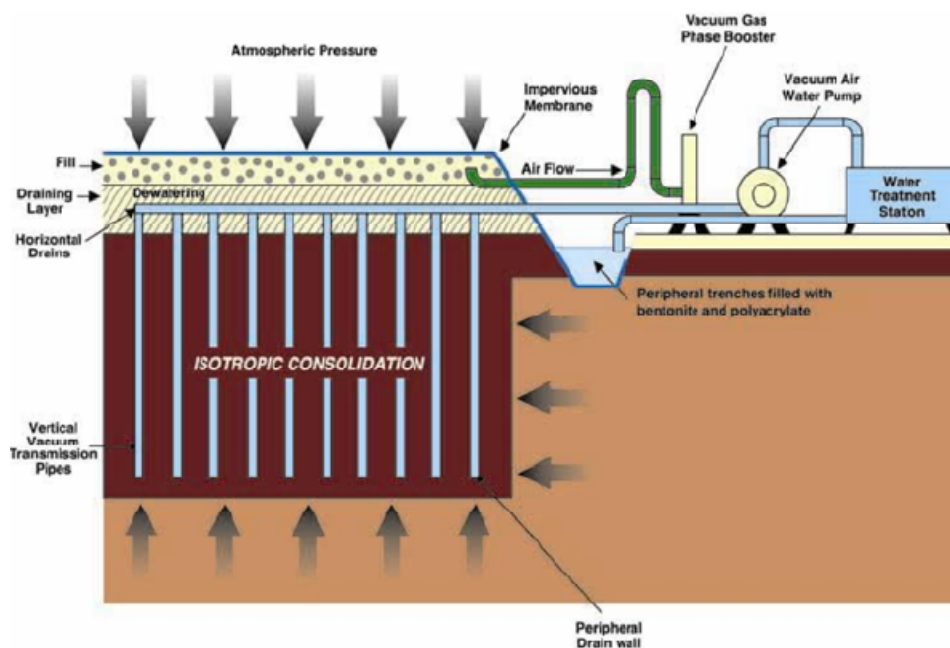


Figure 2.9. Vacuum system (after Masse et al., 2001)

Three layers of thin membranes are often required to seal the area which improved by vacuum. The membranes are buried into a trench at the four boundaries of the area. For this reason the entire soil improvement area often, need to be subdivided into small areas to facilitate the installation of the membranes and capacity of vacuum unit. Then Vacuum pressure is applied continuously for during of preloading stage.

2.5 Degree of Consolidation (DOC)

The degree of consolidation (DOC) is usually used as one of the criteria for assessing the effectiveness of soft soil improvement. It is also used as a design specification in a soil improvement contract. DOC is normally calculated using settlement data, as the ratio of current settlement to ultimate settlement. However, for a soil improvement project, the ultimate settlement (final settlement) is unknown and has to be predicted and several methods are available for estimating the ultimate settlement. On the other hand, the pore water pressure monitored during construction stage is also used to assess the degree of consolidation.

2.5.1 Calculation of Degree of Consolidation by The Settlement (Terzaghi).

The rate of consolidation is defined as the rate of dissipation of the excess pore water pressure in the soil after loading applying. It is important in order to estimate the degree of consolidation, U . The consolidation settlement at an arbitrary time, S_{ult} , is given as

$$S_{ult} = U \cdot S_t \quad (2.14)$$

Where

S_{ult} : the final settlement at end of consolidation (ultimate settlement)

S_c : the settlement at time (t)

Follow Terzaghi, If the applied load is constant, the percentage of primary consolidation U is related to a dimensionless time factor T_v as follows Eq.(2.15):

$$U = 1 - \sum_{m=0}^{\infty} \frac{2}{M^2} \exp(-M^2 T_v); \quad T_v = \frac{C_v t}{H_d^2} \quad (2.15)$$

Where $M = \frac{\pi}{2}(2m + 1)$

Therefore $U = 2\sqrt{\frac{T_v}{\pi}}$ when $U < 0.52$ (52%, $T_v = 0.213$)

And $U = 1 - \frac{8}{\pi^2} \exp(-\frac{\pi^2}{4} T_v)$ when $U > 0.52$

where:

C_v : coefficient of consolidation for vertical drainage,

$$C_v = \frac{k_v}{m_v \gamma_w} \quad (\text{m}^2/\text{sec})$$

k_v : coefficient of vertical permeability, (m/s)

m_v : coefficient of volume change = $\Delta e / \Delta \sigma_v$

γ_w : unit weight of water (kN/m^3)

t : time (year)

H_d : height of drainage path, where $H_d = H/2$ for double drainage because pore water pressure can move downward and upward to escape. $H_d = H$ for single drainage case. (m)

2.5.1.1 Effective diameter of drain (d_e)

When installing drain board, triangle arrangement (Barron, 1948) which is highly economic and square arrangement (Kjellman, 1948) which is easy to apply in practice are used generally. Arrangement method of drain board is shown in **Figure 2.10**

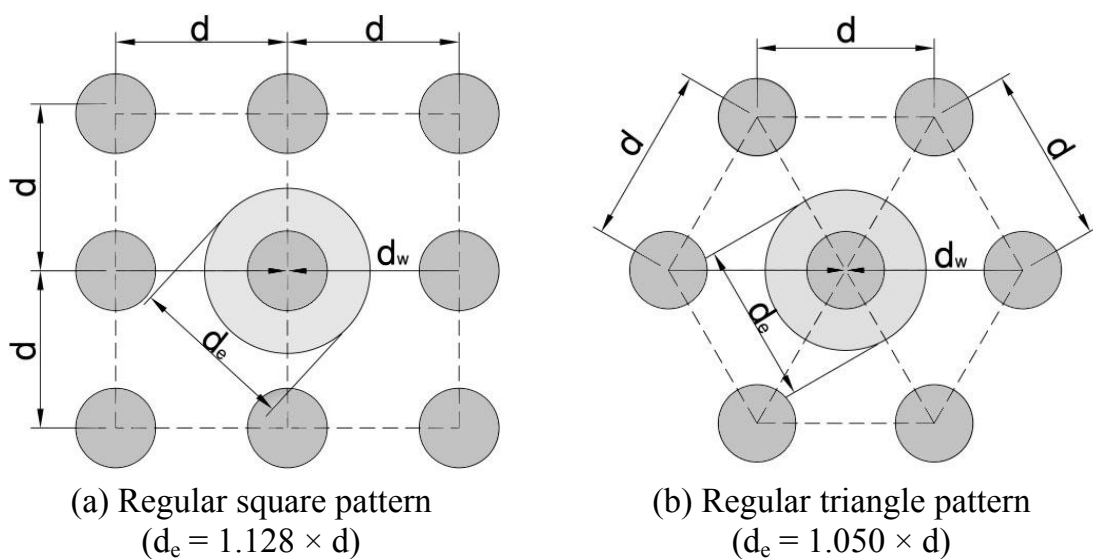


Figure 2.10. Arrangement method of drain board

In analysis regarding the ground where drain board installed, it is calculated after conversion to effective diameter of drain (d_e) due to the complexity in calculation

2.5.1.2 Equivalent diameter of PVD

Since the cross-section of PVD has a shape of plate, it is hard to apply to drainage theory. Therefore, based on equal surface concept, equivalent diameter is calculated, which shown in *Table 2.3*

Table 2.3. Equivalent diameter (d_w) of PVD

Researchers	Proposed d_w	Application
Hansbo(1979)	$d_w = \frac{2(a+b)}{\pi}$	In general, the equivalent diameter is calculated to 5.9~6.6cm, considering safety 5cm is applied
Jansen and den Hoedt(1983)	$d_w = \frac{(a+b)}{2}$	
Fellenius and Castonguay(1985)	$d_w = (1.5\sim 3.0)x \frac{2(a+b)}{\pi}$	
Suits et al.(1986)	38 ~ 64 mm	
Rixner et al.(1986),	$d_w = \frac{(a+b)}{\pi}$	
Hansbo(1983)		

2.5.1.3 Concept for application of C_h

a) Smear effects

- The sub-soils are disturbed during installation of vertical drain depending on the soil's sensitivity and macro fabric. This is so-called "Smear effects"
- The effects of soil disturbance (smear effects) have to be applied in the analysis by assuming an annulus of smear zone of clay layer around the drain.
- Within this annulus of diameter (smear zone), the remolded and disturbed soils has a coefficient of permeability which is lower than the coefficient of permeability for horizontal direction of the undisturbed clay

b) Diameter of smear zone

$$d_s \cong 2.0d_m (d_s / d_m \cong 2.0) \quad \text{Bergado et.al (1991)}$$

Where:

d_s : Diameter of smear zone

d_m : Conversion diameter of mandrel

c) Permeability of smear zone

$$k_s \cong 1.0k_v (k_s / k_v \cong 1.0) \quad \text{Hansbo(1987), Bergado et.al (1991)}$$

Where:

k_s : Permeability of smear zone

k_v : Permeability of vertical direction for clay

d) Coefficient of consolidation of horizontal direction

$$C_h \cong 1.5C_v (C_h / C_v \cong 1.5)$$

$$C_h / C_v \cong k_h / k_v \quad \text{Bergado et.al (1991)}$$

$$k_h / k_v = k_h / k_s = 1.5$$

Where:

k_h : Permeability of horizontal direction for clay

k_s : Permeability of smear zone

k_v : Permeability of vertical direction for clay

C_h : Coefficient of consolidation of horizontal direction

C_v : Coefficient of consolidation of vertical direction

2.5.2 Yoshikuni 's Method (1979)

Since Yoshikuni's equation is derived from without smear effects, the analysis of degree of consolidation in case of considering the smear effects has to be carried out based on that the coefficient of consolidation of horizontal direction (C_h) is equal to that of vertical direction (C_v). Because the permeability of smear zone (k_s) is equal to that of vertical direction (k_v) for undisturbed clay layer, the degree of consolidation is defined as the Eq. (2.16).

$$U_h = 1 - \exp\left(\frac{-8T_h}{F(n) + 0.8L}\right) \quad (2.16)$$

Where:
$$F(n) = \frac{n^2}{n^2 - 1} \log n - \frac{3n^2 - 1}{4n^2}; \quad L = \frac{32}{\pi^2} \times \frac{k_c}{k_w} \times \left(\frac{H}{d_w}\right)^2$$

T_h : Time factor

n : Ratio of spacing ; $n = d_e/d_w$

d_e : Effective diameter of drain (m)

d_w : Conversion diameter of drain material (m)

k_w : Permeability of vertical drain (*cm/sec*)

k_c : Permeability of clay (*cm/sec*)

H_d : height of drainage path, where $H_d = H/2$ for double drainage because pore water pressure can move downward and upward to escape. $H_d = H$ for single drainage case. (*m*)

2.5.3 Hansbo's Method (1981)

Hansbo's equation is derived from with smear effects, following conditions of parameters has to be applied.

- Coefficient of consolidation of horizontal direction is 1.5 times larger than that of vertical direction ($C_h/C_v = 1.5$)
- Therefore, permeability of horizontal direction is 1.5 times larger than that of smear zone ($k_h/k_v = 1.5$)
- Diameter of smear zone is 2.0 times larger than that of mandrel ($d_s/d_m = 2.0$).
DOC defined as the Eq.(2.17).

$$U_{hz} = 1 - \exp\left[-\frac{8T_h}{F}\right] \quad (2.17)$$

Where

$$\begin{aligned} F &= F(n) + F(s) + F(w) \\ &= \left[\ln\left(\frac{d_e}{d_w}\right) - 0.75\right] + \left[\left(\frac{k_h}{k_s} - 1\right) \ln\left(\frac{d_s}{d_w}\right)\right] + \left[\pi z(2H_d - z) \frac{k_h}{q_w}\right] \end{aligned}$$

T_h : Time factor

d_e : Effective diameter of drain (*m*)

d_w : Conversion diameter of drain material(*m*)

k_h : Permeability of horizontal direction for clay (*cm/sec*)

k_s : Permeability of smear zone (*cm/sec*)

z : Depth of soft clay (*m*)

q_w : Discharge Capacity of drain (cm^3/sec)

2.5.4 Car-rillo Theory to Calculate DOC

Car-rillo's theoretical solution (1942) is used to combine the vertical and radial drainage effects to estimate the degree of consolidation as the Eq.(2.18);

$$U_{vr} = 1 - (1 - U_v)(1 - U_r) \quad (2.18)$$

where:

U_v, U_r : the average degree of consolidation due to vertical and radial drainage, respectively.

This equation used to apply in vacuum preloading method which presents three- dimensional consolidation solutions and based upon the assumption that the total stress remain constant, so that the rate of change of excess pore pressure is equal to the rate of change of volume at all points in the soil. The formulas for degree of consolidation are shown in the *Table 2.4*.

Table 2.4. The period method to define the DOC

Proponent	Formula	Apply
Terzaghi	$U = 1 - \sum_{m=0}^{m=\infty} \frac{2}{M^2} \exp(-M^2 T_v)$	- Surcharge only
Yoshikuni (1979)	$U_h = 1 - \exp\left(\frac{-8T_h}{F(n) + 0.8L}\right)$	- Without smear zone - Drain
Hansbo (1981)	$U_h = 1 - \exp\left(\frac{-8T_h}{F}\right)$	- Concern Smear zone - Drain
Car-rillo (1942)	$U_{vr} = 1 - (1 - U_v)(1 - U_r)$	-Horizontal consolidation -Vertical consolidation

2.5.5 Asaoka (Empirical Method)

The method of Asaoka (1978) for prediction of settlement magnitude and Hansbo (1979) for prediction of settlement rate will be combined together to analyze the field observation data of CVM. The measured settlements will be then compared with the predictions. The comparison of settlement behavior CVM is plotted with time.

It is also often used as a design specification (Chu and Yan, 2005). The degree of consolidation is normally calculated as the ratio of the current settlement to the ultimate settlement. However, for a soil improvement project, the ultimate settlement is unknown and has to be predicted.

2.5.6 Degree of Consolidation Based on Pore Water Pressure

Once the pore water pressures at different depths are measured during preloading, the initial and final pore water pressure distributions with depth can be plotted (Chu et al. 2000). For generality, a combined fill surcharge and vacuum load case is considered. The typical pore water pressure distribution profiles for a combined loading case are shown schematically in Figure 2.10. Using this profile, the average DOC, U_{avg} , can be calculated as Eq.(2.21)

$$U_{avg} = 1 - \frac{\int [u_t(z) - u_s(z)] dz}{\int [u_0(z) - u_s(z)] dz} \quad (2.21)$$

Where

$$u_s(z) = \gamma_w z - s \text{ (kPa)}$$

$u_0(z)$: initial pore water pressure at depth z ;

$u_t(z)$: pore water pressure at depth z at time t ;

$u_s(z)$: suction line, z =depth;

γ_w : unit weight of water;

s : suction applied,

The integral in the numerator in Eq. (2.21) is the area between the curve $u_t(z)$ and the suction line $u_s(z)$, and the integral in the denominator the area between the curve $u_0(z)$ and the suction line $u_s(z)$.

The method shown in Eq. (2.21) has the following advantages over the method using settlement data:

- The DOC calculated using Eq.(2.21) relies only on field pore water pressure data, whereas when calculating the DOC using settlement data, the ultimate settlement has to be predicted;
- Not only the final DOC, but also the DOC at any time can be calculated using Eq.(1), as $u_t(z)$ represents the pore water pressure at any time, t ;
- And for consolidation involving multiple layers, Eq. (2.21) can be applied to any single layer to calculate the DOC achieved in a particular layer. In this case, the upper and lower limits of the integrals in Eq. (2.21) are set to be the top and bottom of that soil layer. However, it is

not easy to calculate the DOC for each layer for multilayer soils using settlement, as the settlement of each layer may not be monitored directly and the ultimate settlement of each layer has to be predicted, too.

The schematic illustration of pore water pressure distributions versus depth under vacuum preloading is shown as in **Figure 2.11**.

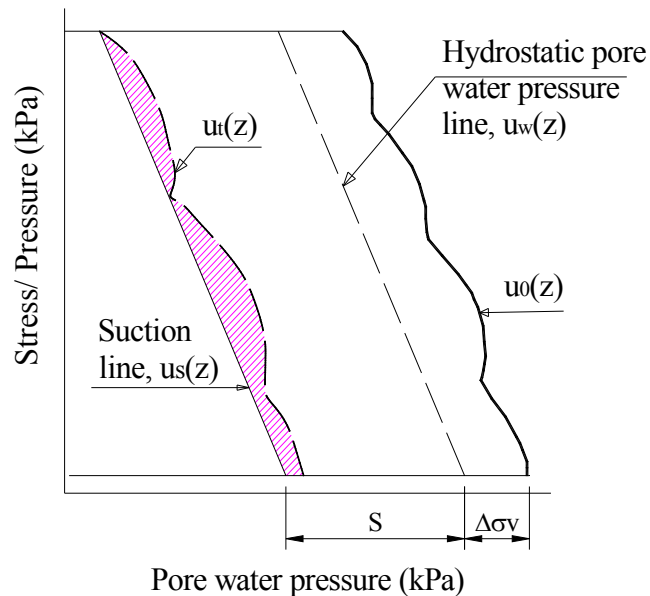


Figure 2.11. Pore water pressure distributions under vacuum preloading

2.6 Laboratory Test

The Tri-axial Shear Test is one of the most reliable methods available for determining the shear strength parameters. It is widely used for both research and conventional testing. The test is considered for the following reason:

- It provides information on the stress-strain behavior of the soil that the direct shear test does not.
- It provides more uniform stress conditions than the direct shear test does with its stress concentration along the failure plane.
- It provides more flexibility in term of loading path.

Three standard types of tri-axial test are generally conducted:

- Consolidation – Drained test or drained test (CD test)
- Consolidation – Undrained test (CU test)
- Unconsolidation – Undrained test (UU test)

In this researching the CU test will be used to estimate the behavior of soft soil before improvement as well after improvement. To model the soil improvement in the lab, the proceeding of vacuum improvement by tri-axial apparatus simulated by decrease the backpressure after saturating the specimen. However the PVD cannot install inside the specimen therefore this simulation will be conducted by another manner, which discusses in next chapter.

2.7 Field Test Results

To estimate the behavior of soil improvement, beside some test in the laboratory during improvement we need observe the effective of the method by the instruments. Normally the information need to measure such as:

- The bearing capacity of the ground before and after improvement. These parameters we can measure by CPT and SPT test at the field.
- The deformation of the embankment includes the vertical settlement and lateral deformation.
- The stability of the embankment during improvement. This task can control by inclinometers and observe the deformation of the ground in time.
- Pore water pressure in the soil.
- The discharge of water squeezes out the soil ground.

2.8 Numerical Method

For estimation the behavior of Vacuum Consolidation method by FEM, so many research success in this field. Such as: The three-dimensional (3D) and two dimensional (2D) numerical analysis of a case study of a combined vacuum and surcharge preloading project for a storage yard at Tianjin Port, China, Buddhima Indraratna (2008). At this site, a vacuum pressure of 80kPa and a fill surcharge of 50kPa were applied on top of the 20 m-thick soft soil layer through prefabricated vertical drains PVD to achieve the desired settlements and to avoid embankment instability.

In 3D analysis, the actual shape of PVDs and their installation pattern with the in situ soil parameters were simulated. In contrast, the validity of 2D plane strain analysis using equivalent permeability and transformed unit cell

geometry was examined. In both cases, the vacuum pressure along the drain length was assumed to be constant as substantiated by the field observations. The finite-element code, ABAQUS, using the modified Cam-clay model was used in the numerical analysis.

The predictions of settlement, pore-water pressure, and lateral displacement were compared with the available field data, and an acceptable agreement was achieved for both 2D and 3D numerical analyses.

It is found that both 3D and equivalent 2D analyses give similar consolidation responses at the vertical cross section where the lateral strain along the longitudinal axis is zero. The influence of vacuum may extend more than 10 m from the embankment toe, where the lateral movement should be monitored carefully during the consolidation period to avoid any damage to adjacent structures.

Hird et al. (1995), Chai et al. (1995), and Indraratna et al. (2005) introduced an *equivalent* two-dimensional (2D) plane strain approach to predict the soft clay behavior improved by the vertical drain system (**Fig. 2.12**).

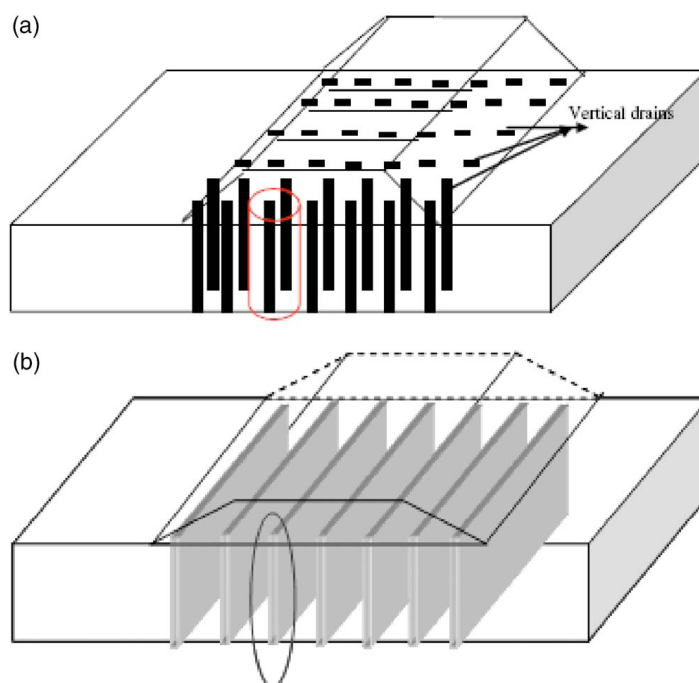


Figure 2.12. PVDs configuration
(a) 3D condition (square pattern); (b) Equivalent plane strain condition

The embankment loading is considered a strip load. This method can be conveniently simulated as a multi-drain system in numerical finite-element modeling. Discrepancies between 2D predictions and observations, especially in terms of excess pore pressure and lateral displacements, are often noted (Cheung et al. 1991).

Since the last decade, improved and user-friendly three-dimensional (3D) finite element codes have emerged as a powerful tool capable of capturing ground response details that cannot be analyzed using traditional 2D (plane strain) finite-element software (Small and Zhang 1991).

2.8.1 Three-Dimensional Finite-Element Analysis

For 3D analysis, a single row of drains with influence zones has been considered, however a smear zone could not be concerned (Cheung et al. 1991; Borges 2004). This study demonstrates that a 3D analysis should be considered for embankments where the 2D plane strain condition may not be appropriate due to the nature of embankment geometry among the other reasons

2.8.2 Two-Dimensional Plane Strain Finite-Element Analysis

To focus on the radial consolidation problem using a plane strain finite-element analysis, the appropriate equivalence between the plane strain and true axisymmetric analysis has to be conducted to obtain realistic predictions. Various conversion procedures have been proposed earlier (e.g., Shinsha et al. 1982; Hird et al. 1992; Bergado and Long 1994; Chai et al. 2001; Indraratna et al. 2005). Cheung et al. (1991) employed the conversion procedure, which assumes that the settlement response at 50% degree of consolidation is the same for both 2D and axisymmetric (3D) conditions (Shinsha 1991).

However, significant differences of the excess pore pressure predictions were found between these two cases. In this study, the conversion method proposed by Indraratna et al. (2005) is adopted for the 2D plane strain analysis. In this approach, not only is the entire degree of consolidation response for the equivalent 2D approach the same as that of the 3D analysis, but also the smear zone was explicitly modeled. Even though this equivalent method may increase the number of elements significantly in the FEM mesh, hence the computational time, the method still provides an acceptable accuracy for multi drain analysis (Indraratna et al. 2004). Indraratna et al. (2005) have further

refined details of the permeability conversion for the equivalent plane strain condition to consider the vacuum consolidation. A summary of the conversion from the axisymmetric to the equivalent plane strain model is presented below, for the benefit of the readers.

To obtain the same consolidation as the axisymmetric condition, the corresponding ratio of the smear zone permeability to the undisturbed zone permeability in plane strain analysis ($k_{s,ps}/k_{h,ps}$) can be obtained by (Indraratna et al. 2005) as shown in Eq.(2.22)

$$\frac{k_{s,ps}}{k_{h,ps}} = \frac{\beta}{\frac{k_{h,ps}}{k_{h,ax}} \left[\ln\left(\frac{n}{s}\right) + \frac{k_{h,ax}}{k_{s,ax}} \ln(s) - \frac{3}{4} \right] - \alpha} \quad (2.22)$$

Where:

$$\beta = \frac{2(s-1)}{n^2(n-1)} \left[n(n-s-1) + \frac{1}{3}(s^2 + s + 1) \right]$$

$$\alpha = \frac{2}{3} \frac{(n-s)^3}{n^2(n-1)}; \quad s = \frac{d_s}{d_w}; \quad n = \frac{d_e}{d_w}$$

where

$k_{s,ax}$ and $k_{h,ax}$: horizontal soil permeability in the smear zone and in the undisturbed zone, respectively,

In the axisymmetric configuration;

d_e : effective diameter of drain;

d_s : diameter of the smear zone;

d_w : equivalent diameter of the drain,

By ignoring both smear and well resistance effects, the simplified ratio of equivalent plane strain to axisymmetric permeability in the undisturbed zone can be attained as Eq.(2.23)

$$\frac{k_{h,ps}}{k_{h,ax}} = \frac{0.67 \frac{(n-1)^2}{n^2}}{\left[\ln(n) - \frac{3}{4} \right]} \quad (2.23)$$

2.8.3 One - D Finite-Element Analysis

Considering that most finite element codes used in practice do not include special drainage element, a simple approximate method for modeling the effect of PVD has been proposed by Chai and Miura (1997). The PVD increases the mass permeability in the vertical direction. Consequently, it is possible to establish a value of the vertical permeability which approximately represents the combined vertical permeability of the natural subsoil and the radial permeability towards the PVD. This equivalent vertical permeability (K_{ve}) is derived based on equal average degree of consolidation together with several assumptions:

The deformation mode of PVD improved subsoil is close to one-dimensional. Thus, one-dimensional consolidation theory can be used to represent the consolidation in the vertical direction and the unit cell theory of Hansbo (1979) for radial consolidation is applicable.

The total degree of consolidation is the combination of vertical and radial consolidation by using the relationship proposed by Scott (1963).

In order to obtain a one-dimensional expression for the equivalent vertical permeability, an approximate equation for consolidation in vertical direction is proposed as follows:

$$U_v = 1 - \exp(-3.54) T_v$$

Where:

T_v : the dimensionless time factor.

$$T_v = \frac{C_v t}{H^2} \quad C_v = \frac{k_{ve}}{m_v \gamma_w} \quad (\text{m}^2/\text{sec})$$

Where:

C_v : vertical consolidation coefficient.

t: time

H: length of vertical drain

m_v : coefficient of volume change $m_v = \Delta e / \Delta \sigma_v$

The equivalent vertical permeability, k_{ve} , can be expressed as:

$$k_{ve} = \left(1 + \frac{2.26.L^2}{F.d_e^2} \cdot \frac{k_h}{k_v} \right) k_v$$

Where

$$F = \ln\left(\frac{d_e}{d_w}\right) + \left(\frac{k_h}{k_s} - 1\right) \ln\left(\frac{d_s}{d_w}\right) - \frac{3}{4} + \frac{\pi 2L^2 k_h}{3q_w}$$

d_e : effective diameter of drain;

d_s : the equivalent diameter of the disturbed zone;

d_w : the equivalent diameter of PVD;

k_h and k_s : the undisturbed and disturbed horizontal permeability of the surrounding soil, respectively;

q_w : the discharge capacity of PVD.

The effects of smear and well resistance have been incorporated in the derivation of the equivalent vertical permeability.

The horizontal deformation ε_r , which is the typical deformation of soft soil improvement by vacuum, could not be measured. So far, the controlling surcharge processing during vacuum construction has not been discussed sufficiently

CHAPTER III

RESEARCH METHODOLOGY

3.1 Introduction

Nowadays the vacuum preloading consolidation method becomes the popular method to improve soft soil. This method is an effective method of improving soft soil conditions. With the merging of new materials and technologies, this method has been further improved in recent years.

The prediction behavior of improved soft soil by vacuum preloading method should be concerned significantly not only in the laboratory but also at the field to avoid the risks of instability and destruction of the embankment during construction. The efficiency of managing the progress of construction under closely control, besides the measurements in the field will reflect the design predictions. The laboratory tests were carried out in Hokkaido University-Japan and the data at Nakhorn Sri Thammarat Airport project was used to analysis the behavior of soft soil before and after vacuum preloading improvement.

3.2 Simulation Vacuum Preloading Method by Tri-Axial Apparatus

It is very important to control any risk of instability of embankment during vacuum construction, the simulation vacuum preloading method using tri-axial apparatus is proposed to predict the behavior of soft soil improvement in the laboratory, as well as to make this method become familiar and easier in the future. The tri-axial apparatus is used instead of the large-scale one, which has been performed by Bergado (1998) and Indaratna (2008). The tri-axial test on small size specimen can be carried out in one week compared to the large-scale apparatus takes one month for big specimen. In addition, the lateral deformation as well as the shear strength increase with time can determine accurately.

The modeling vacuum method to improve soft soil in the laboratory has been performed by Indaratna (2008) using the large-scale apparatus and follows Terzaghi's one-dimensional consolidation theory. The results obtained from this modeling partially evaluated the behavior of soft soil reinforced by vacuum preloading method in the laboratory. Using the large specimen 45 cm x

90 cm in diameter and height respectively in the large-scale apparatus, the time used for this test was more than one month.

The horizontal deformation ε_r during the tested time, which is the typical deformation of soft soil improvement by vacuum, and also the increasing of shear strength, could not be measured. So far, the controlling surcharge processing during vacuum construction has not been discussed sufficiently.

The new method is proposed using tri-axial apparatus to simulate the comprehensive behavior of soil improvement by vacuum preloading method in the laboratory to support the engineering task quickly. In addition, it is desired to make the method become familiar in the future.

The finite element method (FEM) is used to analyze two cases of drainage condition at the boundary and center of the axisymmetric soil cell.

The study aspects to solve these matters are as follows:

- 1) Simulation the behavior of soft soil improved by vacuum method by tri-axial apparatus under axisymmetric consolidation condition;
- 2) The lateral deformation and vertical settlement are concerned during soil improvement by vacuum preloading method;
- 3) Evaluating the degree of consolidation during soil improvement;
- 4) Combination surcharge and vacuum preloading to estimate the increasing shear strength);

3.3 Tri-axial Apparatus

Tri-axial apparatus can clearly evaluate the failure mechanism as well as the capacity of increasing shear strength of soil in the laboratory. From the tri-axial test, the result parameters are used to predict the behavior of soil in the field during construction.

Under vacuum pressure condition alone, the soil mass at depth is subjected the isotropic stress status ($K=1$). With flexible functions of the tri-axial machine is as shown in **Figure 3.1**, the isotropic condition of the soil mass can generate the same vacuum condition by controlling the lateral earth pressure (K).

During vacuum condition, the surcharge loading can be generating as

axial force by the loading rod at top of the machine. The deformations of soil specimen in vertical and horizontal direction are measured during testing to evaluate the behavior of soil specimen.

The specimen is covered by rubber membrane and placed in the water tank; therefore the friction between circular soil specimen and the cell is eliminated, which is different to the oedometer apparatus.

The steel plates at the ends of specimen are as the impervious layer; only radial drainage is induced during consolidation. The filter paper covers around the boundary of specimen and overlaps the porous discs at the both ends of specimen as the drainage layer. For the large-scale oedometer apparatus, the drainage was established at the center of specimen.

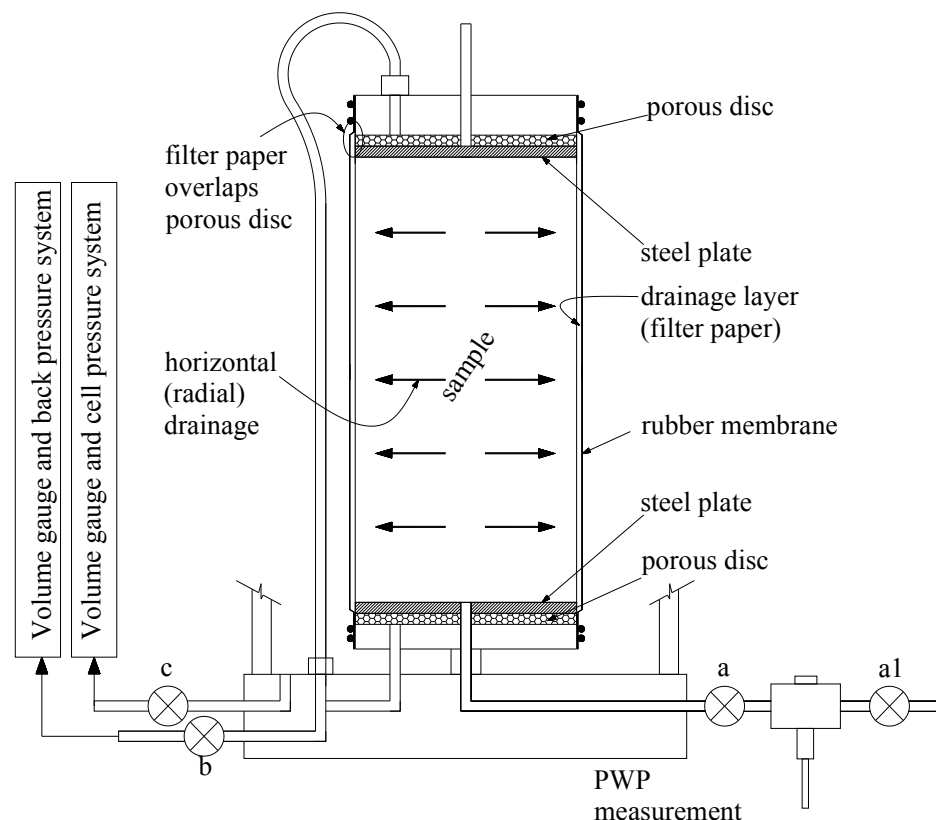


Figure 3.1. Scheme Tri-axial apparatus

The FEM has been used to define the different between the drainage path conditions of specimen, and defines the correction factor for this simulation. The boundary conditions were illustrated in the **Figure 3.2**. The assumptions were used for simulation of vacuum preloading method are as follow:

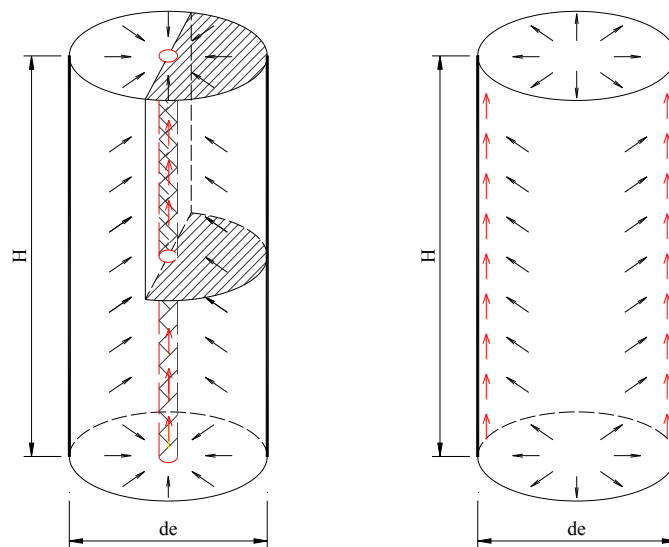
1) Soil mass as subjected vacuum pressure follows axisymmetric consolidation.

2) Under vacuum pressure only, soil mass will be subjected the Isotropic stress state, it mean that the coefficient of horizontal earth pressure (K) equal to one, while for the surcharge only (K) value can calculate from Eq(3.1).

3) For the soil mass, the vacuum pressure is distributed along to the specimen is uniform.

$$K = 1 - \sin \varphi \quad (3.1)$$

Where, φ - the friction angle of soil



a) Drainage at center b) Drainage at outer boundary

Figure 3.2. The modeling of axisymmetric cell in FEM

3.4 Prediction of DOC of Vacuum Preloading Method

3.4.1 Field Monitoring and Instrumentation

The field instrumentations for monitoring of embankment behavior include surface settlement plates, deep settlement gauge, piezometers, and inclinometers. In this project area, the instrumentations include standpipe piezometers, surface settlement plates, and observation wells. The data measured at the site is very important to assessment vacuum consolidation period. There were six types of instruments including surface settlement plates, sub surface settlement gauges, electric type piezometer, inclinometer, and PVC

Automatic Acquisition Unit and water discharge record meters. The types of instrumentation are shown in **Figure 3.3**. List of functions and frequency for different types of instrumentation are shown in *Table 3.1*.

Table 3.1. List of functions and frequency of field instrumentation.

Name of instrument	Item to be measured	Frequency of measurement	
		During construction	After finished of filling works
Surface settlement plate	Vertical settlement	1 time/ day	1 time/ day
Sub Surface settlement gauge	Vertical settlement for subsoil beneath embankment	1 time/ day	1 time/ day
Electric type piezometer	Pore water pressure	Real time records	Real time records
Inclinometer	Vertical and horizontal movement at toe and some distance from toe of embankment	1 time/ day	
Vacuum pressure monitoring box	Vacuum pressure at pump and under vacuum sheets	Real time records	Real time records
Water discharge meter	Rate of water discharge and total volume of water	Real time records	Real time records

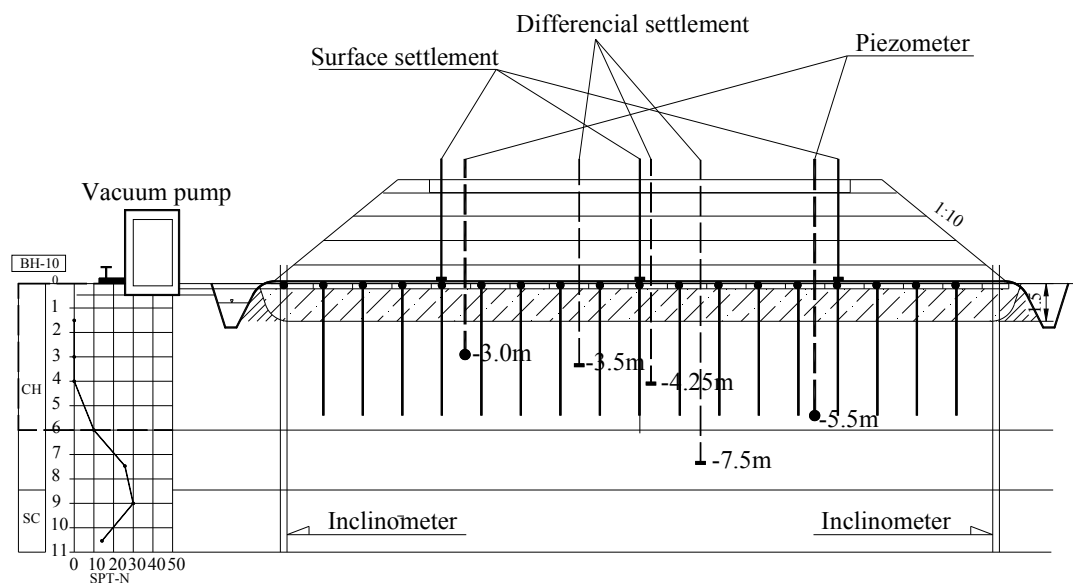


Figure 3.3. Arrangement of instrumentations

3.4.2 Asaoka Method

The Asaoka method (1978) is a method of settlement observation for one-dimensional consolidation in which earlier observations are used to predict the ultimate primary settlement. If necessary, the in situ coefficient of consolidation can also be back calculated after the analysis. The main advantage of this method is its simplicity. In common, settlement analysis conditions such as the initial distribution of the excess pore pressure, the drain length, the final vertical strain of soils, and the coefficient of consolidation are considered to be given in advance of the analysis. It is known that these estimations are quite uncertain. The graphical method can be described as follows (see **Figure 3.4**):

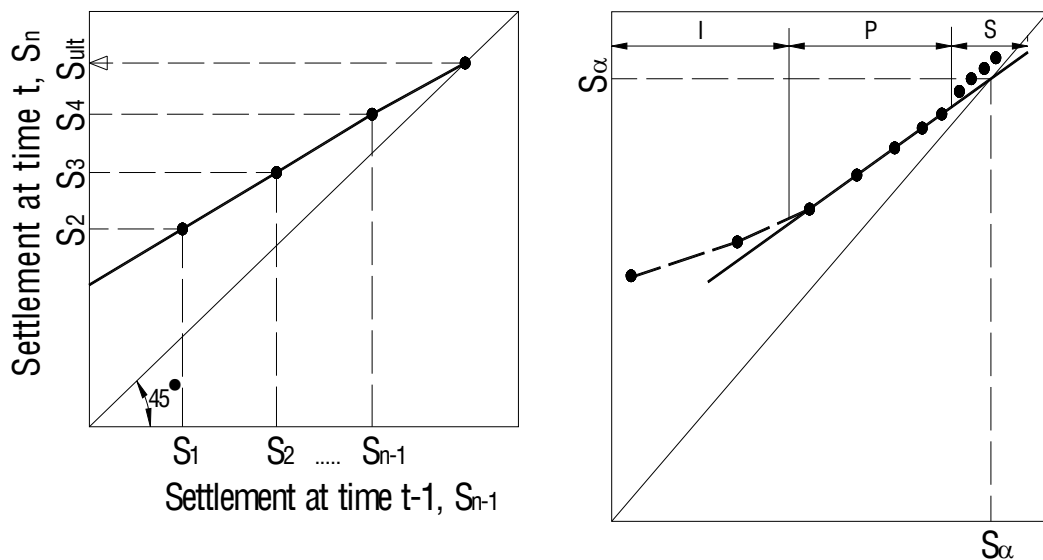


Figure 3.4. Schematic illustration of Asaoka's method

For the Asaoka method neither determination of soil properties nor measuring of the field pore pressure behavior is needed. Asaoka showed that one-dimensional consolidation settlements at certain time intervals could be described as a first order approximation as Eq (3.2):

$$S_n = \beta_0 + \beta_1 \cdot S_{n-1} \quad (3.2)$$

Where S_1, S_2, \dots, S_n are settlements observations. S_n denotes the settlement at time t_n . The time interval $\Delta t = (t_n - t_{n-1})$ is constant. The first order approximation should represent a straight line on a $(S_n \text{ vs } S_{n-1})$ -co-ordinate. The values of β_0 and β_1 are given by the intercept of the fitted straight line with the

S_n - axis and the slope. The ultimate primary settlement can be calculated with the Eq (3.3):

$$S_{ult} = \beta_0 / (1 - \beta_1) \quad (3.3)$$

Which also describes the intercepting point with a 45°-line because S_{ult} is given by $S_n = S_{n-1}$.

- From the time/settlement curve take a series of S_n values.
- From those values plot the points on a (S_n vs S_{n-1}) co-ordinate.
- Find the values β_0 and β_1 and the intercepting point with the 45°-line to determine the ultimate primary settlement

I: Initial stage of compression

P: Primary consolidation with constant C_h or C_v

S: Secondary compression

CHAPTER IV

RESEARCH AND ANALYSIS

4.1 Finite Element Method of Analysis for Drainage Boundary Condition Analysis

4.1.1 *The Theory of Axisymmetric Consolidation*

The unit cell theory representing a single circular drain surrounded by a soil annulus in an axisymmetric condition has been used (e.g. Barron, 1948; Yoshikuni and Nakanodo, 1974; Hansbo, 1981). Most researchers accepted that under embankment loading, the single drain analysis could not provide an accurate prediction due to lateral yield and heave compared to plane strain multi-drain analysis (Indraratna, et al., 1997) although the degree of consolidation (DOC) in this model is acceptable accuracy. In this research, the method is proposed to model the behavior of soft soil improvement by vacuum combine with surcharge preloading method while the lateral displacement is concerned during consolidation.

The following assumptions are based on Hansbo solution (1981) about equal strains (ϵ), the variation of the permeability (k) when void ratio (e) decrease during consolidation and the volume compressibility (m_v).

(1) Soil is homogeneous and fully saturated; the Darcy's law is adopted. Depend on the purposes the outer boundary of unit cell the drainage path is occurred.

(2) Soil strain is uniform at the boundary of the cell. The small strain theory is valid, therefore Hooke's law should be applied for calculation.

(3) For the soil mass, the vacuum pressure distribution along to the drain boundary is uniform during application.

The accuracy of the FEM numerical has checked by solutions of Barron (1948) and Hansbo (1981). According to Barron (1948), the degree of consolidation U for "equal-strain" consolidation is given in Eq.(4.1).

$$U = 1 - \exp\left(-\frac{8T}{\mu}\right) \quad (4.1)$$

With
$$\mu = \left(\frac{n^2}{n^2 - 1} \right) \ln n - \frac{3n^2 - 1}{4n^2}; \quad n = \frac{d_e}{d_w}$$

Where d_e and d_w are diameters of unit cell and equivalent of vertical drain respectively. Hansbo (1981) introduced a circular smear zone (of diameter d_s) in the solution, which resulted in a modified expression for μ

$$\mu = \ln \left(\frac{n}{m} \right) + \frac{k_{ho}}{k_{hs}} \ln m - \frac{3}{4}; \quad m = \frac{d_s}{d_w}$$

For two dimensional consolidation $U(\%)$ can be expressed in terms of integrals of the excess pore water pressure over the unit cell domain as Madhav et al. 1993.

$$U = 1 - \frac{\int \int_{y \ x} u(x, y, T) dx dy}{\int \int_{y \ x} u_0 dx dy} \quad (4.2)$$

Where

$u(x, y, T)$: excess pore water pressure at any point with x, y dimension at a time factor T , u_0 : the initial excess pore water pressure.

Terzaghi-Rendulic proposed differential equation for two-dimensional consolidation as

$$\frac{\partial u}{\partial T} = d_e^2 \left(\frac{\partial^2 u}{\partial x^2} + \frac{\partial^2 u}{\partial y^2} \right) \quad (4.3)$$

$$T = \frac{C_h t}{d_e^2} \quad (4.4)$$

where

C_h : horizontal coefficient of consolidation

As the strains are small, if E' is Young's modulus for effective stress, ν' is Poisson's ratio for effective stress and the material is isotropic, Hooke's law is

$$\begin{Bmatrix} \delta \varepsilon_r \\ \delta \varepsilon_\theta \\ \delta \varepsilon_z \end{Bmatrix} = \frac{1}{E'} \begin{Bmatrix} 1 & -\nu' & -\nu' \\ -\nu' & 1 & -\nu' \\ -\nu' & -\nu' & 1 \end{Bmatrix} \begin{Bmatrix} \delta \sigma'_r \\ \delta \sigma'_r \\ \delta \sigma'_r \end{Bmatrix} \quad (4.5)$$

where:

$\{r, \theta, z\}$ is the principal axes set

$\{\varepsilon_r, \varepsilon_\theta, \varepsilon_z\}$ are the strain in radial, circumferential and vertical respectively.

The coefficient of consolidation C_h in the horizontal direction for axisymmetric plane strain deformation is showed as:

$$C_h = \frac{(1-\nu')E'}{(1+\nu')(1-2\nu')\gamma_w} \frac{k_h}{m_v\gamma_w} = \frac{k_h}{m_v\gamma_w} \quad (4.6)$$

Where;

k_h : horizontal hydraulic conductivity

γ_w : unit weight of water

Dummy research, for the axisymmetric unit cell the coefficient of volume compressibility (m_v) varies during consolidation; m_v calculates by expression (4.7):

$$m_v = \frac{\Delta\varepsilon_v}{\Delta\sigma'_a} \quad (4.7)$$

where:

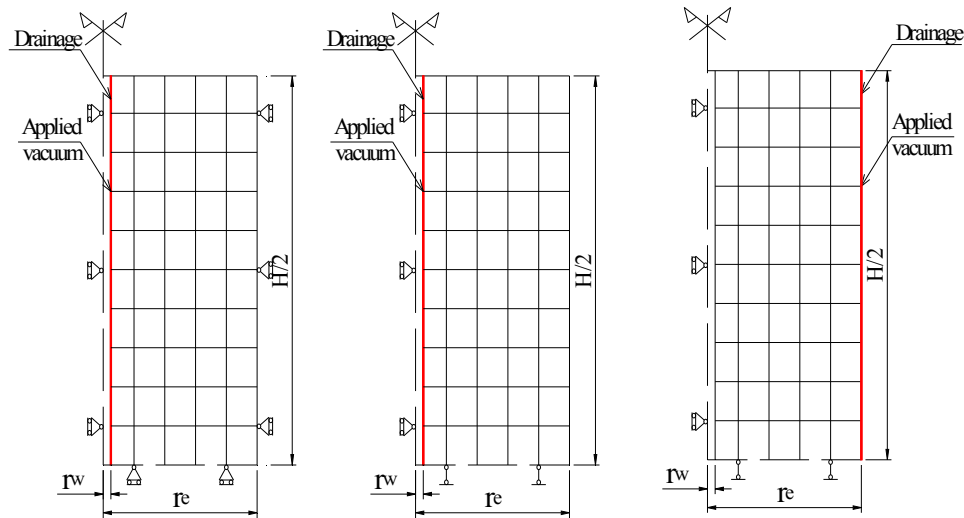
ε_v : volumetric strain of specimen

σ'_a : is the axial effective stress at time reach to degree of consolidation.

4.1.2 Solution for Axisymmetric Unit Cell under Vacuum Pressure

An axisymmetric system of clay unit cell is used to model the behavior of soil specimen improved by vacuum preloading method.

The unit cell with size 7.5cm x 15.0cm in diameter (d_e) and height (H) respectively ($H=2d$), the effective Young's modulus $E'=500$ kN/m², Poisson's ration $\nu'=0.33$, $\lambda = 0.55$, $\kappa =0.06$, the horizontal and vertical hydraulic coefficient $k_h=k_v=4.66E-10$ m/sec and the ratio $n = d_e/d_w$ from 10, 20 are used to analyze. d_w is equivalent diameter of vertical drain as in the **Figure 4.1**. Three cases of axisymmetric unit cells under vacuum preloading only were conducted to verify the relationship about degree of consolidation in the different boundary and drainage condition.



a) Fixed boundary (FC) b) Free boundary (NC) c) Free and drainage at boundary (NB)
Figure 4.1. The boundary condition of axisymmetric cell

The first case, the outer boundary is fixed and drainage occurs at the center (FC) of unit cell. This is the conventional model to estimate the consolidation of axisymmetric unit cell, which has been conducted by several researchers before such as Indraratna (2005), Chai (2006), Tran (2007). One-dimensional consolidation theory is used for this case. As we know that, this case is very suitable for both cases the surcharge loading only and the vacuum zone is infinite. Therefore, this method should not apply well for vacuum preloading.

The second and the third case are proposed to verify the consolidation of axisymmetric unit cell under vacuum preloading in term of the lateral displacement as well as two-dimensional consolidation is concerned, the outer boundary of specimen is free or none (N) combines drainage condition at the center (NC) and the outer boundary of unit cell (NB).

The series of case studies for axisymmetric unit cell were conducted by FEM with Camclay Model, which shown in the **Table 4.1**. The cases from N1 to N12 are to check the accuracy of FEM analysis with vary ratio (n) in 10 and 20 with vacuum pressure applied of 50kPa and 100kPa respectively.

The result presents the relationship between three cases boundary and drainage condition of specimen. (FC), (NC) and (NB). The other cases (case N13 to N16) are to estimate applicable surcharge preloading during vacuum procedure.

Table 4.1. The case studies for axisymmetric unit cell

N0	Case	Boundary condition	Drainage condition	Ratio d_e/d_w	Vacuum Pressure (kPa)	DOC (U%)
N1	FC-1-50	Fixed	Center			
N2	NC-1-50	Free (None)	Center	n=10		
N3	NB-1-50	Free	Boundary		50	100%
N4	FC-2-50	Fixed	Center			
N5	NC-2-50	Free	Center	n=20		
N6	NB-2-50	Free	Boundary			
N7	FC-1-100	Fixed	Center			
N8	NC-1-100	Free	Center	n=10		
N9	NB-1-100	Free	Boundary		100	100%
N10	FC-2-100	Fixed	Center			
N11	NC-2-100	Free	Center	n=20		
N12	NB-2-100	Free	Boundary			
N13	NC-2-50-1	Free	Center			U=70%
N14	NC-2-50-2	Free	Center	n=20	50	U=40%
N15	NB-2-50-1	Free	Boundary			U=70%
N16	NB-2-50-2	Free	Boundary			U=40%

Comparisons were made for the cases of fix and none fix the outer boundary with ratio $n = 10$ and $n = 20$. The results from the FEM were found to compare well with the analytical solutions Baron (1948). The maximum difference in U , for $U > 50\%$, was about 0.26%, occurring at $T = 0.5$ for the case $n = 10$ as shown in **Figure 4.2** and **Figure 4.3**. For the case $n = 20$, the maximum difference in U was 0.17%, occurring at $T = 0.5$ as shown in **Figure 4.4** and **Figure 4.5**. Conclusion the degree of consolidation in both cases fixed boundary (FC) and free boundary (NC) are almost same value and agree with Baron's theory (1948).

For the cases none outer boundary and drainage at the outer boundary (NB), degree of consolidation are almost same in both case $n = 10$ and $n = 20$ as during vacuum preloading. The **Figure 4.6** and **Table 4.2** show the relationship between the modeling of axisymmetric unit cell in free boundary condition, drainage at the center (NC) and at the boundary (NB) during vacuum stage. As the same DOC, the average ratio of time factor for drainage at the center and

outer boundary is T_{hNC}/T_{hNB} about 6.7 and 9.7 for $n=10$, and $n=20$ respectively as showed from case N01 to N12.

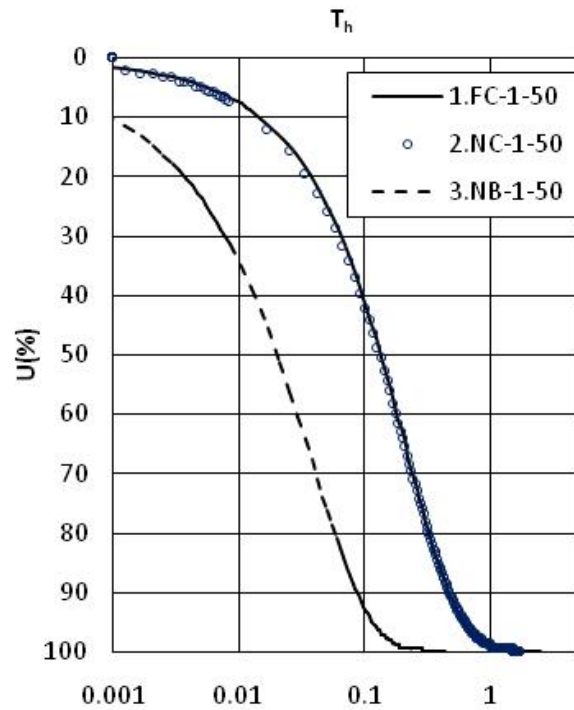


Figure 4.2. Case $n=10$, vacuum only; $V_a=50$ kPa

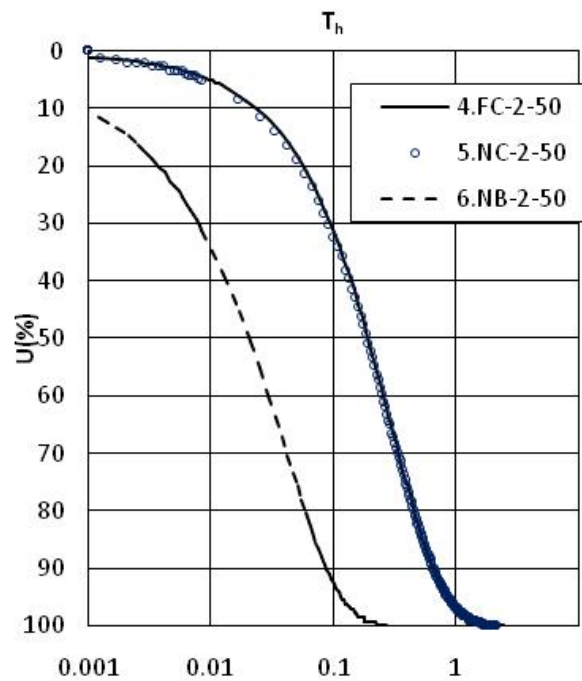


Figure 4.3. Case $n=20$, Vacuum only; $V_a=50$ kPa

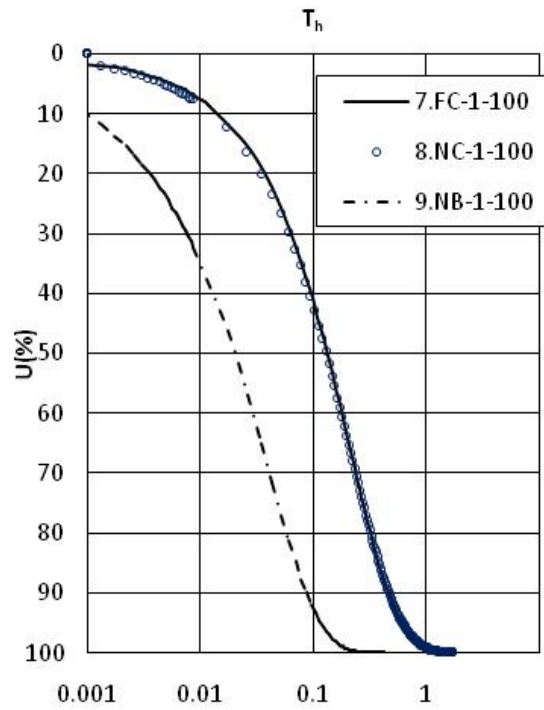


Figure 4.4. Case $n=10$, Vacuum only; $V_a=100\text{kPa}$

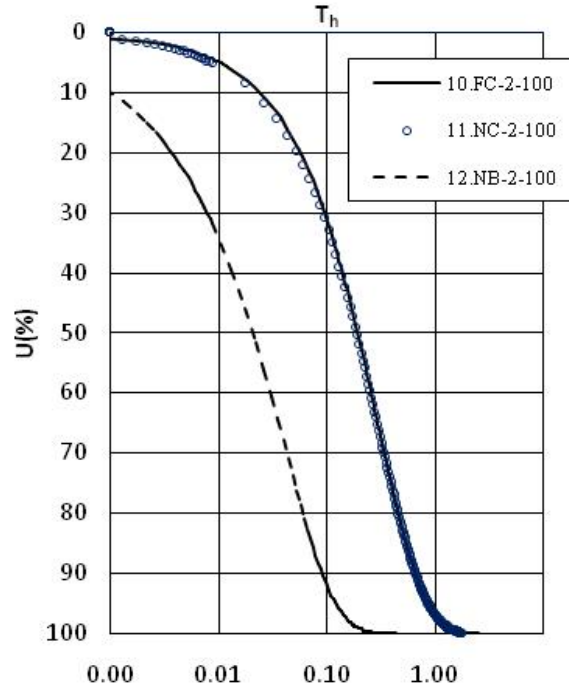


Figure 4.5. Case $n=20$, Vacuum only; $V_a=100\text{kPa}$

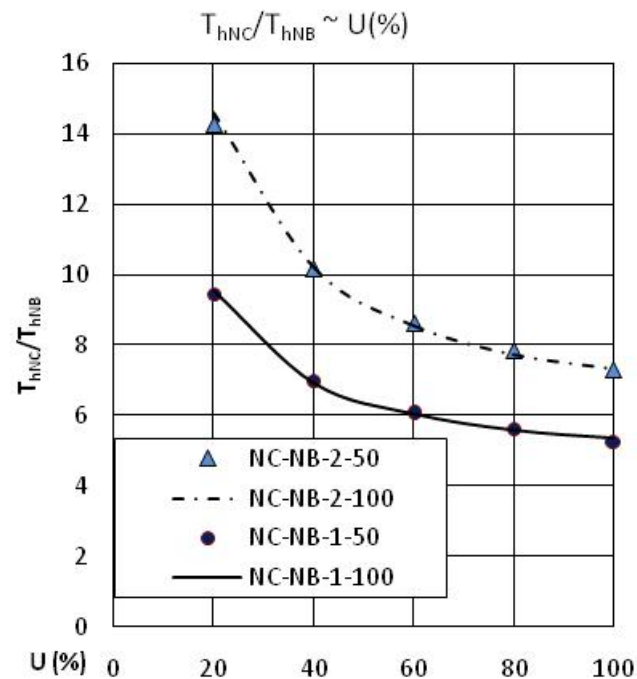


Figure 4.6. Ratio of Time factor $\sim U(\%)$ for Vacuum stage only

The consolidation procedure of unit cell in (NB) case is faster than (NC) case by ratio (T_{hNC}/T_{hNB}). The different values relative to (n) ratio are shown in the **Table 4.2**.

Table 4.2. The ratio of Time factor

U(%)	20	40	60	80	100
n=20	14.6	10.2	8.57	7.76	7.31
n=10	9.56	6.93	6.08	5.59	5.37

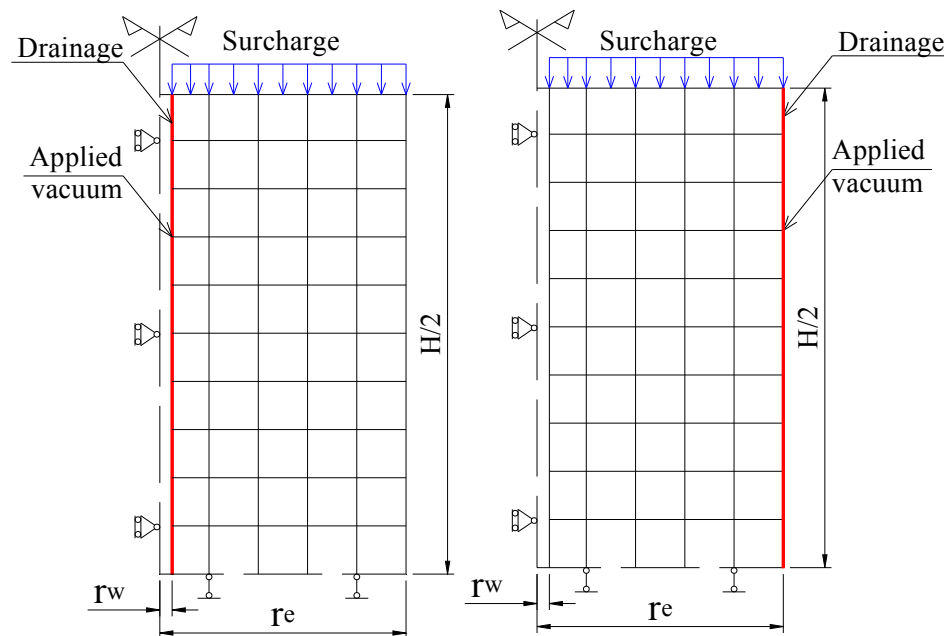
The average coefficient of consolidation (C_h) in both case (NC) and (NB) during vacuum pressure only were found the same value and independent with (n) ratio, $C_{hNC} = C_{hNB} \simeq (2/3)C_{hFC}$.

4.2 Solution for Axisymmetric Unit Cell under Vacuum Combine Surcharge Loading

In this solution, the surcharge is applied after some degree of consolidation induced by vacuum pressure.

Normally, the prefabricated vertical drain (PVD) of dimensions 10cm x 0.4cm is installed by rectangular shape. For this research the equivalent diameter of vertical drain $d_w = 5\text{cm}$ and diameter of cell $d_e = 100\text{cm}$ were used. The

example with $d_e=7.5\text{cm}$ and $d_w=0.3875\text{cm}$, and $n=20$, were used in this analysis and shown in **Figure 4.7**. This unit cell also used to simulate the vacuum preloading in the laboratory test.



a) Drainage at center b) Drainage at outer boundary

Figure 4.7. Vacuum combine surcharge preloading

The surcharge stages are applied in three cases of the degree of consolidation (U) reach to 40%, 70% and 100% as shown in the **Table 4.1**.

There are two stages for vacuum preloading method, the first stage is vacuum preloading only until the degree of consolidation reach to the target, and the second stage is surcharge preloading during the vacuum is maintained.

The surcharge loading estimates equal to 80% of increase vertical effective stress to prevent the failure state, for each case the loadings are 19.8kPa, 29.6kPa, and 42.4kPa respectively when 50kPa vacuum pressure is applying.

The loading rate is 0.5 kPa/min for drainage at the center case (NC), the ration T_{hNC}/T_{hNB} are used from the **Table 4.3**, of 10.2; 8.16 and 7.31 as degree of consolidation 40%; 70% and 100% respectively to define the loading rate when the drainage at outer boundary (NB).

The magnitude and rate of loading determined base on the increasing of effective stress of soil mass. The results are shown as follow:

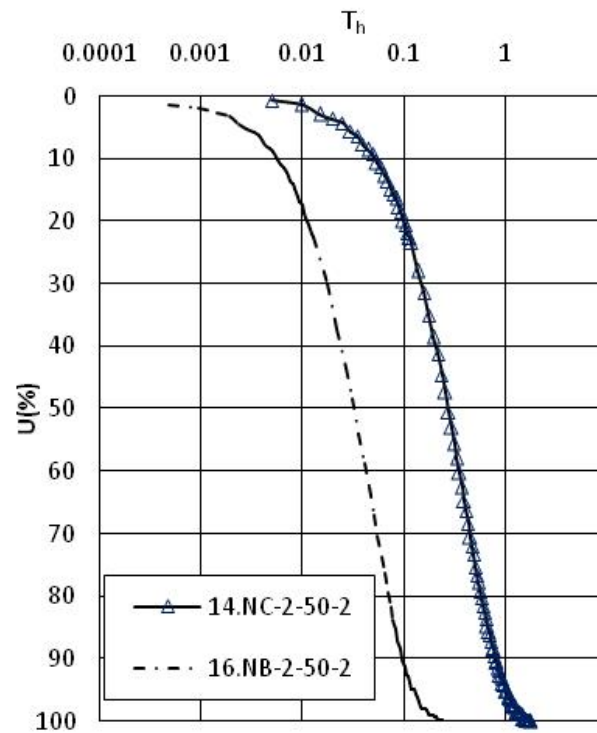


Figure 4.8. Case n=20, Vacuum - Surcharge;
 $V_a=50$ kPa, $U=40\%$; $T_{hNC}/T_{hNB}= 8.65$

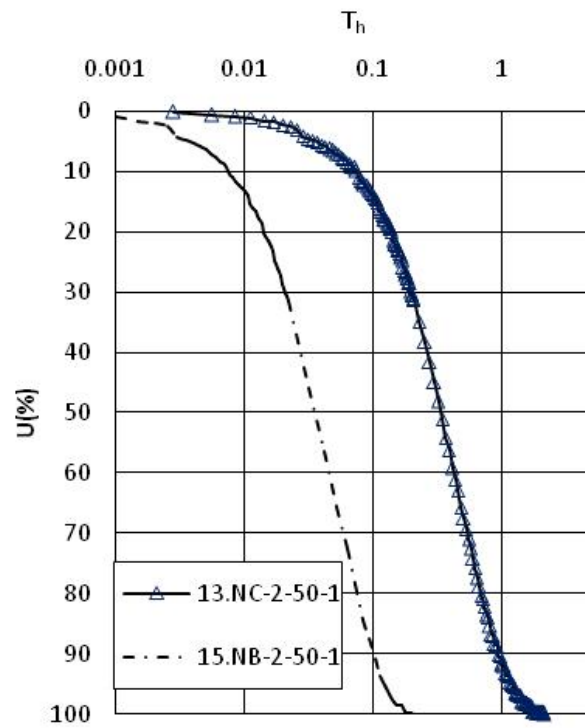


Figure 4.9. Case n=20, Vacuum - Surcharge;
 $V_a=50$ kPa, $U=70\%$; $T_{hNC}/T_{hNB}= 8.71$

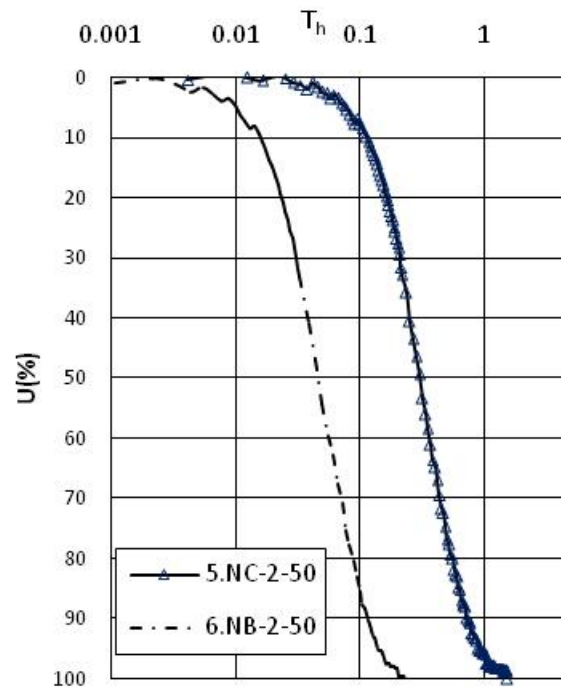


Figure 4.10. Case n=20, Vacuum - Surcharge; $V_a=50\text{kPa}$, $U=100\%$
 From the **Figure 4.11** and **Table 4.3** the average of ratio of time factor are equal to 8.71 & 8.65 for vacuum pressure are 100kPa and 50kPa respectively, when $U=100\%$ the ratio of time factor is nearly same value 7.4

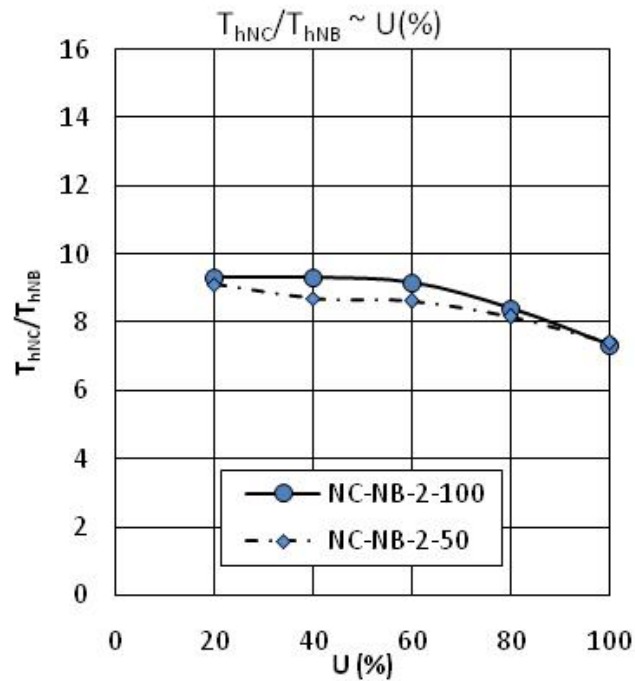


Figure 4.11. Ratio of Time factor $\sim U(\%)$ for Vacuum - Surcharge preloading

Table 4.3. The ratio of time factor for n=20, Vacuum combine surcharge

U(%)	20	40	60	80	100
100kPa	9.33	9.31	9.16	8.41	7.32
50kPa	9.10	8.70	8.63	8.17	7.41

In the **Figure 4.12**, degree of consolidation at 70%, the maximum different in volumetric strain is 1.75% occurring at 420 min for case 40% is almost the same in the **Figure 4.13**.

From the analyzing above, the final volumetric strain in case outer boundary is almost same value as that in drainage at the center as surcharge applied at 40%; 70% and 100%. Under vacuum 50kPa and surcharge was applied, as degree of consolidation is 100%.

The **Figure 4.14** showed the deformation of unit cell (volumetric strain ϵ_v) during time of vacuum and vacuum combine surcharge are same in two cases (NC) and (NB) after adjustment with the ratio of time factor T_{hNC}/T_{hNB} .

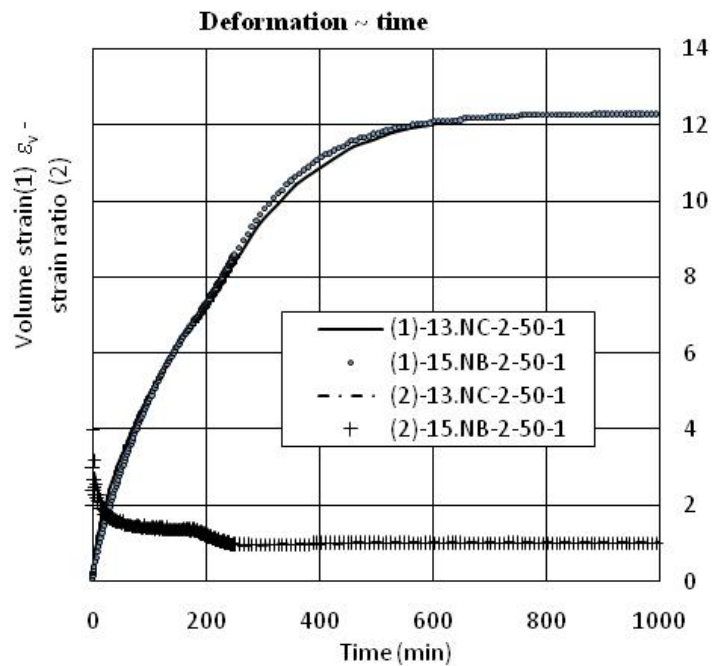


Figure 4.12. Case n=20, Vacuum - Surcharge;
 $V_a=50$ kPa, $U=70\%$; $T_{hNC}/T_{hNB}=8.71$

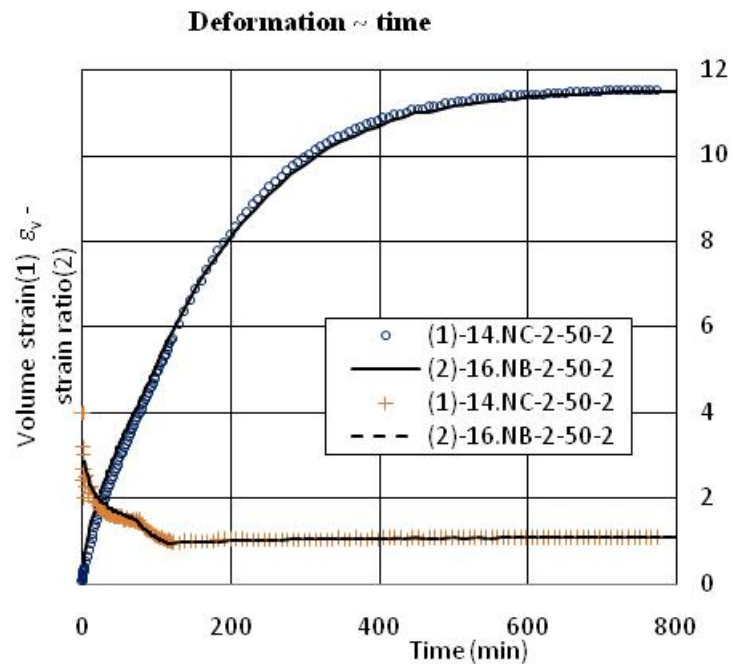


Figure 4.13. Case n=20, Vacuum - Surcharge;
 $V_a=50$ kPa, $U=40\%$; $T_{hNC}/T_{hNB}=8.65$

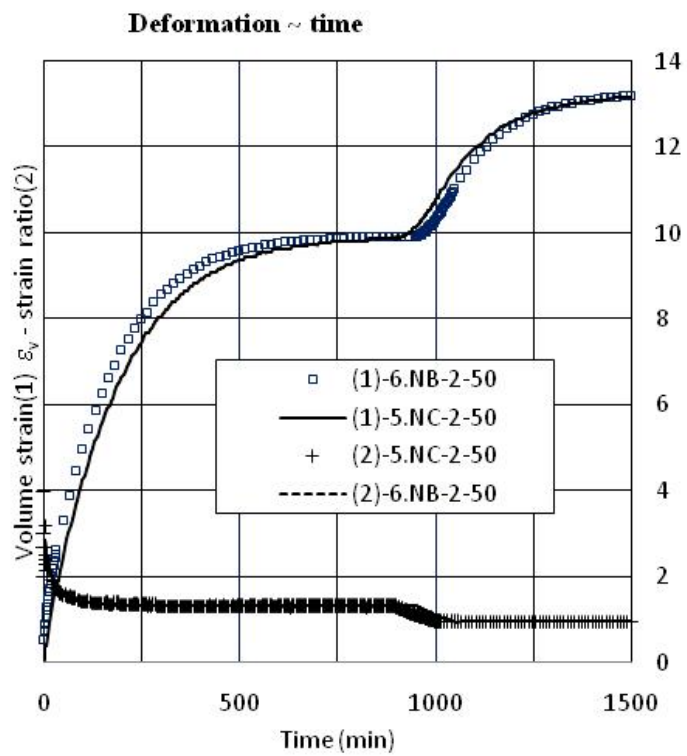


Figure 4.14. Case n=20, Vacuum - Surcharge;
 $V_a=50$ kPa, $U=100\%$; $T_{hNC}/T_{hNB}=7.31$

The strain ration $\varepsilon_r/\varepsilon_a$ are the same in both cases and vary from 4 to 1.3 during vacuum stage and reduce to 0.98 during the surcharge was apply. These results are good agreement with vacuum preloading theory; the lateral deformation of embankment is inward during applying vacuum pressure. These results also agree with the solution above. To make this solution more effectively, the laboratory test by Tri-axial apparatus should be carried out to support this research.

4.3 Simulation in Laboratory Test

4.3.1 Soil Specimen

The serial tests were performed by tri-axial apparatus in the laboratory at Hokkaido University to simulate the behavior of Kasaoka clay improved by vacuum preloading method.

The specimens of clay 75mm x 150mm in diameter and height, respectively were used for this research, which remolded in the laboratory from the commercial Kasaoka clay powder. The specimens are suitable to control consolidation time under vacuum condition by tri-axial apparatus.

The specimens were pre-consolidated under a pressure of 100kPa and OCR=1.25. The effective stresses in vertical and horizontal directions were 80kPa and 40kPa, respectively. Under pre-consolidated condition, the coefficient of horizontal earth pressure at rest is $K_0 = 0.5$. The physical properties of soil are listed in the **Table 4.4**.

Table 4.4. Kasaoka clay's properties

Soil properties	Values
Unit weight, (kN/m ³)	17.5
Water content, w (%)	46.5
Liquid limit, WL (%)	62
Plastic limit, WP (%)	27.5
Plasticity index, PI (%)	34.5
Specific gravity, G _s	2.67
Initial void ratio, e ₀	1.17

The permeability coefficient (k) and compression index (C_c) obtained from the standard odometer test result, were shown in **Figure 4.15**.

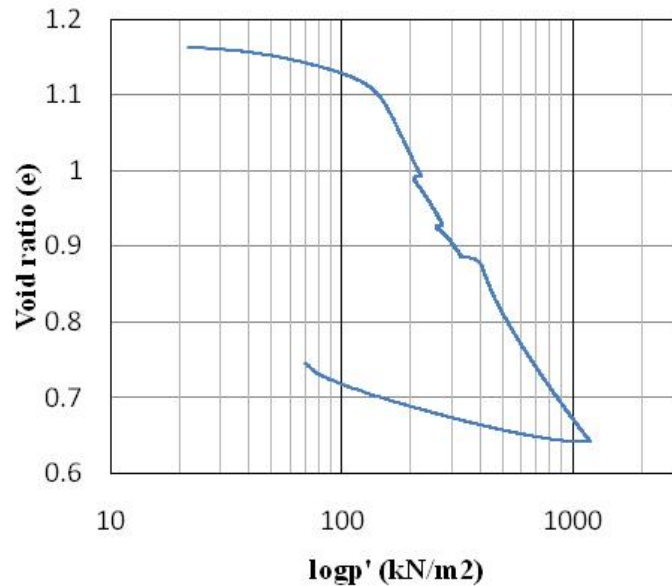


Figure 4.15. Void ratio $\sim \log(p')$ graph

Series conventional tri-axial test were carried out to verify the failure line (K_f) and relationship between the coefficient K and the ratio s_u/σ'_v to predict the shear strength that shown in **Figure 4.16**.

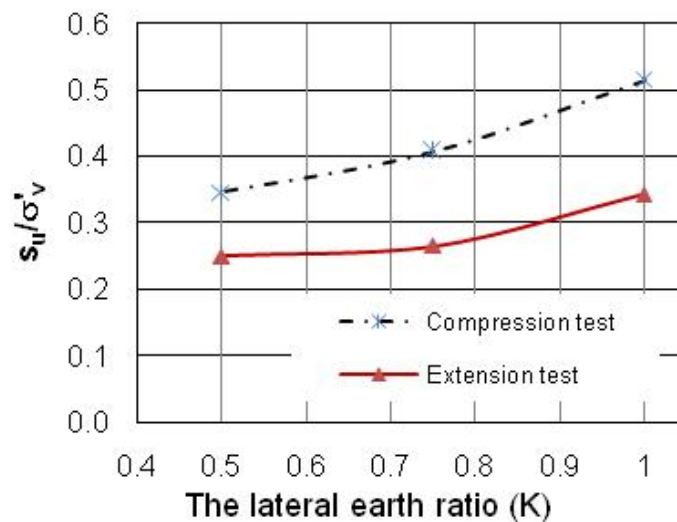


Figure 4.16. Predict shear strength by effective stress and earth ratio

4.3.2 Test Procedure to control the instability of soil specimen under vacuum preloading

It is very important to define the increasing of soil capacity gradually under

vacuum preloading method in the laboratory to avoid any risk in cases applied surcharge over the field soil capacity.

Simulation behavior of soft soil improvement by vacuum and surcharge loading can be carried into five stages as loading step to saturate soil specimen, generating the vacuum pressure condition, applying vacuum, applying surcharge loading, and undrained shearing stage.

The loading and recompression step, the specimen is saturated fully with B value more than 0.98 to reach to the initial pre-compression stress. The effective vertical and horizontal stresses in soil specimen gradually reach to 80kPa and 40kPa, respectively after saturation 24 hours.

The vacuum pressure is simulated by applying the effective stress target with the lateral earth pressure ratio equal to one ($K=1$), the soil specimen is subjected the same condition under vacuum pressure as the period research, the behavior of soil mass under surcharge and vacuum pressure is shown in the **Figure 4.17**.

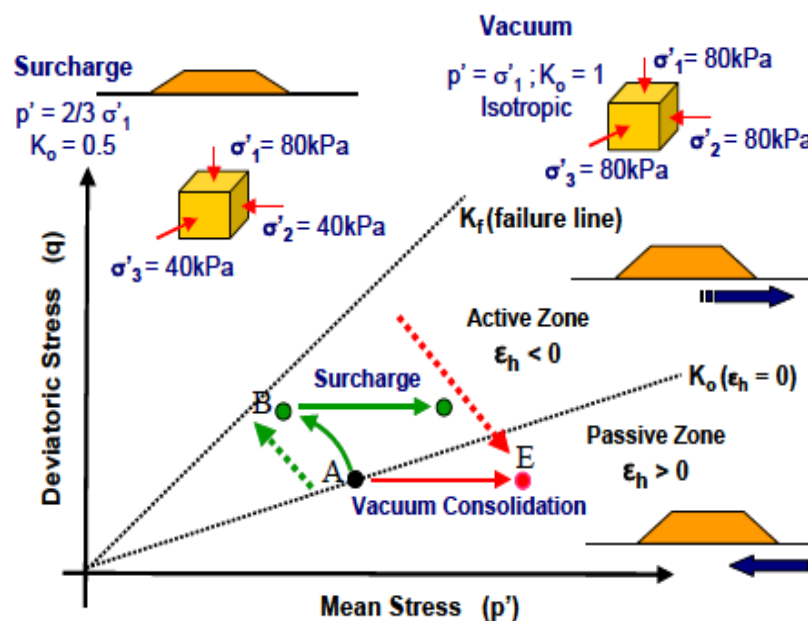


Figure 4.17. Behavior of soil mass under vacuum and surcharge preloading

During the stage of generating vacuum pressure condition, the drainage valve is closed and then excess pore water pressure (PWP) has been increasing up to the desired vacuum pressure. In this research, vacuum pressures are designed at 50kPa and 100kPa to correspond to the depths of specimens. The PWPs was raised up to 250kPa and 300kPa, respectively as shown in

Figure 4.18, vacuum pressure supplying step occurred in the first stage for 155 minutes.

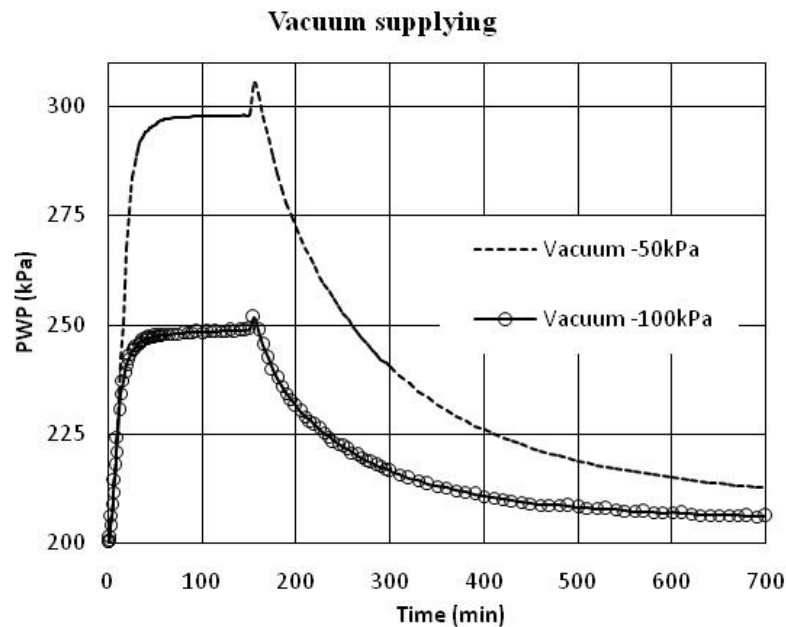


Figure 4.18. Excess pore water pressure in vacuum condition

The vacuum pressure is applied by opening the valve as shown in the second stage, PWP has been reduced while the effective stress is gradually increased until the PWP completely dissipated. Finally, the vertical effective stress target at 130kPa and 180kPa were generated.

The coefficient of horizontal earth pressure (K) is the ratio of the effective horizontal earth pressure due to the confinement from the surrounding soil mass to the vertical effective stress.

From the **Figure 4.19**, K value can estimated as follows:

$$K = \frac{\sigma'_3 + \sigma'_{va}}{\sigma'_1 + \sigma'_{va}} \quad (4.8)$$

During drained progress stage, the consolidation has been occurred due to dissipation of the excess pore water, the effective stress and shear strength of soil will be increase, the behavior is suitable with the vacuum mechanism.

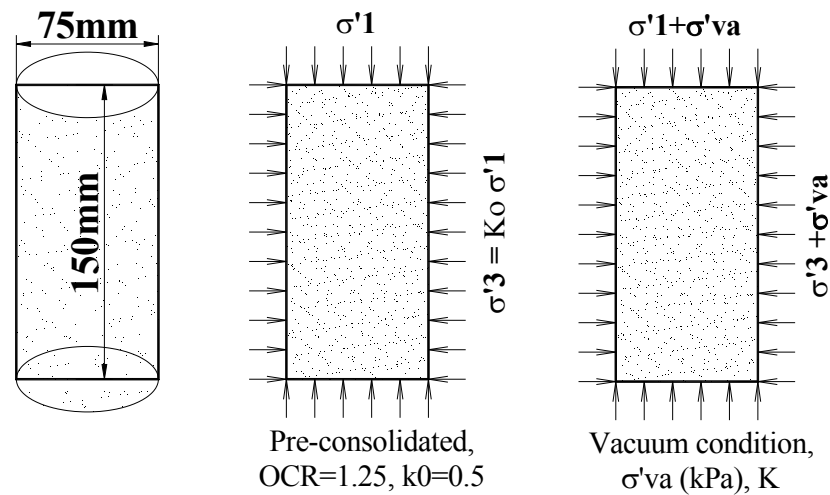


Figure 4.19. Soil specimen under Vacuum condition

When the effective stress increases to the target and the excess pore water dissipates completely the soil is fully consolidated. However, data from laboratory test and FEM showed that the end of primary consolidation (EOP) was gained when the excess pore water pressure was dissipated about 95%. The parameter in vacuum proceed by tri-axial apparatus is shown in Table 4.5 and 4.6.

Table 4.5. Parameter in vacuum proceed by tri-axial apparatus (U=10%)

Step	CP	BP	PWP	σ'_v	σ'_h	(K)
	(kPa)					
Step loading	220	200	200	20	20	1
Recompression	240	200	200	80	40	0.50
Vacuum supplying (50kPa) (Undrained)	290	200	250	80	40	0.50
Vacuum applied	290	200	200	130	90	0.692
Vacuum supplying (100kPa)(Undrained)	340	200	300	80	40	0.50
Vacuum applied	340	200	200	180	140	0.778

Where:

CP - Cell pressure

BP- Back pressure

PWP- Pore water pressure

σ'_v - Vertical effective stress target

σ'_h - Horizontal effective stress target

K – Coefficient of horizontal earth pressure

Table 4.6. Parameter analysis in vacuum proceed by tri-axial apparatus (U=100%, 70%, 40% and 20%)

Recompression $s_u=32.4\text{kPa}$			Vacuum pressure	Target effective stress (Vacuum loading)				U%
σ_1	σ_3	K	σ_{va}	σ'_1	σ'_3	K_{va}	s_u/σ'_v	
				180	140	0.78	0.42	100
80	40	0.5	100	143	103	0.72	0.40	70
				116	76	0.66	0.39	40
				130	90	0.692	0.40	100
80	40	0.5	50	112	72	0.64	0.38	70
				98	58	0.59	0.37	40

Note: All units in kPa

The shearing steps were carried out to define the undrained shear strength of improved soft soil. Depend on the goals; this step could be performed at the time after vacuum loading completely or at the degree of consolidation (DOC) gradually increasing to 40%, 70%, 100% combined with surcharge.

The data was analyzed to verify the capacity of improved soil and to control the preloading surcharge at the site to avoid the soil failure or instability of over surcharge to its capacity.

The capacity of soil predicted by empirical method proposed by Tanaka:

$$s_u = (s_u / \sigma'_v) * 0.8 * \Delta p \quad (4.9)$$

where;

s_u/σ'_v : can be determined from Figure 4.16

Δp : the loading is applied (vacuum pressure or surcharge loading).

The undrained shear strength of soil specimen from lab test result is analysis to check the capacity of soil improved.

4.3.3 Test Results and Analysis

The simulation result was shown in the **Table 4.7**. The surcharges were applied at degree of consolidation of 100%, 70%, and 40% loading.

Table 4.7. The data of vacuum procedure simulation to control instability of soil

Vacuum pressure	Target effective stress (Apply loading)					U%	Prediction s_u	Test s_u
	σ_{va}	$q=2*s_u$ $=\sigma'_1-\sigma'_3$	σ'_1	σ'_3	K_{va}			
100	121.6	261.6	140	0.535	0.358	100	89.08	89.66
	92.176	232.2	140	0.603	0.375	70	82.65	79.36
	71.872	211.9	140	0.661	0.389	40	78.21	75.57
50	82.4	172.4	90	0.522	0.355	100	58.19	62.49
	68.488	158.5	90	0.568	0.366	70	55.15	53.8
	58.336	148.3	90	0.607	0.376	40	45.93	43.2

Note: All units in kPa

These results agree with behavior of soil improvement by vacuum preloading theory. The **Figure 4.20** and **Figure 4.21** are shown the relationship between case (NB) in FEM and lab test, the vacuum pressure of 50kPa was applied only and combination to surcharge respectively. In the both cases the DOC in 100% were induced, the largest different of U is 3.5% between FEM and lab test occurring at $T_h=0.3$.

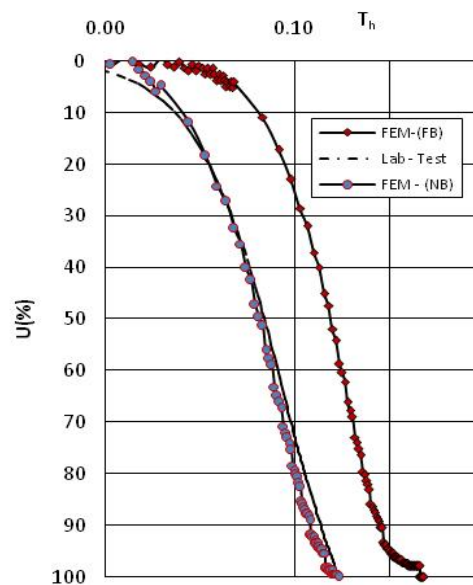


Figure 4.20. Case n=20, Vacuum only; Va=50 kPa, U=100%

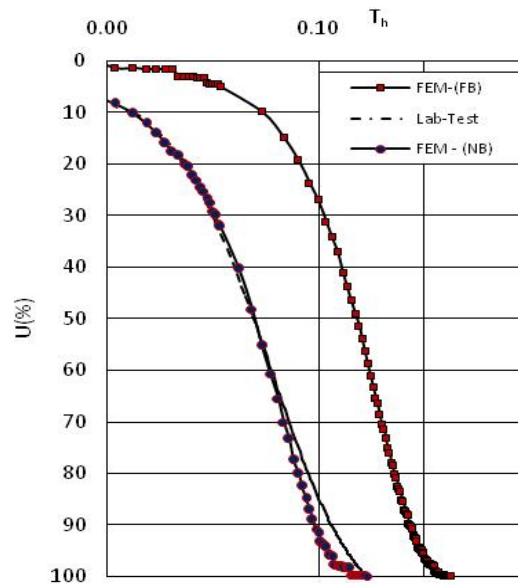


Figure 4.21. Case n=20, Vacuum - Surcharge; $V_a=50\text{kPa}$, $U=100\%$

The final deformation of specimen was nearly same as at end of vacuum stage and vacuum combined with surcharge as shown in **Figure 4.22**. The largest different in volumetric strain 0.3% occurred at 350 min as DOC at 95%.

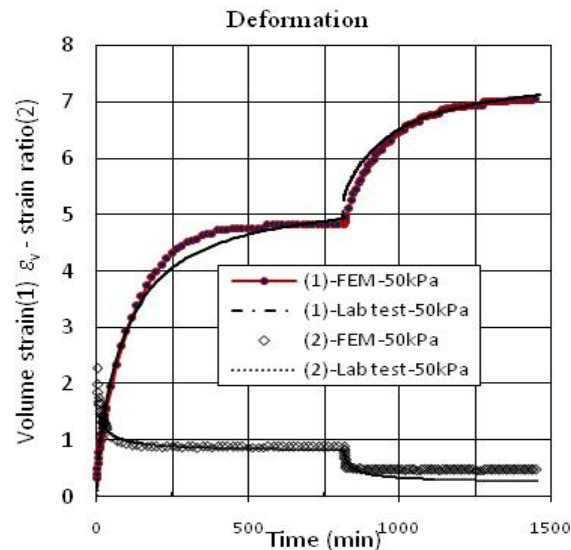


Figure 4.22. Case n=20, Vacuum - Surcharge; $V_a=50\text{kPa}$, $U=100\%$

The volumetric strain of 4.92% and 7.12% were found in both cases FEM and laboratory test. The strain ratio (ϵ_r/ϵ_v) illustrated the inward lateral deformation of specimen subjected isotropic stress. This ratio was nearly one during only applied vacuum pressure and was reduced if surcharge was established. These results agree with behavior of soil improvement by vacuum preloading theory.

The tested undrained shear strength was found to agree well to the predicted s_u as shown in the **Figure 4.23**.

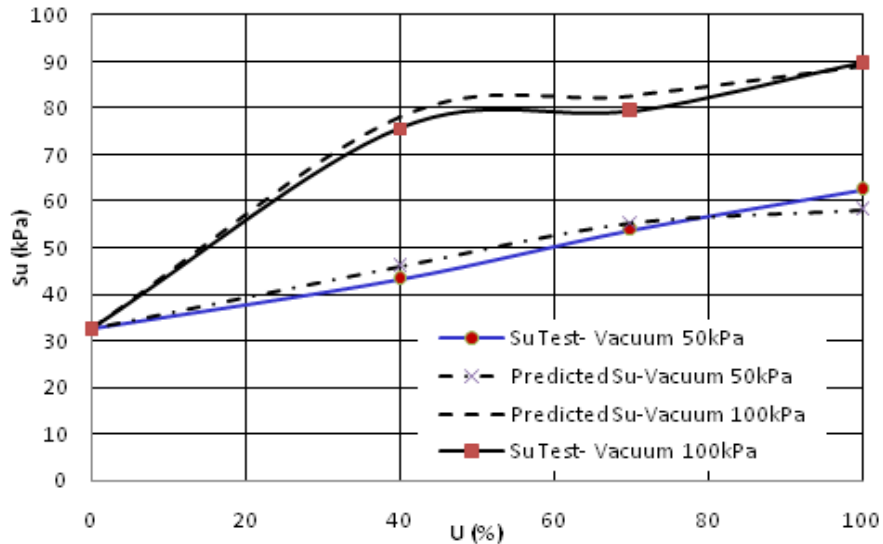


Figure 4.23. Increasing undrained shear strength

The maximum different of shear strength was about 6% and 4% for vacuum pressure at 50kPa and 100kPa, respectively. However, the specimen still stable during surcharge was applied. The stress path was shown in the **Figure 4.24**. There were three stages during vacuum preloading simulate in the laboratory as: pre-consolidation stage (AB), vacuum application stage (BC) and surcharge loading combination stage (CDEF).

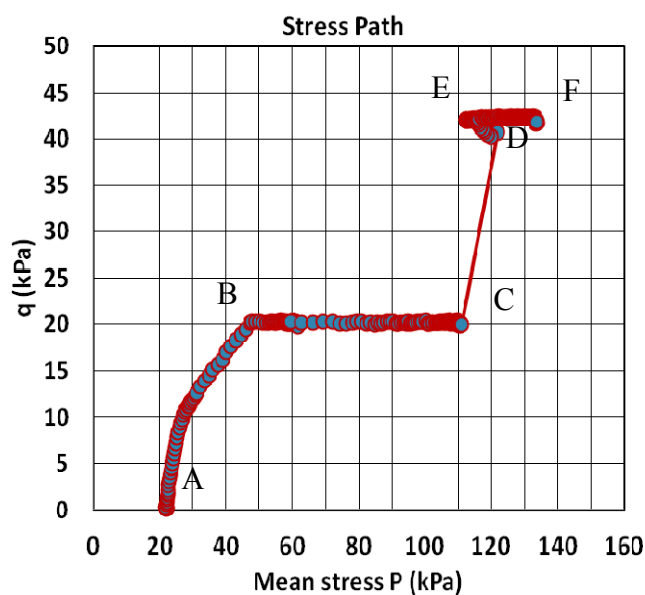


Figure 4.24. Stress path

Under vacuum condition, the stress path of soil moved from B to C which was far from the failure line. Applying surcharge at point B may lead the stress point to the failure line and cause failure the embankment. At point C when the consolidation at 100%, under vacuum pressure, surcharge can be applied safety without any risk of embankment. However the time of construction is longer than apply surcharge at some degree of consolidation.

When surcharge is applied on CD line, the stress path has been changed from D to E and is closed to the failure line, then moves to point F. The behavior of soil specimen under vacuum preloading method simulated by Tri-axial apparatus is matched the before studies as shown in Figure 4.17.

The increasing of undrained shear strength of soil specimen after applied vacuum preloading at some degree of consolidation of 40%, 70% and 100% were shown in **Figure 4.25**. This stage was carried out at end of each test, the failure test were conducted to define the shear strength in undrained condition. The undrained shear strengths defined at 40%, 70% and 100% for vacuum consolidation of 43.2kPa, 53.8kPa and 62.49kPa, respectively. These results agree the approach proposed by Tanaka. The surcharge of each time applied about 10kPa was used for this analysis compare to 0.5m height of embankment.

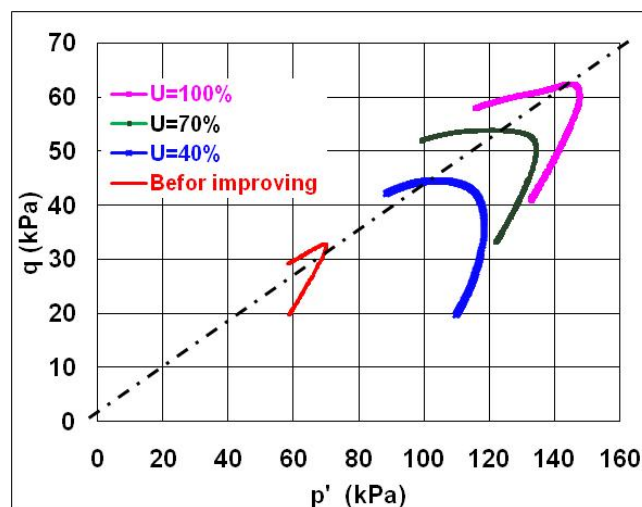


Figure 4.25. Increasing undrained shear strength

4.4 Summary Conclusions

The study has been developed based on the combination of finite element analysis and the results of laboratory experiments to simulate a new appropriate method. This method can be widely applied for soft ground improvement by vacuum preloading method. The results from the study can be summarized as follows:

1) The axisymmetric unit cell used to model the behavior of soil treatment by vacuum preloading as none boundary conditions are considered, the behavior of soil is more close to real soil state in the field.

2) Two cases of drainages boundary showed that time for consolidation in cases outside drainage of unit cell is faster than at the center by T_{hNC}/T_{hNB} ratio. However, the deformations of the specimens in all cases are in same shape and value with the same applied condition.

3) Results of experiments by tri-axial apparatus entirely agree with FEM model. It is suggesting that the theories are given full compliance, highly compelling to predict the behavior of soil improvement by vacuum preloading method.

4.5 Case study of Vacuum Consolidation at Nakhorn Sri Thammarat Air port.

4.5.1 Site Description

The project was separated into 8 zones of soft soil treatment area which is shown in **Figure 4.26**. The area of each zone is between 3000-4000 m², which is matched to the capacity of the vacuum pumping unit and to remain the vacuum pressure more than 70kPa under airtight sheet during construction. The filled sand has been placed on the swamp area of about 1.00 m-1.50 m thick as a working platform.

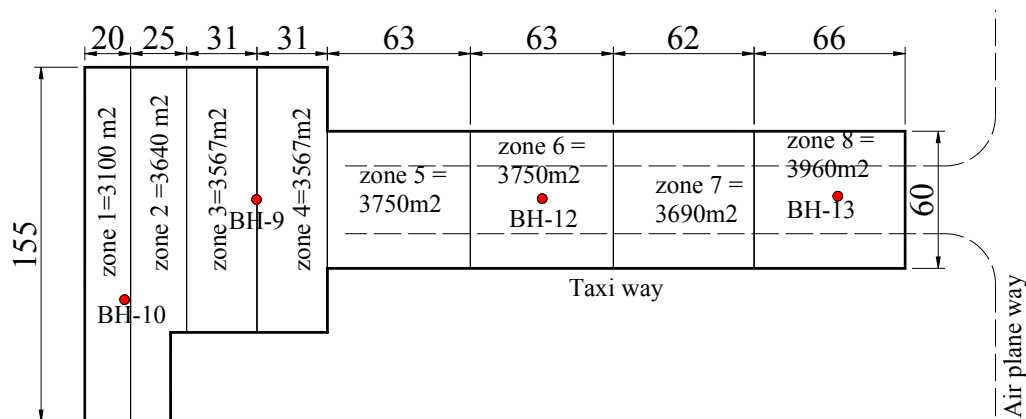


Figure 4.26. The CVM is applied

The purpose of this part is to assess the performance of vacuum consolidation method for very soft soil treatment of 30,000 m² of Apron and Taxiway from field instrumentation work. Using field-monitoring data for monitoring of accelerating the rate of consolidation and increasing of over consolidation ratio (OCR) could reduce the long-term settlement during service period. The cross section of embankment is designed in 4.0m high in sand over the sand mat is used to replace mud on the original ground as shown as **Figure 4.27**.

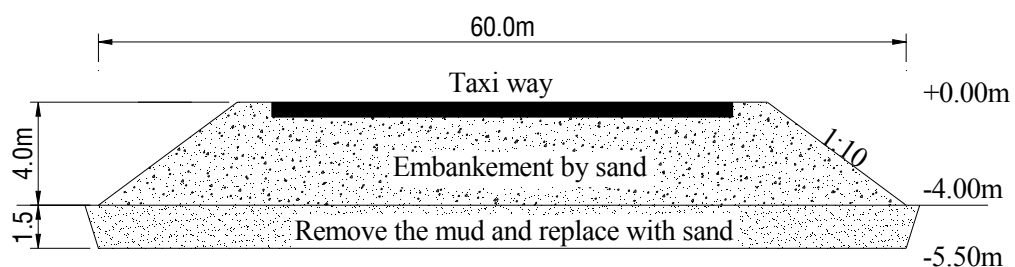


Figure 4.27. The cross section of the Taxiway

The construction area was located on the low land and marshy areas. The high embankment (4.00-4.50 m) was design over the low land and marshy areas.

4.5.2 Soil Conditions

The soil investigations were carried out on beginning of the project. The field investigation for soft soil comprised boring, sampling, in-situ testing. The boring consists of augering, wash boring with in-situ test included Standard Penetration test (SPT), Vane shear test and cone penetration test (CPTu). The field work undertaken during field investigation shown in **Table 4.8**.

Table 4.8. Summary of field investigations in soft soil

Type of investigation	Quantity (Nos)
Boreholes	12
SPT Test	98
Vane shear strength	48
CPTu Test	12

From the soil profile as shown in **Figure 4.28**,

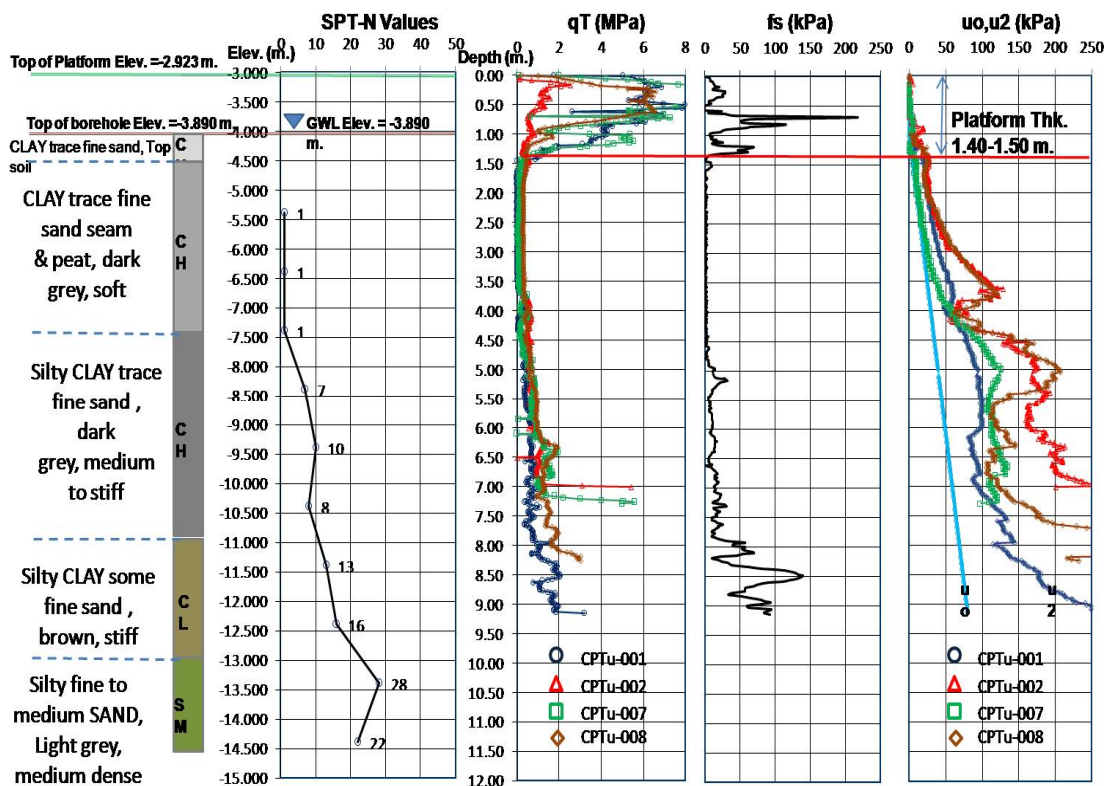


Figure 4.28. Soil profile of the project

The soft soil layer distributed to 5.5m depth from the surface with high content of silt and clay (more than 80% of fine particle). Therefore, the depth for soft soil treatment shall be 5.50m from platform.

Moreover, the possibility of leakage of vacuum pressure at the tip of the band drain is also low. According to the laboratory test, the soil properties at depth 2.00-3.00m from bore hole elevator (depth 3.00-4.00m from platform elevator), are $e_o = 2.492$, $C_c=0.946$, $Cr = 0.271$, and at depth 4.00-5.00m from bore hole elevator (depth 5.00-6.00m from the platform elevator) are $e_o=0.788$, $C_c=0.248$, $Cr=0.139$.

The low compressibility parameter of the medium to stiff clay is presented at depth 4.00-5.00m; hence, the settlement at this layer is less significant compare to the soft clay between 0.00-4.00m. However, the deep settlement gauges installed to check the settlement. At depth 3.75m to 4.25m, the sand lens located with the sand particle content more than 50%. It would be good to install the standpipe piezometer the edge of treatment area the depth of sand lens and compare the rate of decrease of water pressure with the other depth. The index and engineering properties of soft soil at depth 0.0-4.0m from existing ground that found as a soft to very soft clay (CH) are shown in Table 4.9.

Table 4.9. Summary Index and Engineering Properties of soil at depth 0.00-4.00m

No	Index and Engineering properties	Values
1	Moisture contents (%)	75-90
2	Void ratio, e	2.38-2.49
3	Specific gravity, Gs	2.62-2.66
4	Bulk unit weight (g/cm^3)	1.42-1.51
5	Percent of saturation (%), Sr	94-98
6	Compression Index, C_c	0.932-0.945
7	OCR	1.10
8	Coefficient of consolidation, C_v ($m^2/year$)	3.2
9	Undrained shear strength from UU Test (kPa)	10-14
10	Undrained shear strength from Vane Shear Test (kPa)	15-20

The compact vacuum consolidation method used to improve soft clay before construction embankment. The desired deeps of soil improvement by vacuum are shown in the **Figure 4.29**.

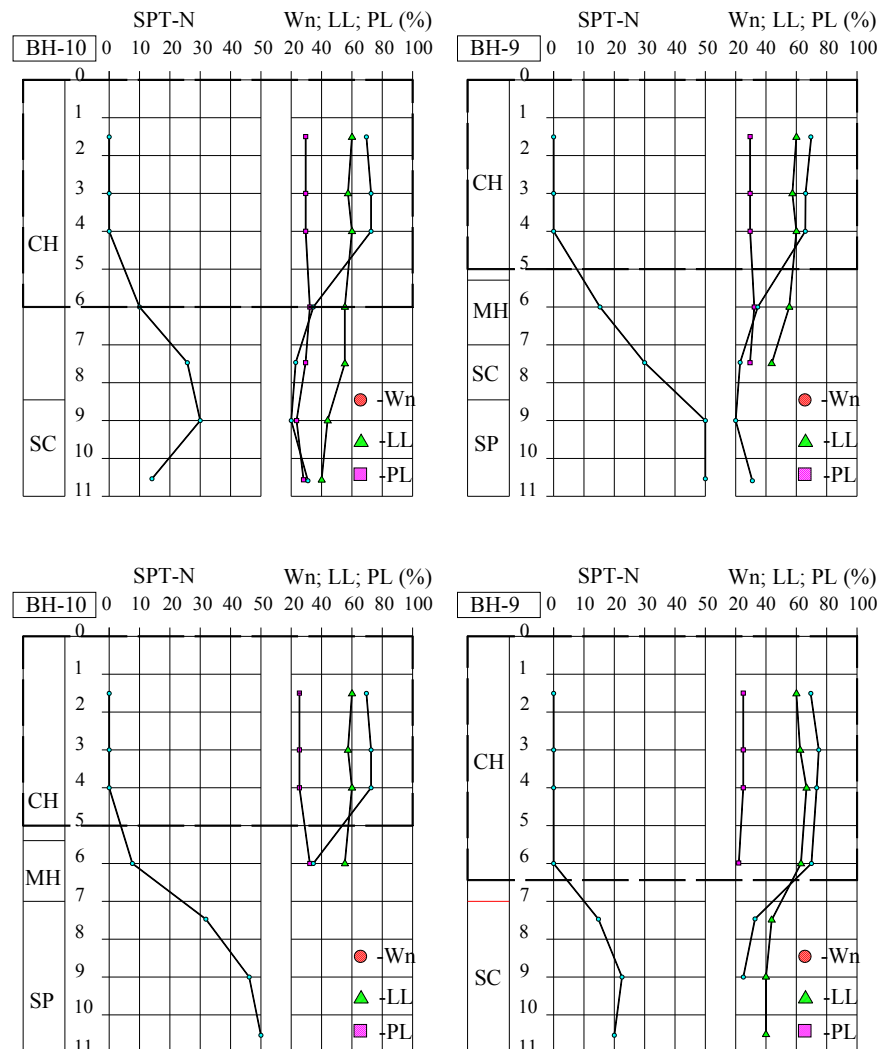


Figure 4.29. Log of boring

As the soil report, soil profile of Nakhorn Sir Thammarat Airport can be classified three sub-layers. **Layer No-1: Clay** trace fine sand seam & peat, dark grey, soft (CH), from surface to about 6.0m depth. **Layer No-2: Silty clay** trace to some fine sand, light grayish brown, stiff. (CH, CL). This layer extends from about 6.0 m to 8.0 m depth. **Layer No-3: Silty** is fine to medium sand, light grey, medium to dense. (SM). This layer extends from about 8.0 m to 10.45 m depth. The ground water level was found at about -4.0m depth, The undrained shear strength of very soft to soft clay layer increased from 15.6 to

23kPa with depth. The soil from surface to 6.0m depth is very soft clay, with high compressive and high water content.

4.5.3 Construction and Field Monitoring Work of Vacuum Preloading Method

The field monitoring work has been beneficial in evaluating soil behavior work under real field conditions, as well as assessing the performance of new materials and the methods used in the design and construction of geotechnical tasks. The stage of construction (embankment filling) was applied for this project. The embankment was constructed on the soft soil with the rate of filling be governed by the increase in soil strength due to consolidation process and requires close monitoring and communication between design engineer, construction and supervising engineers. Geotechnical instrument scheme for ground improvement work was designed to ensure safe and economical construction of embankment. The instrumentations were installed gradually with the vacuum construction technique as follow as:

- (1) The settlement plates and displacement stakes installed at designed locations for the monitoring purpose before doing any activities.
- (2) Placing and spreading the embankment (1.00-1.50m thick) on the original very soft ground surface were carried out to provide a suitable working platform.
- (3) The ARPAS drain KD-100 has been used for the band drain material. The band drain was installed up to 4.50-6.00m depth below working platform to medium clay layer. The band drain was installed in square pattern with 1.00m spacing.
- (4) The piezometers and differential settlement gauges were installed with appropriate depth and locations.
- (5) The perforated pipes were installed in the interval 20-30m in the stabilized area.
- (6) The primary and secondary separate tanks was installed and connected to the all of the pipe line systems.
- (7) The horizontal drains were laid in perpendicular to the perforated pipes and passing under the pipes for accelerating the water flow to the pipes.

- (8) The non woven geo-textile (protection sheets) and airtight sheets was placed to protect the vacuum systems from leakage.
- (9) Excavation of peripheral trenches (1.50m. depth) and laying of the airtight sheets up to the trench and backfilling with the embankment material were carried out to provide the anchorage length for airtight sheets.
- (10) The main tank was connected to vacuum pipes as well as the water and air pipes. The vacuum pumps was capable of generating -100kPa pressure.
- (11) Start vacuum pumping operation. During 1st week of operation, the daily checking to investigate and repair for the leakage points on the airtight sheets.
- (12) Preloading by embankment filling will be performed layer by layer.
- (13) Loading embankment layer 2, 3 and 4; during loading the pore water pressure and settlement as well lateral movement will be measure to control the stability of the embankment; Check the settlement; if it is reach 90% degree of consolidation, the vacuum pump will stop;

There are six types of instruments including surface settlement plates, sub surface settlement gauges, electric type piezometer, inclinometer, PVC Automatic Acquisition Unit and water discharge record meters in the instrumentation program. The types and arrangement of instrumentation are shown in **Figure 4.30**.

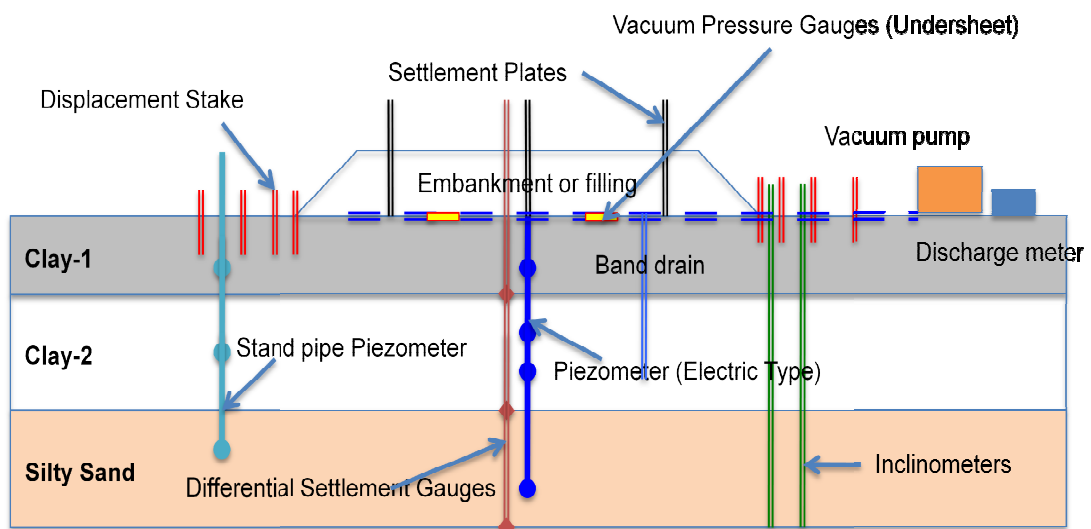


Figure 4.30. Arrangement of instrumentations

List of functions and frequency for different types of instrumentation are shown in **Table 4.10**

Table 4.10. The lists and nos of field instrumentation works

GI-Zone	Piezometer	Settlement plates	Sub-surface settlement	Inclinometer
1	1	8	3	2
2	1	5		
3	2	4	2	
4		3		
5	2	6	2	
6	1	3	2	
7	1	3	2	
8	1	3	2	
Total	9	35	13	2

The Schematic of CVM is shown as Figure 4.31

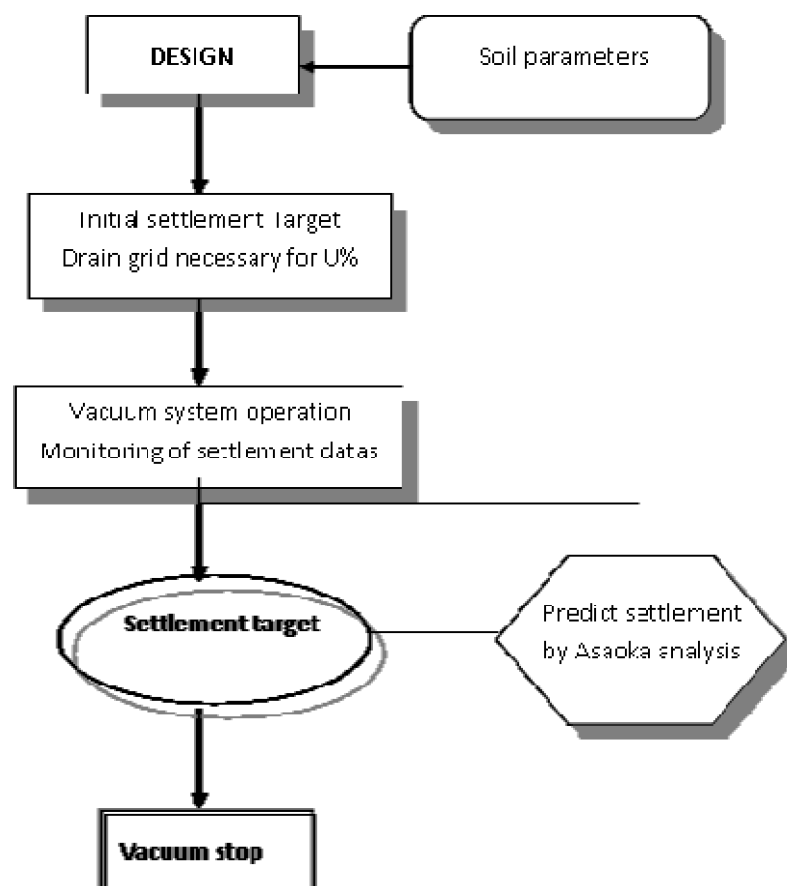


Figure 4.31. The schematic of CVM

4.5.4 Behavior and Performance of Vacuum Consolidation Method

During construction by CVM the behavior and performance of embankment is conducted by field data before and after vacuum preloading. As analysis the important of the data in the **Chapter 2** to estimate the behavior of soft soil improvement by vacuum preloading method, during treatment the soft soil we have to measure the data versus time by the instruments at the field.

The preloading consists of three steps shown in Figure 4.32. The first stage only vacuum pressure was applied for two weeks to check leakage of airtight sheets and create the first consolidation degree of soft ground. The second stage, the sand fill were applied with eight layers for 55 days, with the thickness of each layer about 35 cm. The last stage of loading took place during 65 days. Under this stage the soil was subjected the combination of vacuum pressure and embankment loading. The vacuum is maintained at high pressure of 80kPa during whole construction procedure, the stability of embankment is controlled well, the lateral movement is not presented at the field observation.

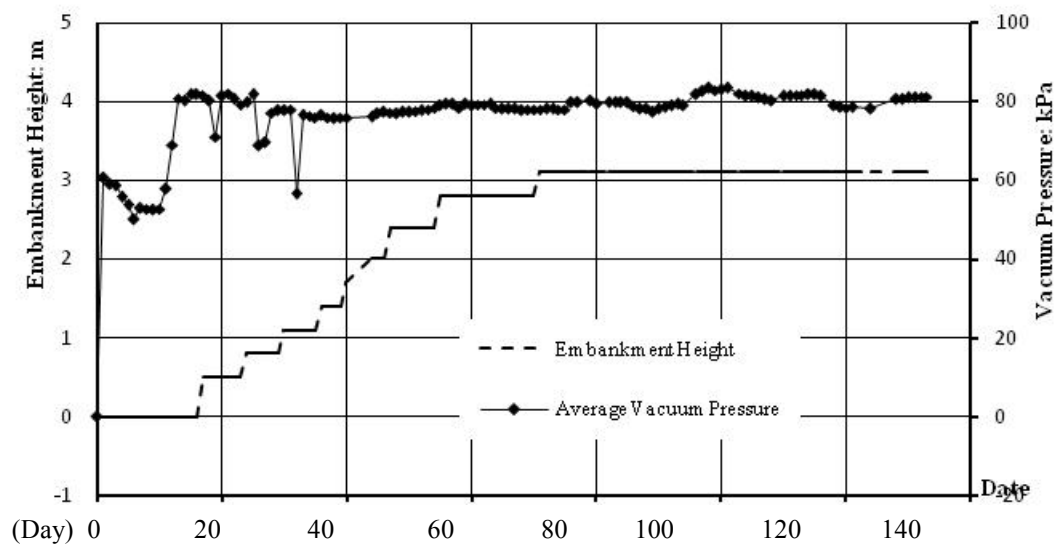


Figure 4.32. The vacuum preloading stages

The construction procedure is completed when the recorded final settlement reached the required value by Asaoka's method (1978) as shown in **Figure 4.33** to control the settlement of improved embankment. The ultimate settlements were 0.55m, 0.35m and 0.10m at the ground surface, 1.5m depth and 3.5m depth, respectively.

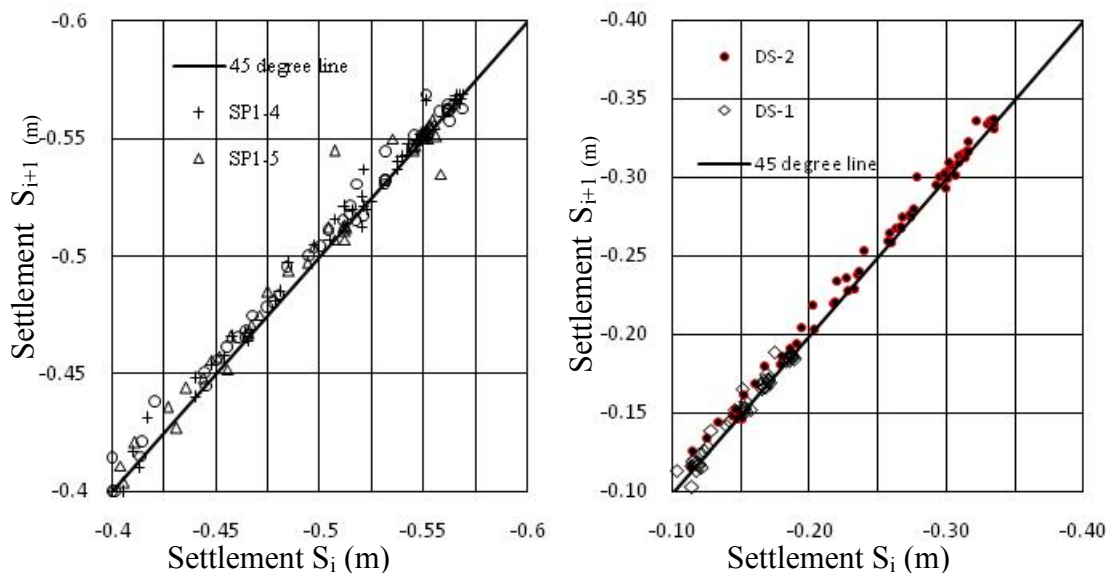


Figure 4.33. The final settlement-Zone GI-1 by Asaoka's method

According to the field instrumentation records, the evaluation criteria for stop vacuum operation was assessed by considering the degree of consolidation and rate of settlement. The settlements at certain time intervals were described by Eq (4.10):

$$S_n = \beta_0 + \beta_1 \cdot S_{n-1} \quad (4.10)$$

Where:

S_1, S_2, \dots, S_n are settlements observations.

S_n denotes the settlement at time t_n .

The time interval $\Delta t = (t_n - t_{n-1})$ is constant. The first order approximation should represent a straight line on a $(S_n \text{ vs } S_{n-1})$ -co-ordinate. The values of β_0 and β_1 are given by the intercept of the fitted straight line with the S_n - axis and the slope. The ultimate primary settlement can be calculated with the expression:

$$S_{\text{lut}} = \beta_0 / (1 - \beta_1) \quad (4.11)$$

These settlements are presented in **Figure 4.34** and **Figure 4.35**, which compared well to finite element method (FEM). The FEM prediction was followed the proposed method for tri-axial test. The different settlement just occurred in the first two weeks, after that they were almost same value, and the final settlement of 0.56m agreed with Asaoka's method and FEM approach.

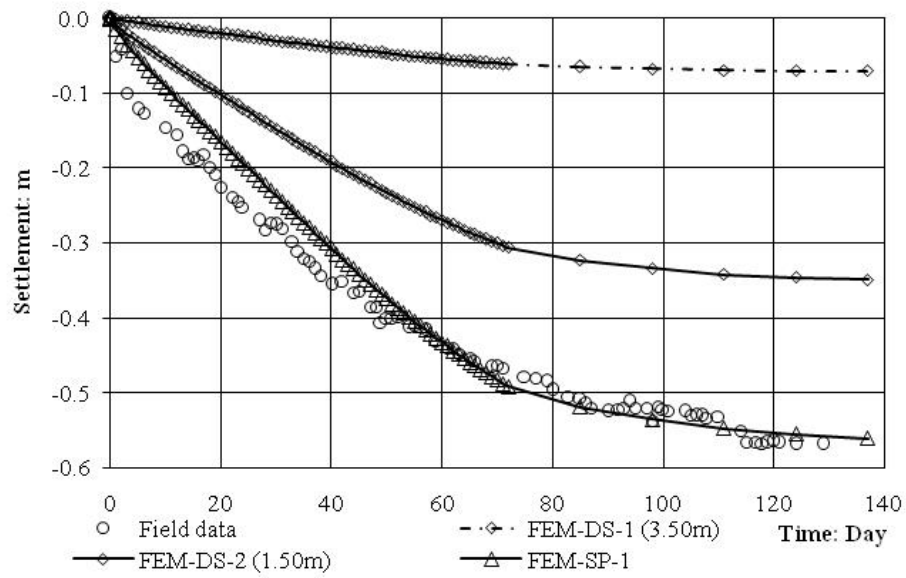


Figure 4.34. The settlement at zone GI-1

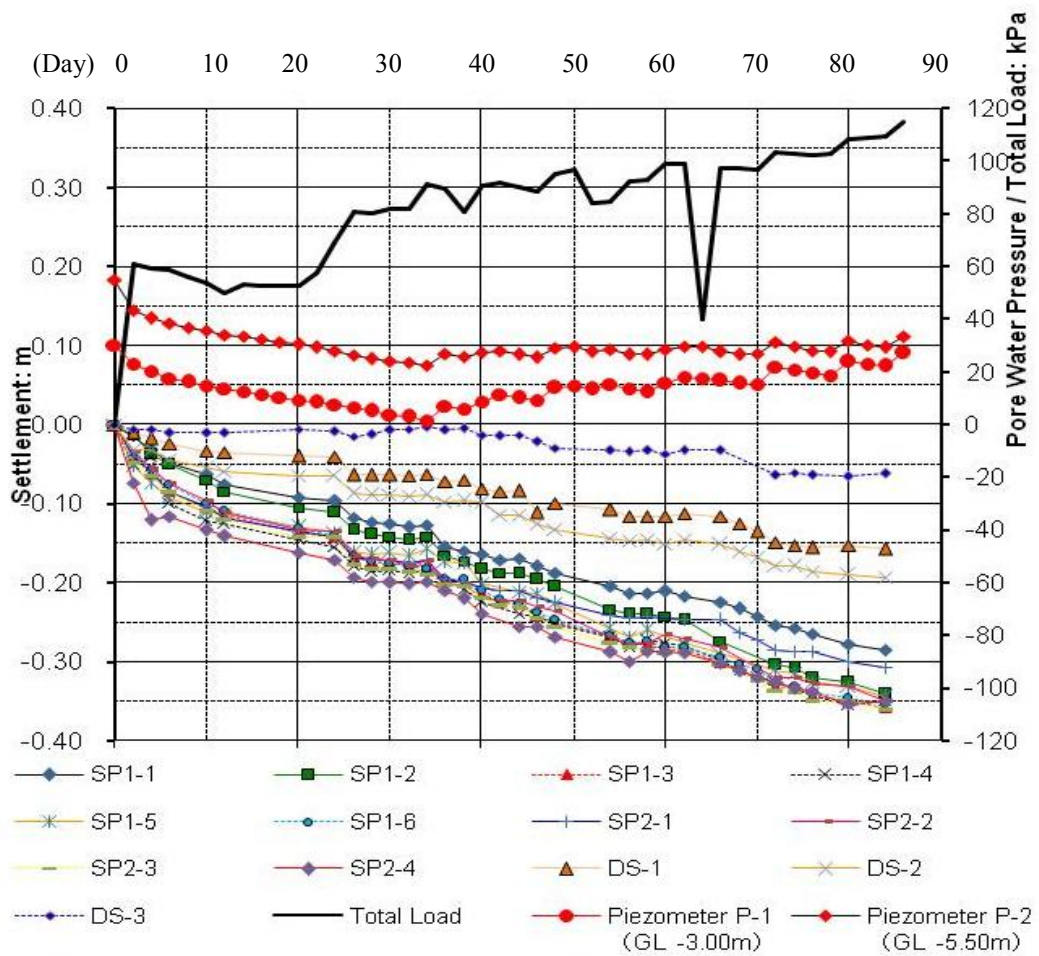


Figure 4.35. Field monitoring Zone 1&2

The excess pore water pressure during construction was shown in the **Figure 4.36** and **Figure 4.37**.

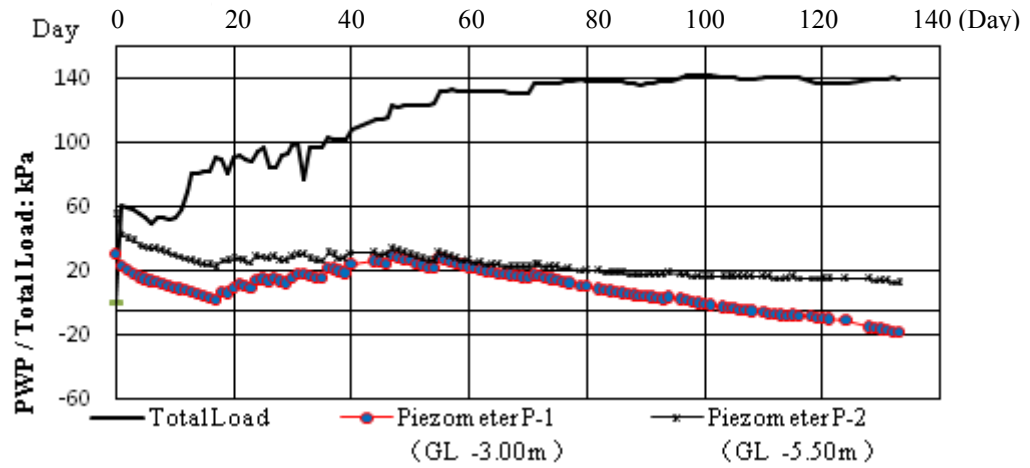


Figure 4.36. Pore water pressure from piezometer data

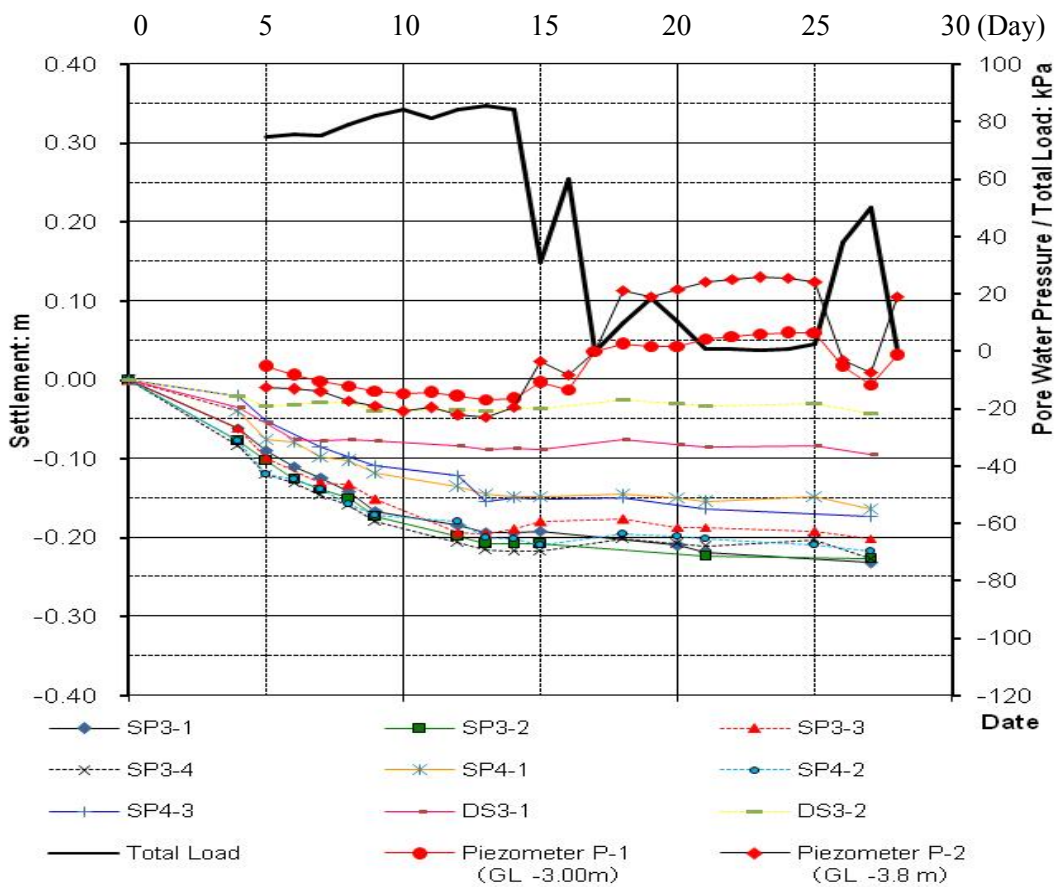


Figure 4.37. Problem during surcharge applying in Zone 3,4

After vacuum pressure apply the excess pore water pressure occurred immediately in negative value gained the vacuum pressure, if the surcharge was fill the excess pore water pressure will be increased during apply surcharge fill stage, then it will be dissipated gradually. However damage of airtight sheet occurred during earthwork construction, the pressure is lose and the pore water pressure raised up, the soft soil is swelled.

The pore water pressure change is shown in the **Figure 4.38**, during surcharge loading the excess pore water pressure increases in first 30 days and 60 days, during the third stage, the pore water pressure reduced and lead to the suction line due to excess pore water dissipated.

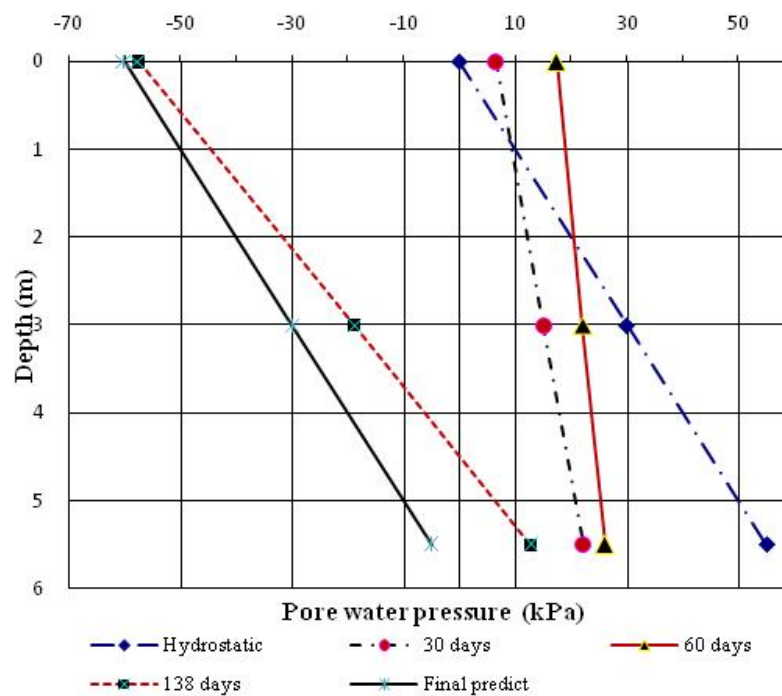


Figure 4.38. Dissipation of excess pore water pressure

The average DOC, U_{avg} , can be calculated as Eq(3):

$$U_{avg} = 1 - \frac{\int [u_t(z) - u_s(z)] dz}{\int [u_0(z) - u_s(z)] dz}; \quad (4.12)$$

where:

$$u_s(z) = \gamma_w z - s \quad (\text{kPa}) \quad (4.13)$$

$u_0(z)$, $u_t(z)$, $u_s(z)$, γ_w , s - initial pore water pressure at depth z ; pore water pressure at depth z at time t ; suction line; unit weight of water; and suction applied.

The Degree of Consolidation predicted from distribution of excess pore water pressure indicated that it reduced with depth of improvement by vacuum. In Figure 4.39, the DOC values was more than 95% and 80% at 3m and 5.5m depth, respectively, therefore the result agrees with prediction.

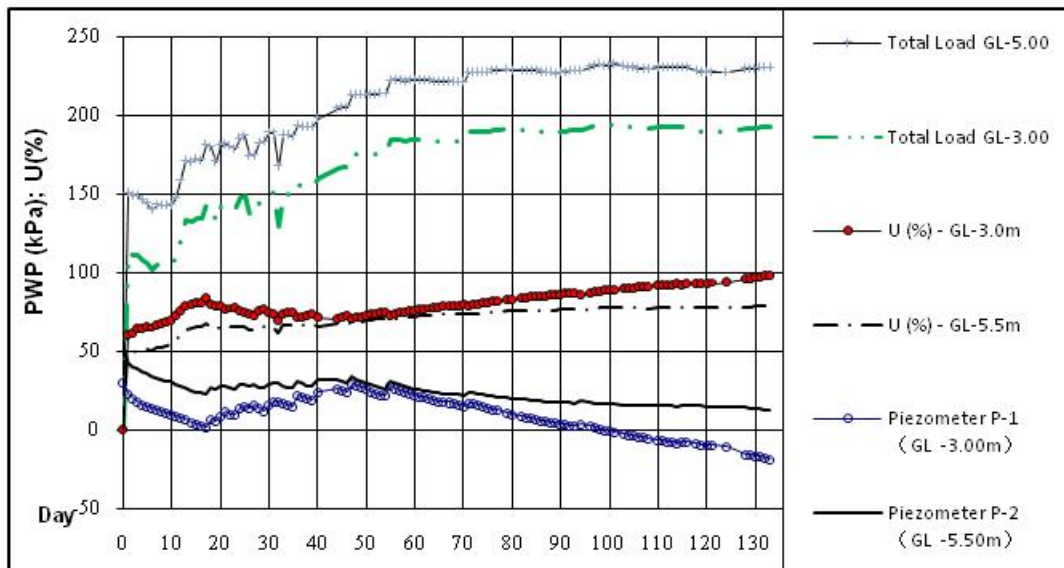


Figure 4.39. Predict DOC by dissipation of the excess pore water pressure (EPWP) The measurement of water discharge was automatically carried out as shown in Figure 4.40. The drained volume constant is marked to stop the vacuum pressure.

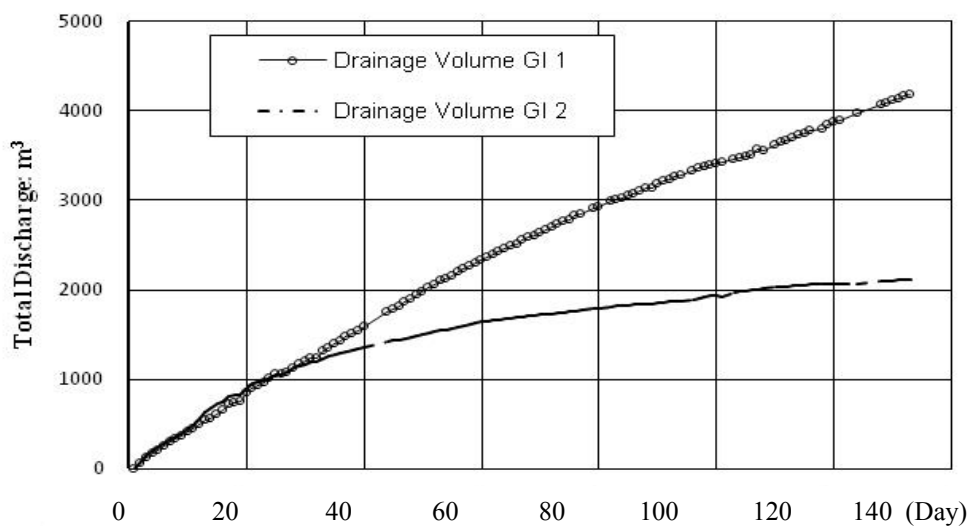


Figure 4.40. The discharge of zone GI-1 & GI-2

The stages of embankment filling at each GI-Zone 1-8 are shown in **Table 4.11**. From the plotted, huge delay on vacuum operation on Zone 3,4,5 and 6

due to the repaired of damage of airtight sheet during earthwork construction and delay of filling works.

Table 4.11. The stage of embankment filling period and vacuum operation

GI-Zone	Date of start of vacuum operation	Date of start filling embankment	Date of finished embankment	Date of stop vacuum operation	Period time (day)	Height of embankment
1	23 Dec 2009	8 Jan 2010	3 May 2010	7 May 2010	135	3.10
2	23 Dec 2009	8 Jan 2010	3 May 2010	7 May 2010	135	3.10
3	9 Jan 2010	20 Jan 2010	4 July 2010	28 July 2010	200	2.80
4	9 Jan 2010	20 Jan 2010	4 July 2010	28 July 2010	200	2.80
5	30 Dec 2009	17 Mar 2010	29 Jun 2010	28 July 2010	210	2.80
6	30 Dec 2009	17 Mar 2010	29 Jun 2010	28 July 2010	210	2.80
7	13 Feb 2010	3 Mar 2010	10 Apr 2010	11 July 2010	148	2.40
8	13 Feb 2010	3 Mar 2010	30 Apr 2010	11 July 2010	148	2.10

The summary of settlement, degree of consolidation, rate of settlement and OCR value for GI Zone 1-8 are shown in Table 4.12.

Table 4.12. Degree of consolidation and rate of settlement

GI-Zone	Avg Sett	DOC	Rate of settlement	OCR value	
	(m)			(%)	(mm/day)
1	0.55	95.10	0.63	1.1	1.25
2	0.57	95.80	1.00	1.1	1.25
3	0.53	N.A	0.50	1.1	1.20
4	0.53	N.A	0.58	1.1	1.20
5	0.52	N.A	0.63	1.1	1.20
6	0.55	N.A	0.22	1.1	1.20
7	0.58	93.90	1.00	1.1	1.30
8	0.55	91.67	0.90	1.1	1.50

During the earthwork construction some settlement plates and depth settlement gaugers were damaged, the data could not be used as a reference in monitoring records. The average of final settlement was found about 0.55m after 135 days with

the degree of consolidation at more than 90% and the rate of settlement almost less than 1mm per day.

After reach the target of degree of consolidation, the vacuum operations finished, applying of vacuum pressure act as pre-loading pressure in sub-soil. The sub-soil was a over consolidated state, the OCR were evaluated as the actual loading (dead load and live load) which could be applied in the future.

The **Figure 4.39** is proposed to illustrate real excess pore water pressure of soft soil under vacuum consolidation preloading method.

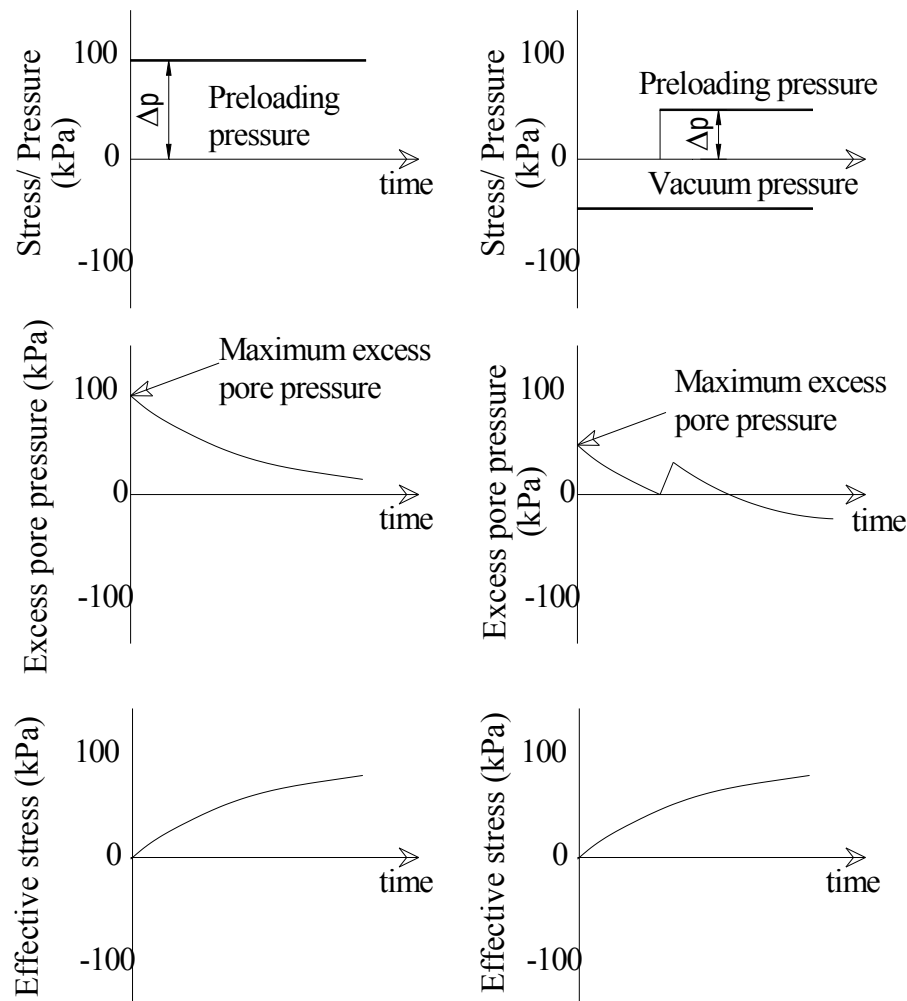


Figure 4.41. The real excess pore water pressure

4.5.5 Summary Conclusions

Based on the field monitoring records and the analysis of soil improvement by vacuum consolidation method for Apron and Taxi way of Nakorn Srithammarat Airport, It can be concluded as follows:

(1) The primary consolidation settlement of soft to very soft clay found in range 0.5-0.65m, with the degree of consolidation more than 90% after only 135days vacuum operation. The period construction accelerated significantly compare to the conventional method. The 1mm/day rate of settlement was measured at last 12 days before stop vacuum operation.

(2) The degree of consolidation evaluated from dissipation of excess pore water were varied with depth, it was reduced with the depth of soil improvement, due to the various distribution of vacuum pressure along to the vertical drain.

(3) The 70 to 85kPa of vacuum pressure was generated the overconsolidated state of soil with the minimum OCR values equal to 1.20.

CHAPTER V

CONCLUSIONS AND DISCUSSIONS

5.1 Research Conclusions

5.1.1 The Gain of the Research

The study has been developed based on the combination of finite element analysis and laboratory experiments to propose a new appropriate method, which can be widely applied for soft ground improvement by vacuum preloading method. To avoid the risks of instability of embankment, the prediction behavior of soft soil during performance of vacuum preloading method should be concerned significantly not only in the laboratory but also at the field. The simulation vacuum preloading method using tri-axial apparatus is proposed to predict the behavior of soft soil improvement and the increasing of undrained shear strength of soil specimen at any degree of consolidation in the laboratory at Hokkaido University. The undrained shear strengths of soil, at 40%, 70% and 100% of vacuum consolidation, are gained at 43.2kPa, 53.8kPa and 62.49kPa, respectively by using tri-axial apparatus.

None boundary axisymmetric soil cell has been used to model the behavior of soft soil treatment by vacuum preloading method. This condition suits the on-site real soil condition. Two cases of drainage boundary of soil cell indicated that the consolidated time of drainage at boundary is faster than at center of the soil cell by ratio T_{hNC}/T_{hNB} . However, deformations of the specimens are in the same shape and value with the same preloading condition. Results of experiments by tri-axial apparatus agree with FEM model. It is suggested that the solution is highly reliable and technologically feasible to predict the behavior of soft soil improvement during the performance of vacuum preloading method.

The simulation by Tri-axial apparatus is the effective method to determine the increasing rate of soil strength corresponding to loading rate during consolidation process. In addition, its aim is to restrict using field test, which can cause damage of the airtight sheet membrane and loss of vacuum pressure during vacuum preloading construction. In this simulation, the normal size of

specimen, which can be retrieved from the field, is conducted only one week instead of one month with large specimen.

The performance of vacuum consolidation for soft ground at Nakhorn Sri Thammarat Airport by applying technology from Maruyama Company, Japan, has achieved the required objectives. Vacuum pressure was maintained at high magnitude of 80kPa even more than 90kPa via the collection tank system to split water and air separately throughout the construction process. The average settlement is gained at 57cm, with more than 90% degree of consolidation after 135-day vacuum operation only. The construction period accelerated significantly compared to the conventional method. The settlement rate of 1mm/day was measured at the last 12 days prior to closing vacuum operation. These results indicate the effectiveness of this approach.

The vacuum pressure were generated overconsolidated state of soil, the minimum OCR values gained at 1.20. The embankment improved by surcharge and vacuum pressure can be compensated the actual loading in the future.

5.1.2 The Advantages of Using the Vacuum Preloading Method

The advantages of using the vacuum preloading method as follows

- Vacuum preloading causes isotropic stress increment in both vertical and horizontal directions in sub soil, and the corresponding lateral displacement occurred inward. Consequently, the risk of shear failure can be minimized even at higher rate of embankment construction, resulting in an increased rate of soft soil consolidation.
- The average vacuum pressure from 70 to 85kPa, generated under membrane sheets by pumping, is equivalent to 3.50m - 4.50m height of embankment. The embankment at the beginning earthwork can be constructed rapidly without any risk. The height of surcharge can be replaced by vacuum pressure to gain the same degree of consolidation.
- It is not necessary to design the land manes to restrict the instability of embankment due to large lateral deformation, which always occurs during soft soil improve by conventional method.

- The pollution in the environment does not exist during performance of vacuum consolidation method because only non-chemical material is used in this method.

5.1.3 The Factors Effect on Effectiveness of This Method

The increasing bearing capacity of soft soil can not be determined via the usual method during vacuum preloading. Hence, field data measurement and laboratory prediction are very important to control instability of the embankment, and to ensure the effectiveness of performance of vacuum consolidation. The instrumentations are used effectively to control and minimize the instability of the embankment at the site.

The dropping of water head and soft soil subsidence causes vacuum pressure reduction, which can be disappear completely as the large thick soft soil layer improved by conventional vacuum technique. Applying the separated tank the vacuum pressure can be maintained during construction.

The effectiveness of this method based on many factors however can determine some main factors as shown below:

- Capacity of vacuum pumping systems
- The sealing and protection of the airtight sheets method
- Soft soil condition and ground water level
- Effectiveness of the vertical band drains.

5.2 Limitations and recommendations of the Study:

Because of limited research time, the Kasaoka clay samples in Japan were used to simulate behavior of soft soil improvement by vacuum consolidation instead of the extruded soil samples from the site at Nakhorn Sri Thammarat Airport in order to ensure the results obtained from simulation are accurate and consistent.

The membrane damage, caused by using sand and rock particles instead of a uniform sand layer, leads to extend the construction time of some zones to fix the leaked vacuum pressure points during earthwork. Finally, the total construction budget has increased significantly and affected whole project.

The construction process must be done carefully during performance of vacuum consolidation method. It is very important and necessary to protect the airtight sheet membrane. Three 0.3mm thickness layers of airtight sheet should be designed to prevent any risk that may occur during construction.

REFERENCES

- Das, B.M. **Fundamentals of geotechnical engineering**. 7th Edition. USA : Cengage Learning, 2010.
- Manfred, R.H. **Engineering principles ground modification**. Singapore : McGraw-Hill Publishing Company, 1990.
- William , T.L., Robert., V.W. **Soil mechanics, SI version**. New York: John Wiley & Sons, 1979.
- Nagaraj, T.S., Miura, N. **Soft clay behaviour analysis and assessment**: Taylor & Francis, 2001.
- Terzaghi, K. **Theoretical soil mechanics**. New York: John Wiley & Sons, 1943.
- Asaoka, A. **Observational procedure of settlement prediction**. Soils and Foundations, Japanese Society of Soil Mechanics and Foundation Engineering 18, 4, 1978.
- Barron, R.A. **Consolidation of fine-grained soils by drain wells**. Trans. ASCE 1948: 718–742.
- Bergado, D.T., Balasubramaniam, A.S., Fannin, R.J., and Holtz, R.D. **Prefabricated vertical drains (PVDs) in soft Bangkok clay: a case study of the new Bangkok International Airport project**. Canadian Geotechnical Journal 39, 2 2002: 304-315.
- Chai, J.C., Carter, J.P., Hayashi, S. **Vacuum consolidation and its combination with embankment loading**. Canadian Geotechnical Journal 2006: 985–996.
- Chai, J.C., Shen, S.L., Miura, N., and Bergado, D.T. **Simple method of modeling PVD improved subsoil**. Journal of Geotechnical Engineering, ASCE 2001: 965-972.
- Chu, J., and Yan, S.W. **Application of vacuum preloading method in soil improvement project**. Case Histories Book 3, Edited by Indraratna, B., and Chu, J., Elsevier, London 2005: 91-118.

- Chu, J., Yan, S.W., and Indraratna, B. **Vacuum preloading techniques - recent developments and applications**. GeoCongress, New Orleans, Geosustainability and Geohazard Mitigation GPS 178, Reddy, KR, Khire, MV, Alshawabkeh, AN (eds) 2008: 586-595.
- Chu, J. and Yan, S.W. **Estimation of degree of consolidation for vacuum preloading projects**. International Journal of Geomechanics, ASCE 5, 2 2005: 158-165.
- Hansbo, S. **Aspects of vertical drain design: Darcian or non-Darcian flow**. Geotechnique, 47, 5 1997: 983-992.
- Hansbo, S. **Consolidation of fine-grained soils by prefabricated drains**. Proc., 10th Int. Conf. on Soil Mechanics and Foundations Engineering, Stockholm, Sweden 3 1981: 677-682.
- Hanzawa, H. and Tanaka, H. **Normalized undrained strength of clay in the normally consolidated state and in the field**. Soils and Foundations 32, 1 1992: 132-148
- Indraratna B., and Redana, I.W. **Laboratory determination of smear zone due to vertical drain installation**. Journal of Geotechnical and Geoenvironmental Engineering, ASCE 124, 2 1998: 180-184.
- Indraratna B., and Redana, I.W. **Plane strain modeling of smear effects associated with vertical drains**. Journal of Geotechnical and Geoenvironmental Engineering, ASCE 123,5 1997: 474-478.
- Indraratna, B. **Recent advancements in the use of prefabricated vertical drains in soft soils**, Australian Geomechanics Journal, March issue 2008: 29-46.
- Indraratna, B., and Redana, I. W. **Laboratory determination of smear zone due to vertical drain installation**. J. Geotech. Eng., ASCE 125, 1 1998: 96-99.
- Indraratna, B., and Redana, I.W. **Numerical modeling of vertical drains with smear and well resistance installed in soft clay**. Canadian Geotechnical Journal 37 2000: 133-145.

- Indraratna, B., Bamunawita, C., and Khabbaz, H. **Numerical modeling of vacuum preloading and field applications.** Canadian Geotechnical Journal 41 2004: 1098-1110.
- Indraratna, B., Rujikiatkamjorn C., and Sathananthan, I. **Analytical and numerical solutions for a single vertical drain including the effects of vacuum preloading.** Canadian Geotechnical Journal 42 2005: 994-1014.
- Indraratna, B., Rujikiatkamjorn, C., Balasubramaniam, A.S., and Wijeyakulasuriya. **Prediction and observations of soft clay foundations stabilized with geosynthetic drains and vacuum surcharge.** Ch. 7, Ground Improvement Case Histories 2005.
- John, D., McKinley. **Coupled consolidation of a solid, infinite cylinder using a Terzaghi formulation.** Computers and Geotechnics 23 1998: 193-204.
- Kjellman, W. **Consolidation of clay soils by atmospheric pressure.** Proceedings of a conference on soil stabilization, Massachusetts Institute of Technology, Boston 1952: 258-263.
- Rujikiatkamjorn, C., Indraratna, B. **Soft ground improvement by vacuum-assisted preloading.** Australian Geomechanics Journal 2007: 19-30.
- Tanaka, H., Shiwakoti, D.R., and Tanaka, M. **Applicability of SHANSEP method to six different natural clays, using triaxial and direct shear tests.** Soils and Foundations 43, 3, 2003: 43-56
- Watabe, Y., Tanaka, M., Tanaka, H. and Tsuchida, T. **Ko-consolidation in a triaxial cell and evaluation of in-situ Ko for marine clays with various characteristics.** Soils and Foundations 43, 1 2003: 1-20

BIBLIOGRAPHY

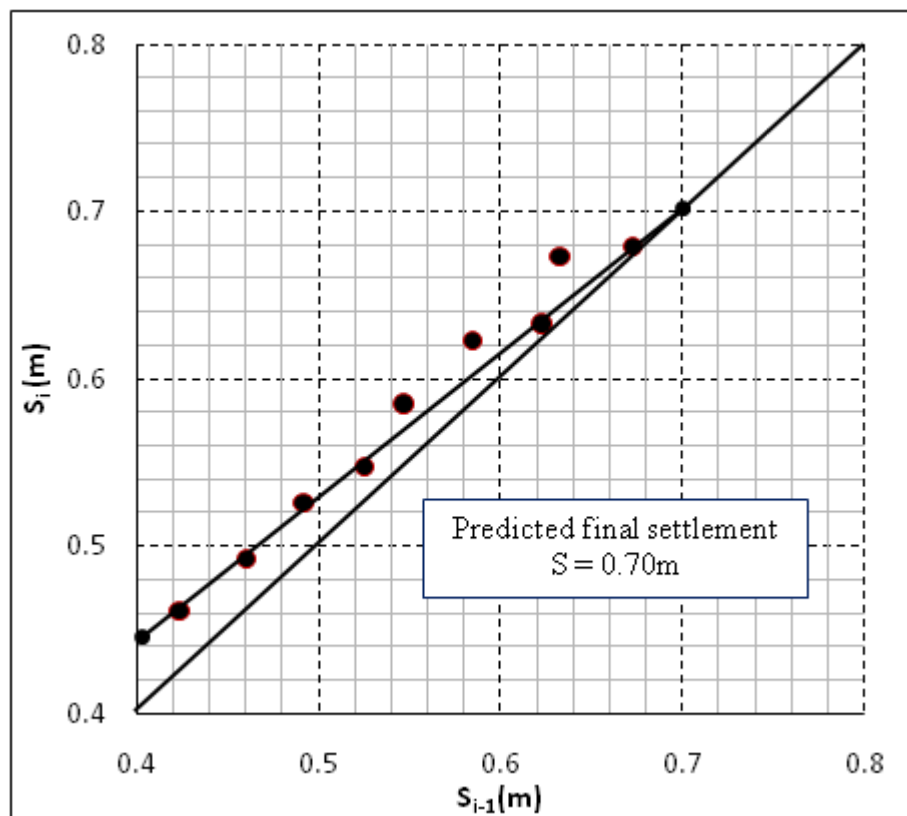
- Minna, K., Martino, L. **Geotechnics of soft soils – focus on ground improvement**. Proceedings of the 2nd International Workshop held in Glasgow, Scotland, 2008.
- Indraratna B., and Chu, J. **Ground improvement – Case histories book 3**. London, Elsevier, 2005.
- Chen, H., and Bao, X.C. **Analysis of soil consolidation stress under the action of negative pressure**. Proc. 8th European Conf. on Soil Mech. and Found. Eng., Helsinki 2 1983: 591-596.
- Chu, J., Bo, M.W., and Choa, V. **Practical considerations for using vertical drains in soil improvement project**. Geotextiles and Geomembranes 22 2004: 101-117.
- Chu, J., Yan, S.W., and Yang, H. **Soil improvement by the vacuum preloading method for an oil storage station**. Geotechnique 2000: 625-632.
- Hibbitt, Karlsson, Sorensen. **ABAQUS/standard user's manual**, Published by HKS Inc, 2004.
- Mohamedelhassan, E., and Shang, J.Q. **Vacuum and surcharge combined one-dimensional consolidation of clay soils**. Canadian Geotechnical Journal 39 2002: 1126-1138.
- Qian, J.H., Zhao, W.B., Cheung, Y.K., and Lee, P.K.K. **The theory and practice of vacuum preloading**. Computers and Geotechnics 13 1992: 103-118.
- Sharma, J. S., and Xiao, D. **Characterization of a smear zone around vertical drains by large-scale laboratory tests**. Canadian Geotechnical Journal 37, 6 2000: 1265–1271.
- Tuan, A.T, Toshiyuki, M. **Equivalent plane strain modeling of vertical drains in soft ground under embankment combined with vacuum preloading**. Computers and Geotechnics 3 2008: 5655–672.

APPENDIX

Asaoka's Plot and Estimated Degree of Consolidation for SP-7-1

Date	Settlement (m)	Remarks
8-Apr-10	0.424	Day Zero
18-Apr-10	0.461	S-1
28-Apr-10	0.492	S-2
8-May-10	0.526	S-3
18-May-10	0.547	S-4
28-May-10	0.585	S-5
7-Jun-10	0.623	S-6
17-Jun-10	0.633	S-7
27-Jun-10	0.673	S-8
7-Jun-10	0.679	S-9

Asaoka's Plot

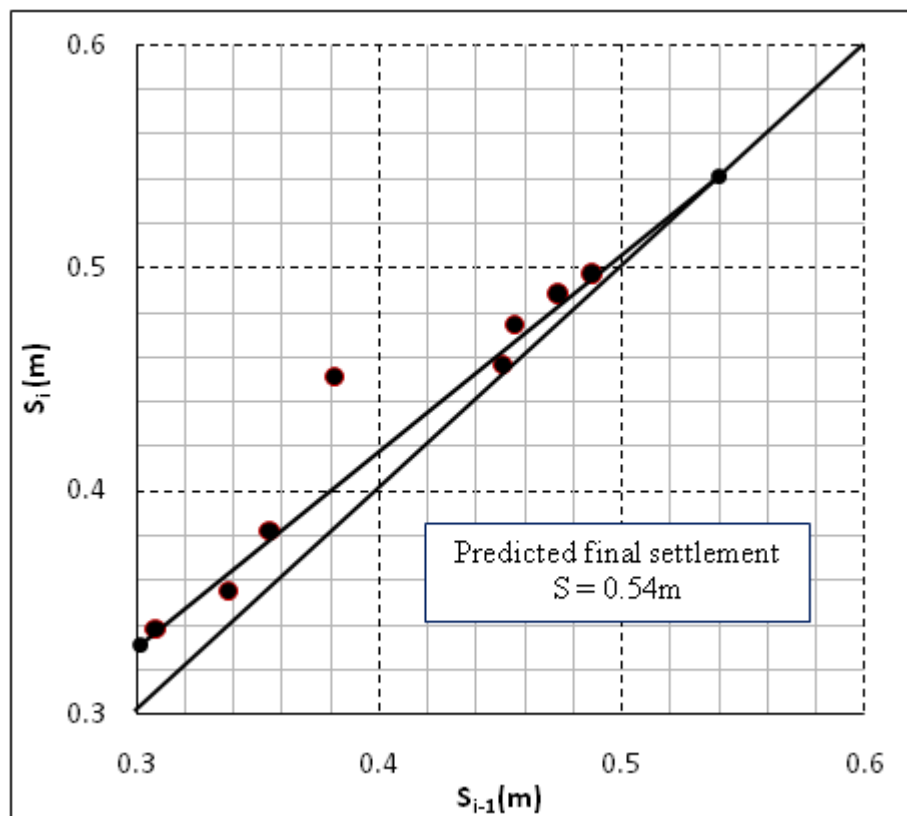


Total settlement (m)	0.7
Actual settlement (m)	0.679
Degree of Consolidation (%)	97
Rate of settlement (last 10days)(mm/day)	0.6

Asaoka's Plot and Estimated Degree of Consolidation for SP-7-2

Date	Settlement (m)	Remarks
8-Apr-10	0.284	Day Zero
18-Apr-10	0.308	S-1
28-Apr-10	0.338	S-2
8-May-10	0.355	S-3
18-May-10	0.382	S-4
28-May-10	0.451	S-5
7-Jun-10	0.456	S-6
17-Jun-10	0.474	S-7
27-Jun-10	0.488	S-8
7-Jun-10	0.497	S-9

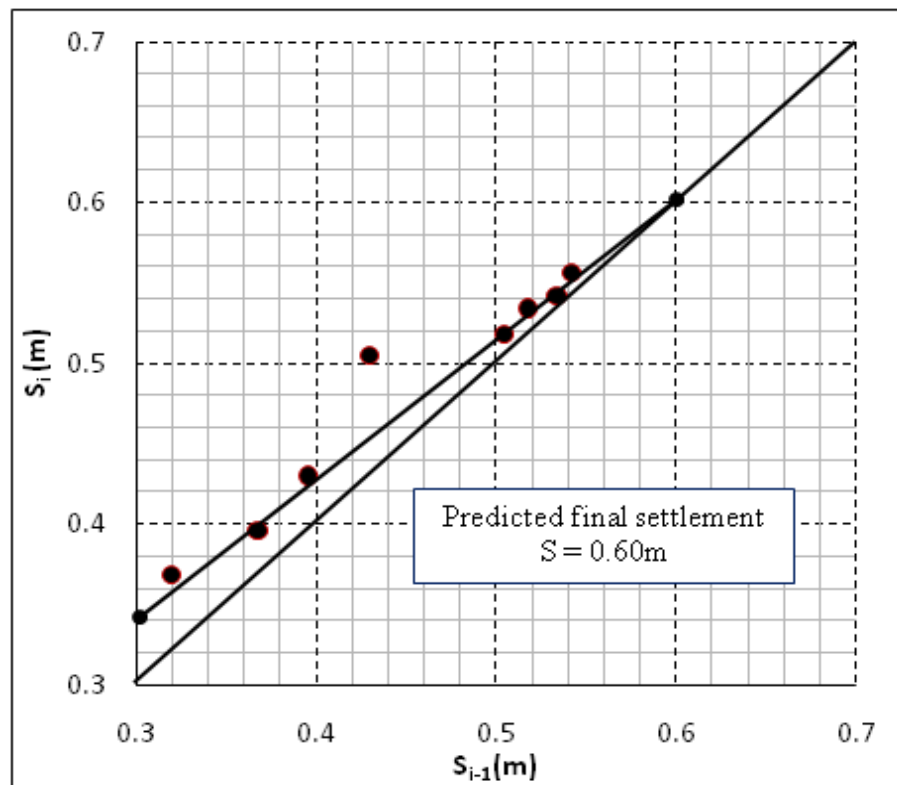
Asaoka's Plot



Total settlement (m)	0.54
Actual settlement (m)	0.497
Degree of Consolidation (%)	92.0
Rate of settlement (last 10days)(mm/day)	0.90

Asaoka's Plot and Estimated Degree of Consolidation for SP-7-3

Date	Settlement (m)	Remarks
8-Apr-10	0.284	Day Zero
18-Apr-10	0.32	S-1
28-Apr-10	0.368	S-2
8-May-10	0.396	S-3
18-May-10	0.43	S-4
28-May-10	0.505	S-5
7-Jun-10	0.518	S-6
17-Jun-10	0.534	S-7
27-Jun-10	0.542	S-8
7-Jun-10	0.556	S-9

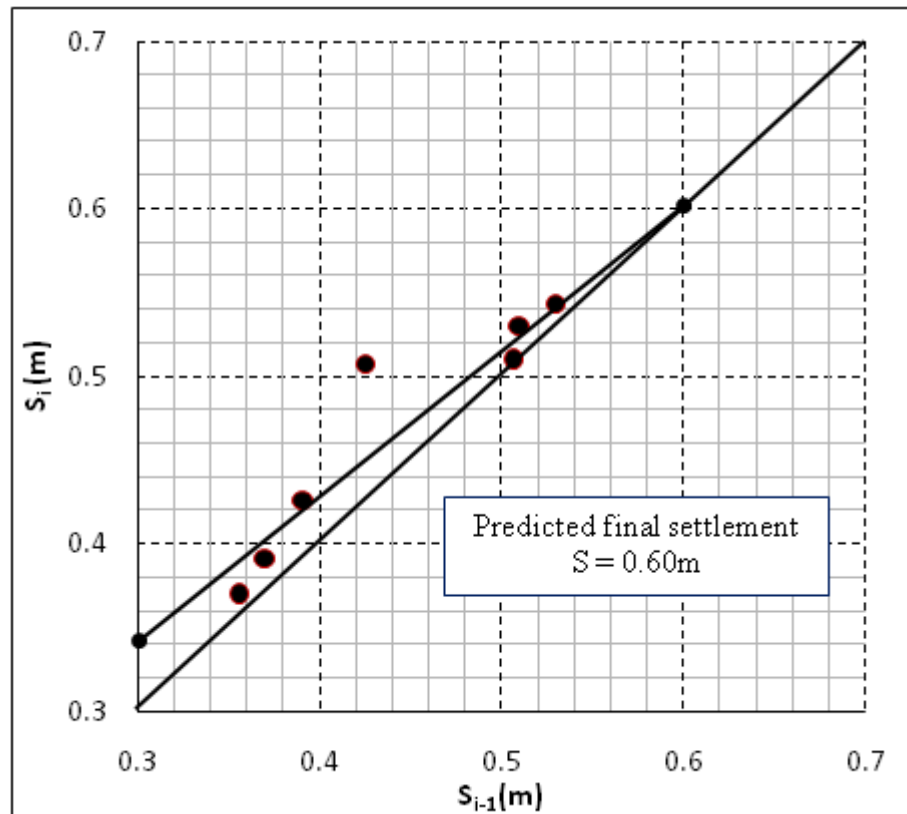


Total settlement (m)	0.6
Actual settlement (m)	0.556
Degree of Consolidation (%)	92.7
Rate of settlement (last 10days)(mm/day)	1.40

Asaoka's Plot and Estimated Degree of Consolidation for SP-8-1

Date	Settlement (m)	Remarks
30-Apr-10	0.356	Day Zero
10-May-10	0.37	S-1
20-May-10	0.391	S-2
30-May-10	0.426	S-3
9-Jun-10	0.507	S-4
19-Jun-10	0.51	S-5
29-Jun-10	0.53	S-6
9-Jul-10	0.543	S-7

Asaoka's Plot

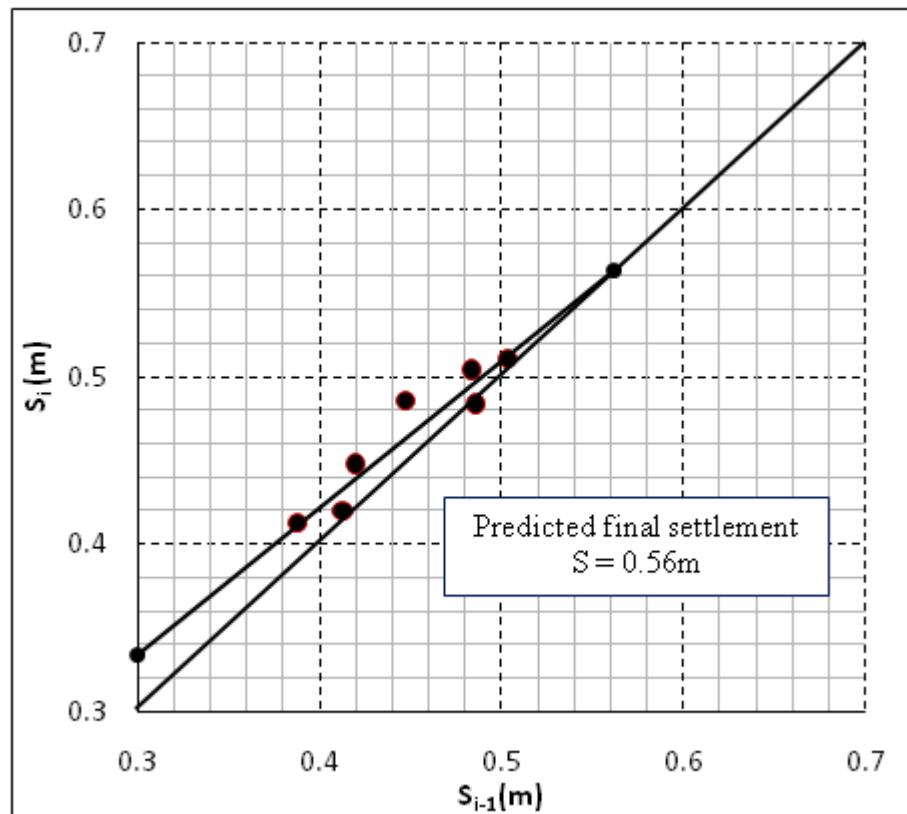


Total settlement (m)	0.6
Actual settlement (m)	0.543
Degree of Consolidation (%)	90.5
Rate of settlement (last 10days)(mm/day)	1.30

Asaoka's Plot and Estimated Degree of Consolidation for SP-8-2

Date	Settlement (m)	Remarks
30-Apr-10	0.388	Day Zero
10-May-10	0.413	S-1
20-May-10	0.42	S-2
30-May-10	0.448	S-3
9-Jun-10	0.486	S-4
19-Jun-10	0.484	S-5
29-Jun-10	0.504	S-6
9-Jul-10	0.511	S-7

Asaoka's Plot

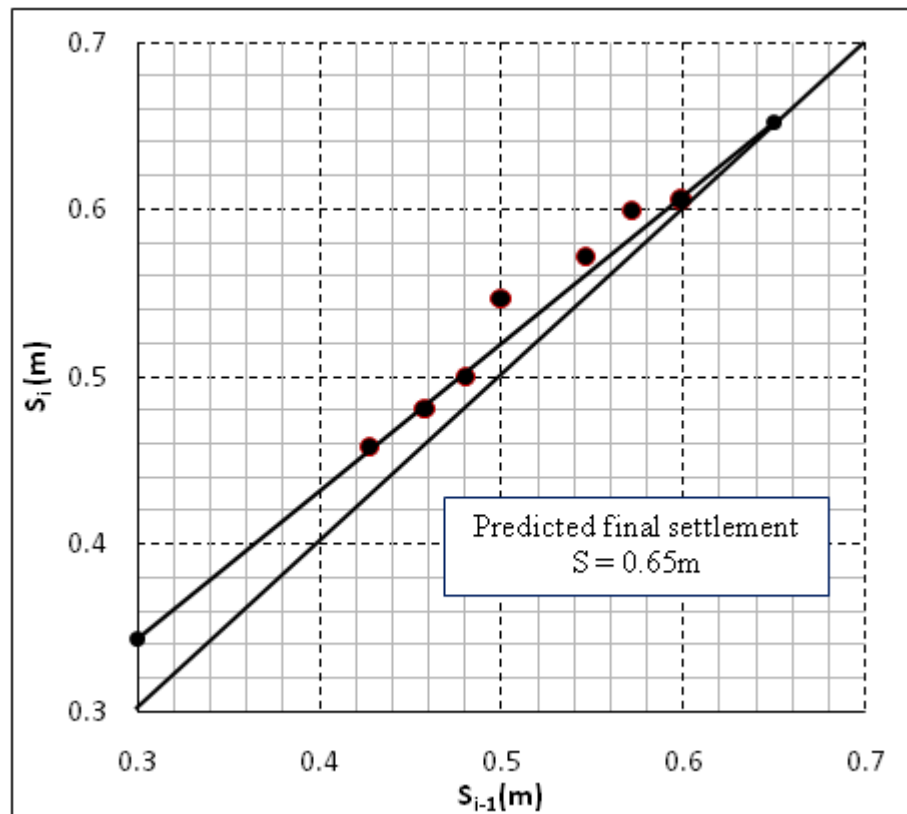


Total settlement (m)	0.56
Actual settlement (m)	0.511
Degree of Consolidation (%)	91.3
Rate of settlement (last 10days)(mm/day)	0.70

Asaoka's Plot and Estimated Degree of Consolidation for SP-8-3

Date	Settlement (m)	Remarks
30-Apr-10	0.428	Day Zero
10-May-10	0.458	S-1
20-May-10	0.481	S-2
30-May-10	0.5	S-3
9-Jun-10	0.547	S-4
19-Jun-10	0.572	S-5
29-Jun-10	0.599	S-6
9-Jul-10	0.606	S-7

Asaoka's Plot

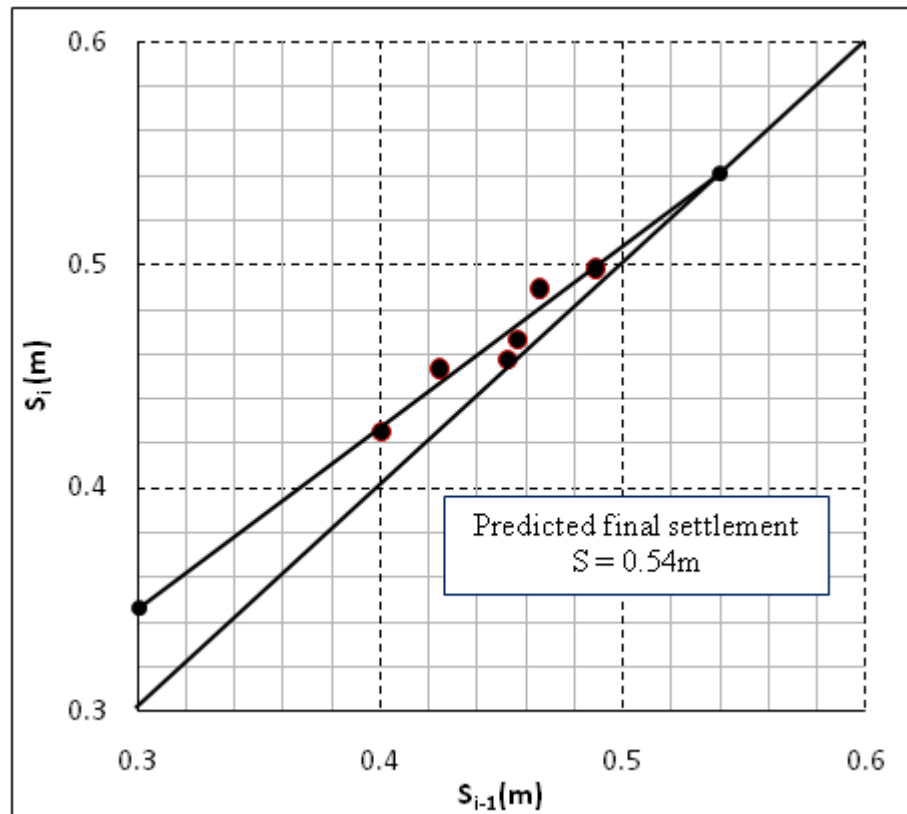


Total settlement (m)	0.65
Actual settlement (m)	0.606
Degree of Consolidation (%)	93.2
Rate of settlement (last 10days)(mm/day)	0.70

Asaoka's Plot and Estimated Degree of Consolidation for SP-1-1

Date	Settlement (m)	Remarks
4-Mar-10	0.401	Day Zero
14-Mar-10	0.425	S-1
24-Mar-10	0.453	S-2
3-Apr-10	0.457	S-3
13-Apr-10	0.466	S-4
23-Apr-10	0.489	S-5
3-May-10	0.498	S-6

Asaoka's Plot

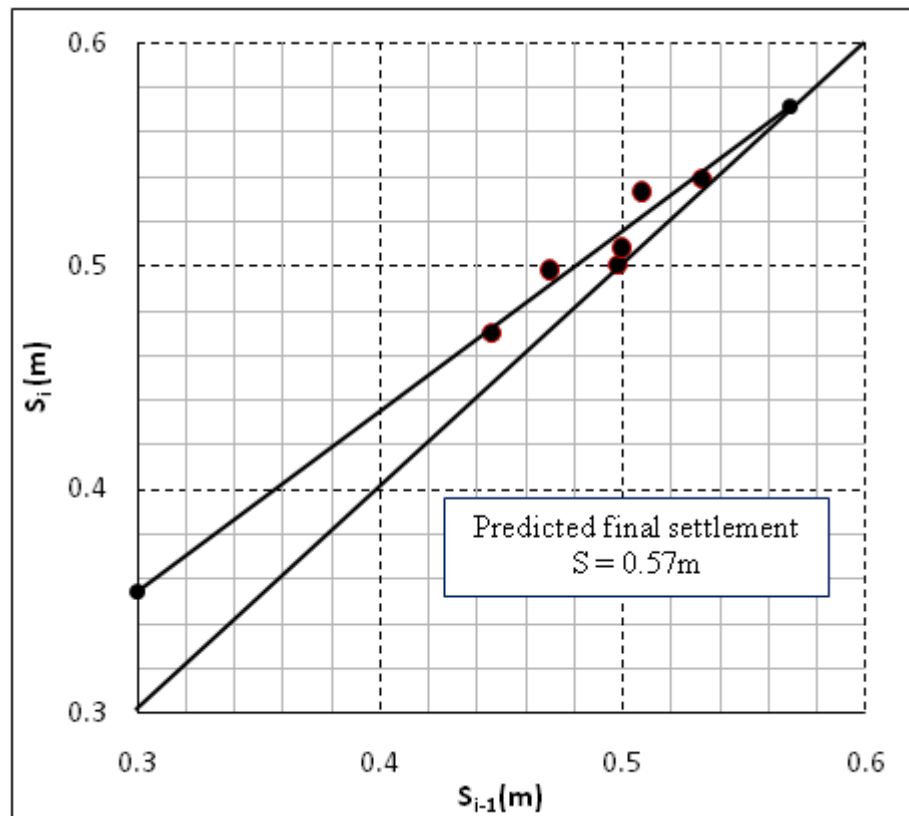


Total settlement (m)	0.54
Actual settlement (m)	0.498
Degree of Consolidation (%)	92.2
Rate of settlement (last 10days)(mm/day)	0.90

Asaoka's Plot and Estimated Degree of Consolidation for SP-1-2

Date	Settlement (m)	Remarks
4-Mar-10	0.446	Day Zero
14-Mar-10	0.47	S-1
24-Mar-10	0.498	S-2
3-Apr-10	0.5	S-3
13-Apr-10	0.508	S-4
23-Apr-10	0.533	S-5
3-May-10	0.539	S-6

Asaoka's Plot

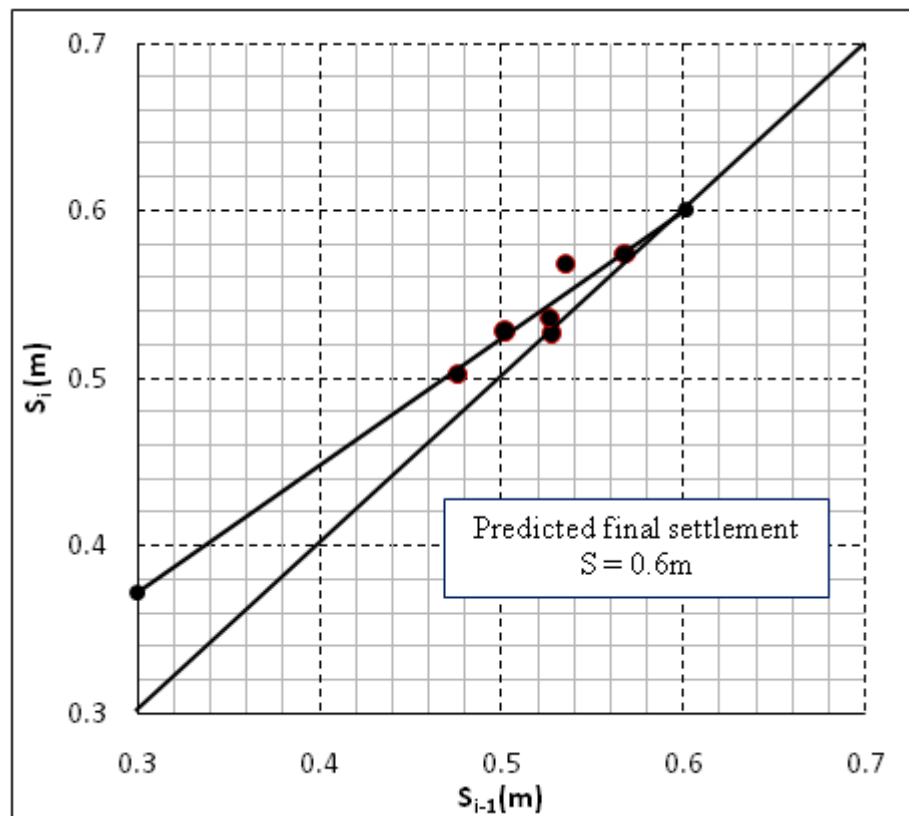


Total settlement (m)	0.57
Actual settlement (m)	0.539
Degree of Consolidation (%)	94.6
Rate of settlement (last 10days)(mm/day)	0.60

Asaoka's Plot and Estimated Degree of Consolidation for SP-1-3

Date	Settlement (m)	Remarks
4-Mar-10	0.476	Day Zero
14-Mar-10	0.502	S-1
24-Mar-10	0.528	S-2
3-Apr-10	0.527	S-3
13-Apr-10	0.536	S-4
23-Apr-10	0.568	S-5
3-May-10	0.574	S-6

Asaoka's Plot

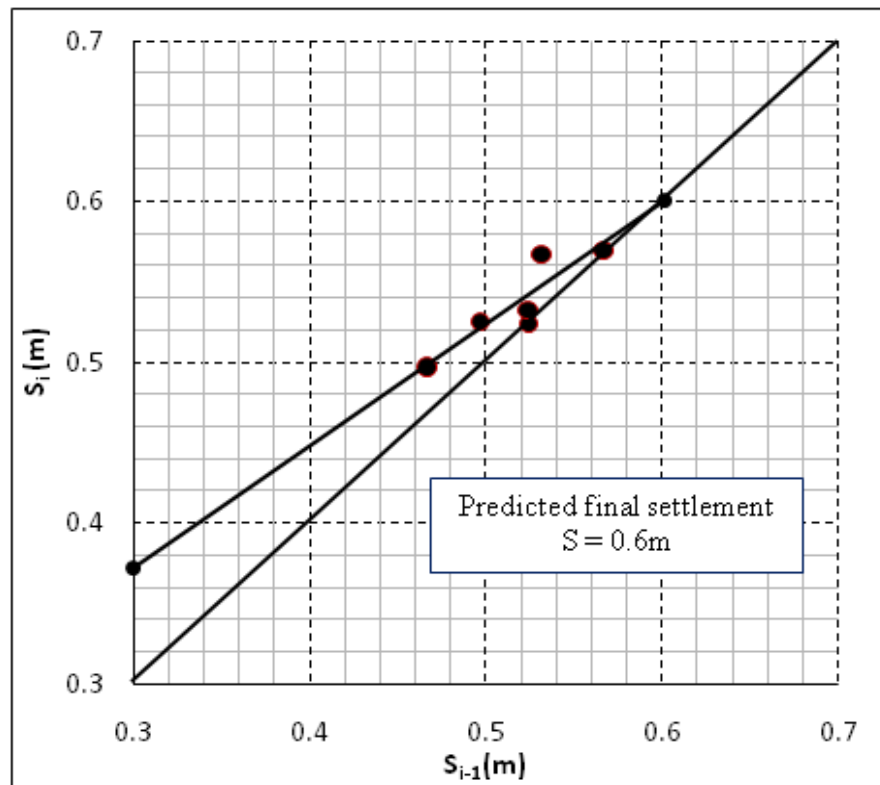


Total settlement (m)	0.6
Actual settlement (m)	0.574
Degree of Consolidation (%)	95.7
Rate of settlement (last 10days)(mm/day)	0.60

Asaoka's Plot and Estimated Degree of Consolidation for SP-1-4

Date	Settlement (m)	Remarks
4-Mar-10	0.467	Day Zero
14-Mar-10	0.497	S-1
24-Mar-10	0.525	S-2
3-Apr-10	0.524	S-3
13-Apr-10	0.532	S-4
23-Apr-10	0.567	S-5
3-May-10	0.569	S-6

Asaoka's Plot

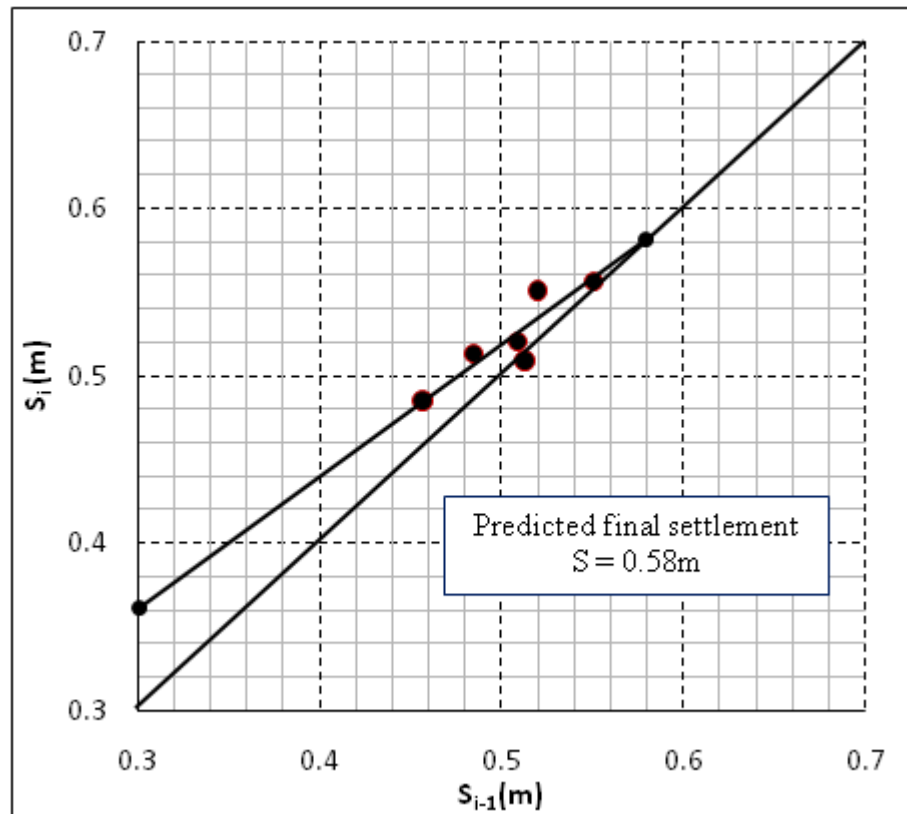


Total settlement (m)	0.6
Actual settlement (m)	0.569
Degree of Consolidation (%)	94.8
Rate of settlement (last 10days)(mm/day)	0.20

Asaoka's Plot and Estimated Degree of Consolidation for SP-1-5

Date	Settlement (m)	Remarks
4-Mar-10	0.457	Day Zero
14-Mar-10	0.485	S-1
24-Mar-10	0.513	S-2
3-Apr-10	0.509	S-3
13-Apr-10	0.52	S-4
23-Apr-10	0.551	S-5
3-May-10	0.556	S-6

Asaoka's Plot

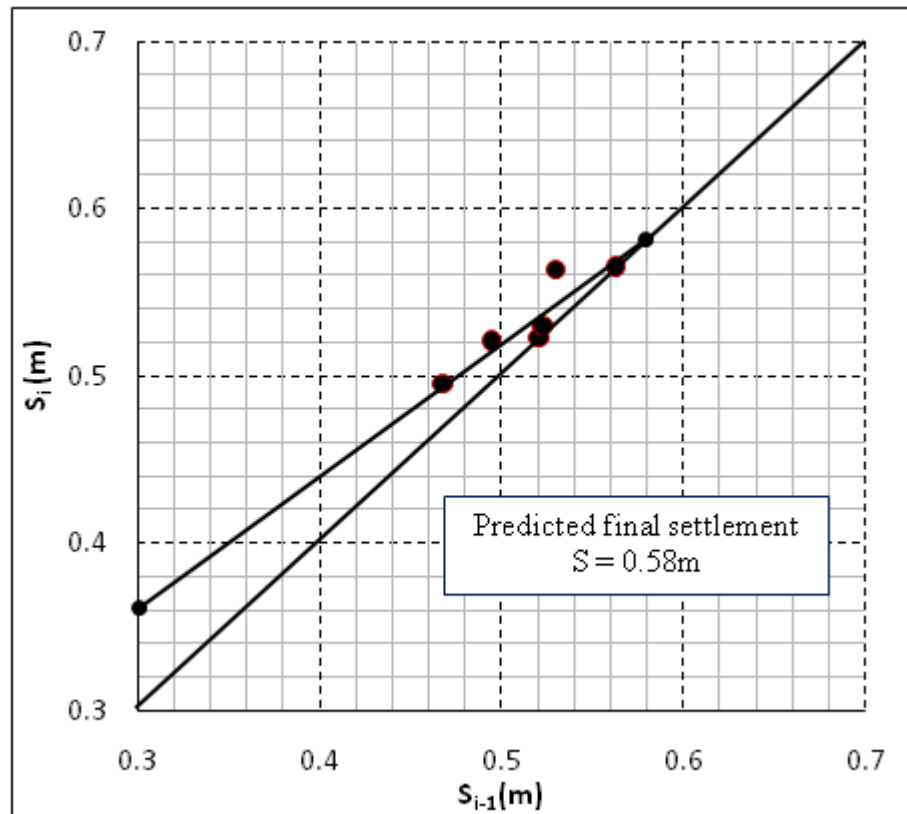


Total settlement (m)	0.58
Actual settlement (m)	0.556
Degree of Consolidation (%)	95.9
Rate of settlement (last 10days)(mm/day)	0.50

Asaoka's Plot and Estimated Degree of Consolidation for SP-1-6

Date	Settlement (m)	Remarks
4-Mar-10	0.468	Day Zero
14-Mar-10	0.495	S-1
24-Mar-10	0.521	S-2
3-Apr-10	0.523	S-3
13-Apr-10	0.53	S-4
23-Apr-10	0.563	S-5
3-May-10	0.565	S-6

Asaoka's Plot

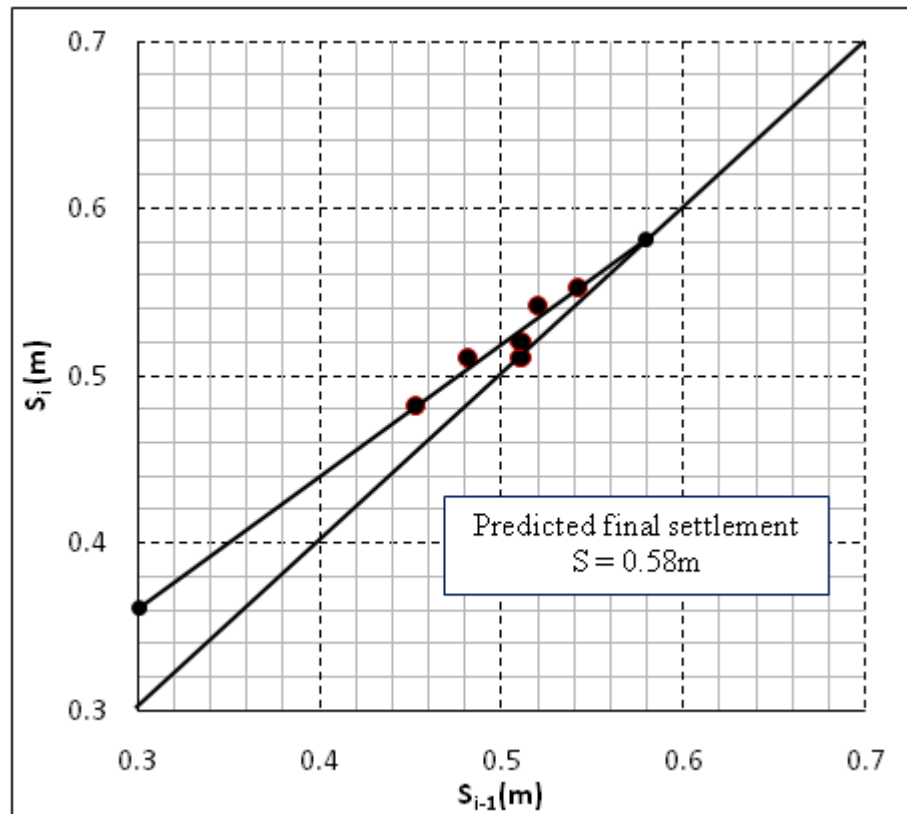


Total settlement (m)	0.58
Actual settlement (m)	0.565
Degree of Consolidation (%)	97.4
Rate of settlement (last 10days)(mm/day)	0.20

Asaoka's Plot and Estimated Degree of Consolidation for SP-2-2

Date	Settlement (m)	Remarks
4-Mar-10	0.453	Day Zero
14-Mar-10	0.482	S-1
24-Mar-10	0.511	S-2
3-Apr-10	0.511	S-3
13-Apr-10	0.52	S-4
23-Apr-10	0.542	S-5
3-May-10	0.553	S-6

Asaoka's Plot

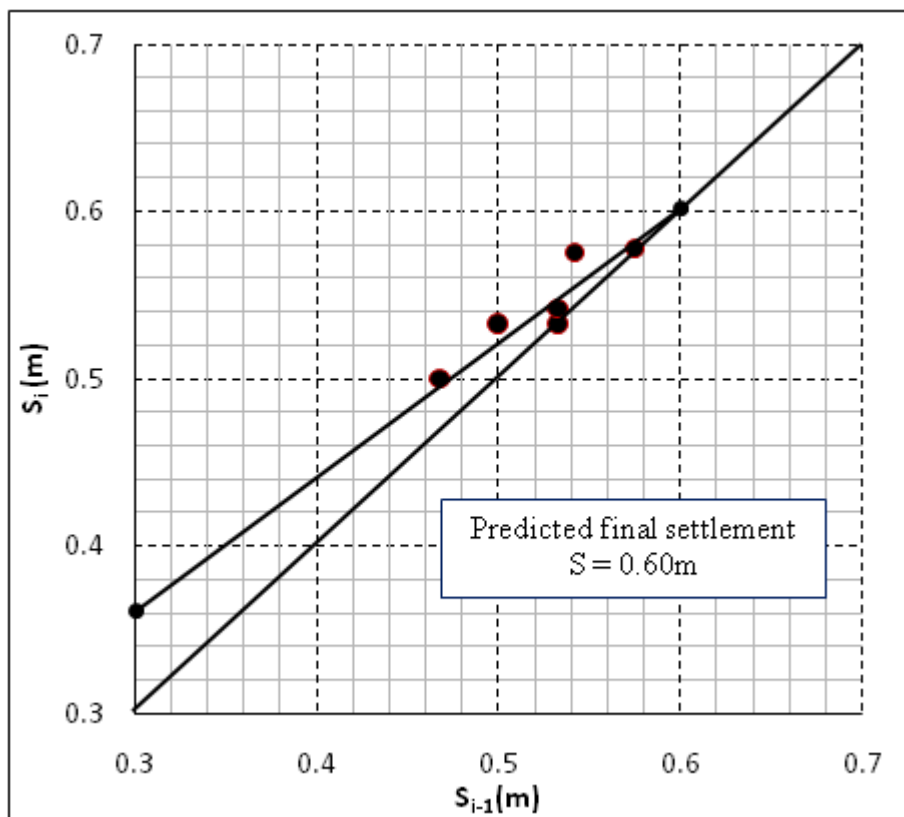


Total settlement (m)	0.58
Actual settlement (m)	0.553
Degree of Consolidation (%)	95.3
Rate of settlement (last 10days)(mm/day)	1.10

Asaoka's Plot and Estimated Degree of Consolidation for SP-2-2

Date	Settlement (m)	Remarks
4-Mar-10	0.468	Day Zero
14-Mar-10	0.5	S-1
24-Mar-10	0.533	S-2
3-Apr-10	0.533	S-3
13-Apr-10	0.542	S-4
23-Apr-10	0.575	S-5
3-May-10	0.578	S-6

Asaoka's Plot



Total settlement (m)	0.6
Actual settlement (m)	0.578
Degree of Consolidation (%)	96.3
Rate of settlement (last 10days)(mm/day)	0.30